Estimates of Evapotranspiration to Support the Klamath River Revised Natural Flow Study

Matt Bromley
Blake A. Minor
Christopher Pearson
Christian Dunkerly
Charles Morton
Justin L. Huntington

Draft – August 2024

Publication No. 41XXX

Prepared by
Division of Hydrologic Sciences, Desert Research Institute

Prepared for
U.S. Bureau of Reclamation

(Cover Picture: Mosaic of photographs of the Klamath River Basin; Attribution: USBR)

Estimates of Evapotranspiration to Support the Klamath River Revised Natural Flow Study

Matt Bromley
Blake A. Minor
Christopher Pearson
Christian Dunkerly
Charles Morton
Justin L. Huntington

August 2024

Publication No. 41XXX

Prepared by

Division of Hydrologic Sciences, Desert Research Institute

Prepared for

U.S. Bureau of Reclamation

THIS PAGE LEFT INTENTIONALLY BLANK

ABSTRACT

The Desert Research Institute (DRI) prepared this work as part of the Klamath River Revised Natural Flow Study (KRRNFS). In 2020 as part of the Klamath Basin Science Initiative, the United States (U.S.) Department of the Interior (DOI) tasked Reclamation with estimating refined natural streamflow estimates throughout the Klamath River Basin in a comprehensive NFS. For the NFS, we define natural streamflow as the streamflow that would have occurred in the absence of land use changes (agriculture, forestry, etc.), major development (roads, railroads, municipalities, etc.), and water management (dams, hydroelectric plants, etc.). This study aims to advance science in the Klamath River Basin, and thereby support future analyses and studies throughout the basin. Primarily, the KRRNFS leverages current science, data, methods, and tools to develop revised natural streamflow estimates for the Klamath River Basin, while improving upon limitations of previous estimates (Reclamation, 2005; Hardy & Addley, 2006) and incorporating comments provided by the National Research Council (NRC) (2008). The resulting natural streamflow estimates may be of use in habitat studies, drought planning, and water supply allocation decision making.

This report describes the Evapotranspiration task to support the KRRNFS with the development of annual estimates of 1) actual ET (ET_a), effective precipitation, and net ET for croplands, 2) ET_a and net ET for wetlands, 3) groundwater ET (ET_g) from phreatophyte shrubland vegetation. This work included the development of numerous supporting and derived geospatial datasets describing irrigated area, irrigation system type, and cropland field boundary extents. These datasets are fundamental for quantifying the hydrologic budget, consumptive water use, and model boundary conditions that will support conceptual and numerical modeling activities being conducted by the Bureau of Reclamation's Technical Service Center (TSC) and the USGS to arrive at daily naturalized streamflow estimates in the Klamath River Basin over water years 1981–2020.

This work improves on previous analyses which relied on assumed or static rates of ET and effective precipitation, through the application of the best available science which combines cutting-edge cloud-computing, manually-edited agricultural field boundaries depicting the maximum irrigated extent, long-term remote sensing data provided by Landsat (1985–2020), and daily calculations of meteorological conditions produced by gridMET (1979–2020). The produced data were dynamic over the period of study and represent real, on-the-ground conditions of the study area. The primary results from this effort are compiled into a series of field specific .csv files which are formatted for use in modeling and analysis using computer scripting languages. The data produced by the ET task may be aggregated to irrigation districts or to hydrologic units as suitable for analysis and implementation into the KRRNFS. The crop ET and effective precipitation estimates were provided for the purpose of estimating surface water irrigation deliveries. Irrigation delivery and wetland ET estimates are primary inputs in the development of natural streamflow estimates for the Klamath River Basin.

THIS PAGE LEFT INTENTIONALLY BLANK

CONTENTS

LIST OF FIGURES

LIST OF TABLES

LIST OF ABBREVIATIONS

AWC	Available Water Capacity
ASCE	American Society of Civil Engineers
BMM	Beamer-Minor Method
BR	Bowen Ratio
CDL	Cropland Data Layer
CDWR	California Department of Water Resources
CGDD	Cumulative Growing Degree Days
CI	Confidence Interval
CIMIS	California Irrigation Management Information System
CLU	Common Land Unit
CN	Curve Number
CONUS	Contiguous United States
CRS	Coordinate Reference System
CU_{irr}	Consumptive Use of Irrigation
DEM	Digital Elevation Model
DOQ	Digital Orthophoto Quadrangle
DRI	Desert Research Institute
EBC	Energy Balance Closure
EC	Eddy Covariance

EDF	Environmental Defense Fund
EFC	Effective Full Cover
EBR	Energy Balance Ratio
EROS	Earth Resources Observation and Science
ET	Evapotranspiration
ET_a	Actual Evapotranspiration
ET_c	Potential Crop Evapotranspiration
ET_g	Groundwater Evapotranspiration
ET_o	Grass Reference Evapotranspiration
ET_oF	Fraction of Grass Reference Evapotranspiration
ET_r	Alfalfa Reference Evapotranspiration
ET*	Normalized Actual Evapotranspiration
ET+	ET Plus
ETM+	Enhanced Thematic Mapper Plus
FAO	Food and Agriculture Organization of the United Nations
GEE	Google Earth Engine
GIS	Geographic Information System
GWIS	Oregon Water Resource Department's Groundwater Information System
HUC	Hydrologic Unit Code
KBAO	Klamath Basin Area Office
K_e	Soil Surface Evaporation Coefficient
K_{cb}	Basal Crop Coefficient
KRRNFS	Klamath River Revised Natural Flow Study
K_s	Stress Coefficient
LaSRC	Landsat Surface Reflectance Code
LEDAPS	Landsat Ecosystem Disturbance Adaptive Processing System
LST	Land Surface Temperature
MAE	Mean Absolute Error
MAD	Maximum Allowable Depletion
METRIC	Mapping EvapoTranspiration at high Resolution with Internalized Calibration
MSWE	Maximum Surface Water Extent
NAIP	National Agriculture Imagery Program
NASA	National Aeronautics and Space Administration

NCGDD	Normalized Cumulative Growing Degree Days
NDVI	Normalized Difference Vegetation Index
NIR	Near Infrared
NIWR	Net Irrigation Water Requirement
NLDAS	North American Land Data Assimilation System
NRCS	Natural Resources Conservation Service
NWI	Normalized Wetness Index
NWIS	U.S. Geological Survey's National Water Information System
NWR	National Wildlife Refuge
OLI	Operational Land Imager
OSIP	Oregon State Imagery Program
OWRD	Oregon Water Resources Department
PM	Penman-Monteith
PPT	Total Annual Precipitation
P_{rz}	Precipitation Residing in the Root Zone Available for Either Evaporation or Transpiration
PI	Prediction Interval
QA/QC	Quality Assurance and Quality Control
R^2	Coefficient of Determination
RF	Random Forest
RMSE	Root-Mean-Square Error
SEB	Surface Energy Balance
SCAN	Soil Climate Analysis Network
SSURGO	Soil Survey Geographic Database
STATSGO	State Soil Geographic Dataset
T_{30}	30-day Average Temperature
TM	Thematic Mapper
TSC	U.S. Bureau of Reclamation's Technical Service Center
USBR	U.S. Bureau of Reclamation
USDA	U.S. Department of Agriculture
USGS	U.S. Geological Survey
VI	Vegetation Index
WGS	World Geodetic System

WRS	Worldwide Reference System

THIS PAGE LEFT INTENTIONALLY BLANK

INTRODUCTION

The Desert Research Institute (DRI) prepared this work summarizing evapotranspiration (ET) as part of the Klamath River Revised Natural Flow Study (KRRNFS). In 2020, as part of the Klamath Basin Science Initiative, the United States (U.S.) Department of the Interior (DOI) tasked Reclamation with estimating refined natural streamflow estimates throughout the Klamath River Basin in a comprehensive NFS. For the KRRNFS, natural streamflow was defined as the streamflow that would have occurred in the absence of land use changes (agriculture, forestry, etc.), major development (roads, railroads, municipalities, etc.), and water management (dams, hydroelectric plants, etc.). This study aims to advance science in the Klamath River Basin, and thereby support future analyses and studies throughout the basin. Primarily, the KRRNFS leverages current science, data, methods, and tools to develop revised natural streamflow estimates for the Klamath River Basin, while improving upon limitations of previous estimates (Reclamation, 2005; Hardy et al., 2006) and incorporating comments provided by the National Research Council (NRC) (2008). The resulting natural streamflow estimates may be of use in habitat studies, drought planning, and water supply allocation decision making.

ET is the combined process of evaporation from soil and transpiration from vegetation. ET is the largest discharge component of the hydrologic budget and largest consumptive use of water diverted from the Klamath River (Figure 1). Therefore, quantifying ET from natural discharge and cropland areas is of primary importance in estimating and assessing naturalized streamflow in the Klamath River Basin. Annual and monthly ET from irrigated agriculture is primarily a function of water availability, atmospheric water demand, crop type, and vegetation conditions. The use of remote sensing data acquired from thermal and optical sensors on-board the Landsat series of satellites is ideal for quantifying multi-decadal ET estimates for native and agricultural vegetation given the field-scale and sub-monthly resolution of data and provides data continuity dating back to 1984. This report summarizes modeling and data processing steps specific to the ET analysis subtask of the KRRNFS. Additional details regarding ET data applications and incorporation in groundwater and surface water modeling components can be found within the respective subtask reports.

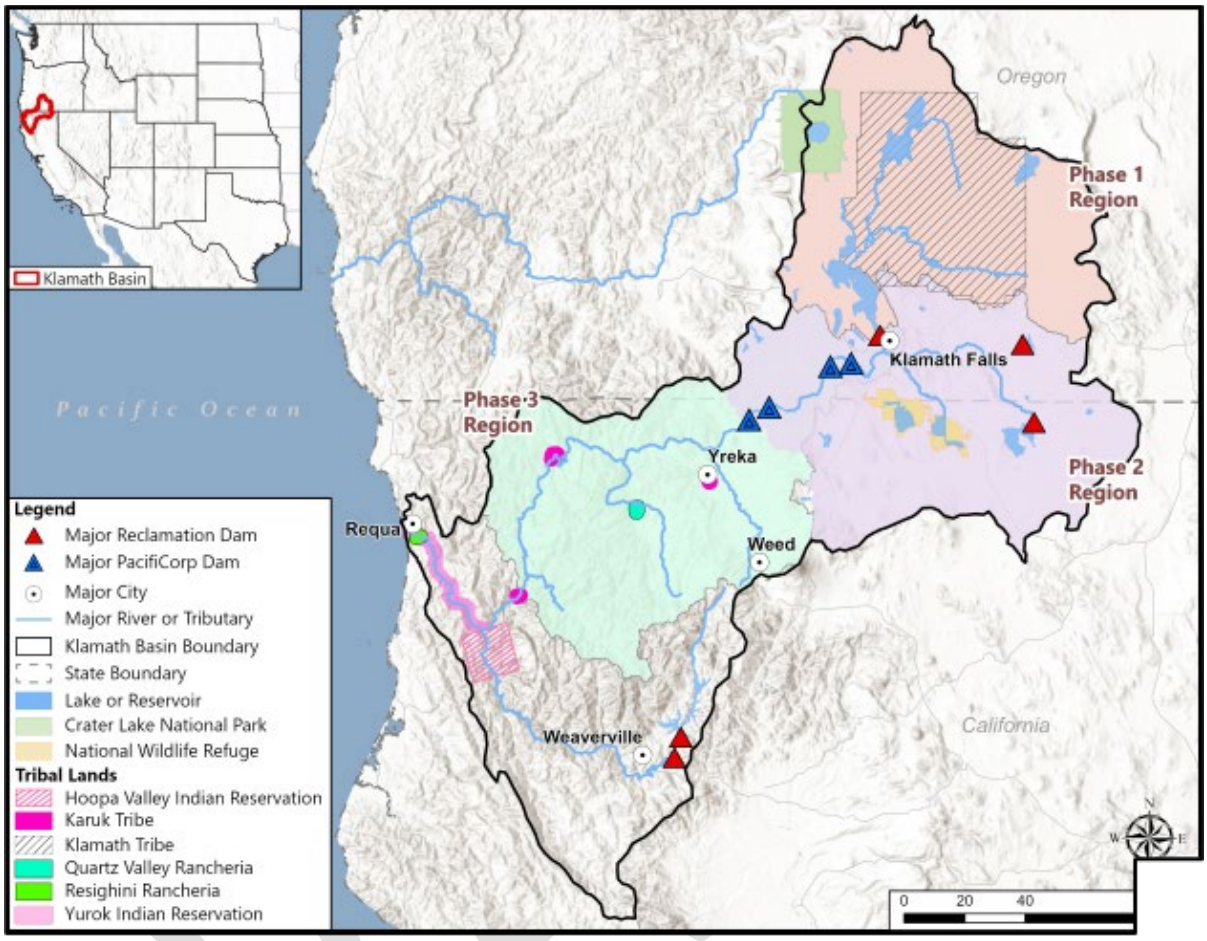

Figure 1. Geographical extent of project phases in the Klamath River Revised Natural Flow Study (KRRNFS). Image provided by USBR.

Basin Description

The Klamath River flows west from its headwaters near Crater Lake in southern Oregon to its outflow at the Pacific Ocean in northern California. The Klamath River Basin has a diverse environment, spanning multiple distinct climate zones and ecological habitats, and is typically divided into two portions: Upper and Lower Klamath Basins. The Upper Klamath Basin (UKB) drains all catchments above the location of Iron Gate Dam and is primarily in Oregon. Located in the rain shadow on the eastern side of the Cascade Mountain Range, this portion of the basin has an arid climate. Vegetation within the UKB is primarily drought-tolerant trees, such as lodgepole and ponderosa pines, along with shrubs, grasslands, and even wetlands in the lower elevations and near lakes. However, despite its aridity, the UKB features Oregon's largest natural lake by surface area—Upper Klamath Lake (UKL)—extensive wetlands, abundant wildlife, and widespread urban and agricultural development. The Lower Klamath Basin (LKB) consists of the catchments below the location of Iron Gate Dam and is primarily California. In contrast, located in the Pacific Coastal Range, the LKB receives ample rainfall. The LKB is well forested by a palette of northern California and Pacific Northwest conifers and hardwoods. While the LKB has no major natural lakes and less urban and agricultural development than in the UKB, it is home to the federally

recognized tribal lands of multiple Native American Tribes. The Klamath River was historically home to multiple thriving fish populations, including: Lost River and shortnose suckers, bull trout, and chinook and coho salmon (Guertin, 2022).

Indigenous people have inhabited the Klamath River Basin since time immemorial (Beckham, 2006). Presently, the basin is home to six federally recognized Native American Tribes: the Yurok Tribe; Hoopa Valley Tribe; Karuk Tribe; the Klamath Tribes, comprised of Klamath, Modoc, and Yashookin; Quartz Valley Indian Community; and Resighini Rancheria (77 FR 47868). Numerous additional native groups that are not federally recognized, such as the Shasta people, inhabit parts of Northern California and Southern Oregon. Although they are not federally recognized, some have been inducted into the Karuk Tribe (Beckham, 2006). The Klamath River and canyon and many of the fish species throughout the basin are considered sacred by the native tribes and have played a critical role in their survival and cultural identity (Bureau of Land Management, 1990). Management practices of native people left much of the natural landscape unchanged prior to non-native settlement.

Early non-native settlers began entering the region in the early 1800s and focused on agricultural production, including farming, fishing, and ranching. The abundance of large, flat, grassy meadows with lakes and marshy areas to provide water encouraged the expansion of grazing in the UKB (Stene, 1994). In 1905, Congress authorized Reclamation to begin the Klamath Project, a federal irrigation project designed to locate and contract irrigation networks designed to support productive agricultural communities. The Klamath Project was unique to other federal-sponsored projects in the arid west due to the nature of the landscape. Rather than transform arid lands into farmlands, Reclamation sought to drain the wetlands located around the natural lakes—Upper Klamath Lake (UKL), Lower Klamath Lake (LKL), and Tule Lake—and transform them into reclaimed agricultural lands. To accomplish this vision, over the next 20 years Reclamation constructed a complicated system of diversion canals, dams, and drainage canals to facilitate this alteration of the basin. In addition to the Klamath Project, with the arrival of the railroad in 1909, timber harvesting activities grew in the basin.

Land use, development, and water management practices directly impacting the UKB and affecting the flow regime and ecology of the LKB have greatly altered the Klamath River Basin from its natural state. While once the third most productive salmon run on the West Coast, fish populations in the Klamath River have dwindled and include multiple Federally listed endangered species. The current streamflow regime is significantly altered from the natural streamflow regime that would exist without the above-mentioned changes to the basin.

Project Purpose and Overall Approach

The KRRNFS study aims to both improve upon previous estimates of unimpaired streamflow (Reclamation, 2005; Hardy et al., 2006) and incorporate comments provided by the NRC (2008) on those estimates. The NFS uses current science, methods, and tools to develop revised natural streamflow estimates for the Klamath River Basin. To this end, we estimate streamflow for both pre-development and current conditions:

- Pre-development Conditions – the landscape and hydrologic conditions that existed in approximately 1900, prior to major development of the region for irrigated agriculture, forestry, and other purposes.
- Current Conditions – the landscape and water demand conditions throughout the past four decades, as a result of land use, development, and water management practices.

Although natural streamflow is often defined as that which would occur in the absence of human intervention, we define natural streamflow estimates as that which would occur under pre-development conditions in approximately 1900. While development prior to 1900 included minor diversions and irrigation of small portions of the watershed (Stene, 1994), historical documentation suggests that these had overall a small impact on the natural hydrologic system. Through use of multiple models and mass balance techniques, we remove the effects of existing development from the observed streamflow records for 1981 to 2020 to develop daily estimates of natural streamflow.

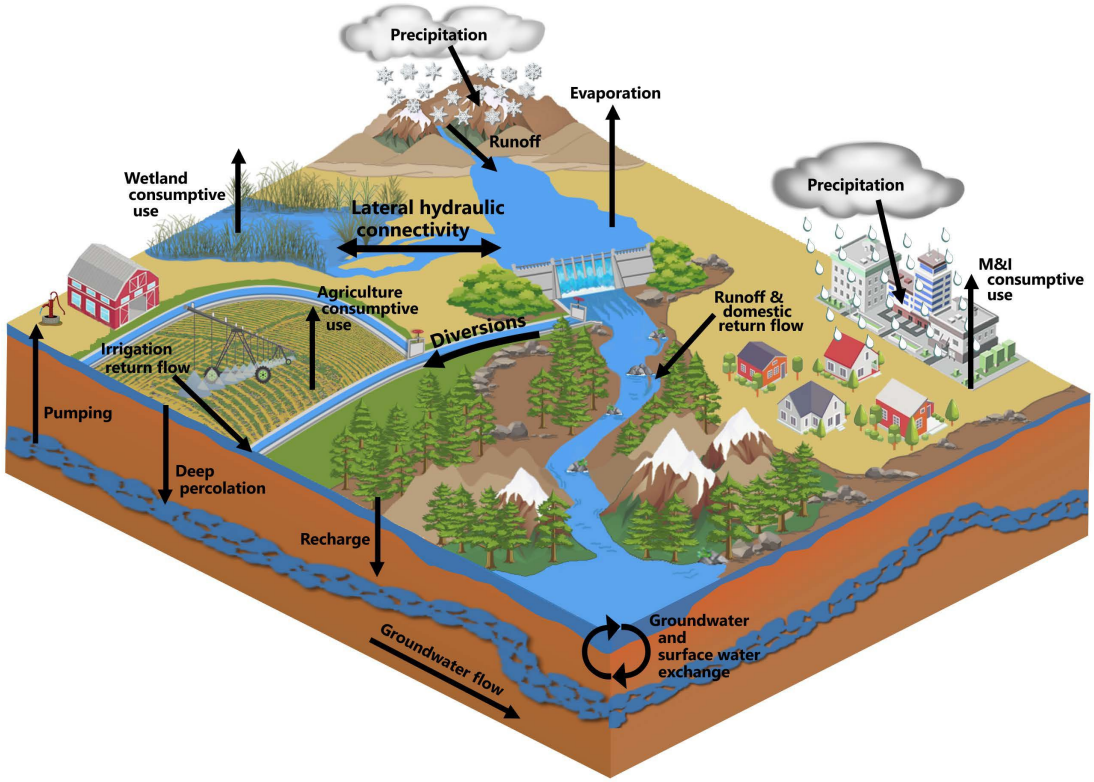

Figure 2. Conceptual diagram of the models and data needed to develop natural flow estimates for the Klamath Basin. Image provided by USBR.

The NFS evaluates both pre-development and current conditions by integrating six numerical modeling components (Figure 2) through implementation of a mass balance model in RiverWare. These components are interconnected:

1. Surface hydrology modeling quantifies distributed precipitation recharge. The groundwater model uses this distributed precipitation recharge output.
2. Groundwater modeling simulates groundwater conditions and estimates groundwater levels, groundwater storage, pumping, groundwater recharge from deep percolation of irrigation, interception of groundwater by drains, evapotranspiration from groundwater, and subsurface flow. In the LKB, groundwater modeling focuses on groundwater and surface water interactions in the Scott and Shasta River basins. The mass balance model uses the groundwater model output for baseflow to streams and seepage to and from lakes and reservoirs.
3. Consumptive use modeling estimates net evapotranspiration (ET) (ET subtract effective precipitation), deep percolation of irrigation water to groundwater, and ET estimates for groundwater dependent vegetation. Multiple other models use the resulting ET estimates, including groundwater (e.g., ET discharge and deep percolation recharge are connected to the groundwater model), surface water (e.g., consumptive use estimates are used to calibrate the surface hydrology model), and mass balance (e.g., consumptive use demands met by surface water are key inputs to the mass balance model).
4. Open water evaporation modeling quantifies evaporation rates from lakes and reservoirs. The mass balance and surface water models use these evaporation rates as a component in modeling the mass balance of lakes and reservoirs (current condition only) and calibration, respectively.
5. Hydraulic modeling quantifies the natural storage capacities, hydraulic controls, and interconnectedness of rivers, lakes, and wetlands in the basin. The mass balance model uses resulting hydraulic information to represent surface flow exchanges from the Klamath River to and from the Lost River basins, and the open water evaporation model uses resulting estimated average lake/reservoir depths through use of digital elevation models.
6. Mass balance modeling incorporates streamflow observations, direct output from the other models (e.g., baseflow contributions to streams, evaporation from lakes, etc.), hydraulic controls, lake and reservoir capacities, and physical features of the river system, to estimate natural streamflow at specific locations. Together, the mass balance model aims to quantify pre-development era streamflow by accounting for changes in hydrologic inputs and losses contributing to flow at identified locations.

For the NFS, the study area was divided into three geographic regions, referred to as "phases" (Figure 1). UKB was split into two phases: Phase 1 includes all inflows to UKL such as the Wood River, Sprague River, and Williamson River, with the downstream boundary at Link River Dam; and Phase 2 includes the UKB between Link River Dam and Iron Gate Dam. Phase 3 includes most of the LKB, encompassing the contributing areas downstream of Iron Gate Dam to the Klamath River upstream of its confluence with the Trinity River.

This report describes estimates of ET for all modeling phases of the KRRNFS. Other modeling reports and geographic extents will be published upon completion. Once all modeling components are complete an overall report will summarize methods and findings for all components and geographical extents.

OBJECTIVES

The objective of this study was to collaborate with the USBR to develop rates and volumetric estimates of 1) ET_a and net ET (ET less effective precipitation) from agricultural, 2) ET_a and net ET from wetlands, and 3) the groundwater component of ET (ET_g) from phreatophyte shrublands. This process included development of numerous supporting and derived geospatial datasets such as irrigated area, irrigation system type, cropland field boundary extents, and applied water through time to support the KRRNFS. ET, net ET, and supporting geospatial datasets characterize fundamental components of the hydrologic budget and will support conceptual and numerical hydrologic modeling activities being conducted by the Bureau of Reclamation's Technical Service Center (TSC) and the USGS (Figure 3). More specifically, estimates of net for agricultural lands will be used to estimate surface water irrigation deliveries in areas where in situ observations are limited to main canals. Irrigation delivery and wetland ET estimates are primary inputs in the development of the Klamath River Basin natural streamflow estimations.

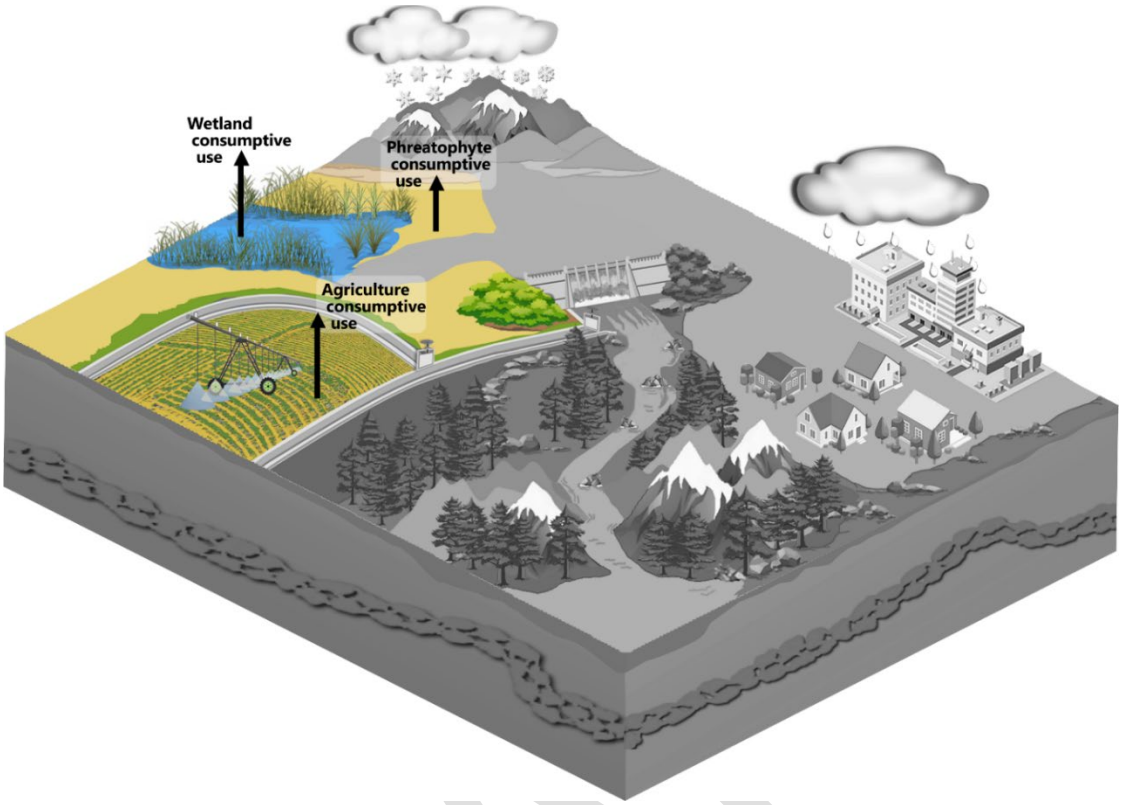

Figure 3. Conceptual diagram of the hydrologic cycle within the Klamath River Basin, with emphasis on the ET components of the KRRNFS. Image provided by USBR.

APPROACH

The general approach of this study combines remotely sensed ET with soil water balance derived effective precipitation estimates to summarize ET and net ET (ET minus effective precipitation) for agricultural, phreatophyte shrubland, and wetland vegetation throughout the Klamath Basin from 1980–2020. Several spatial datasets including agricultural field boundaries, crop and landcover type, irrigation status, and system type were also developed to support spatial ET and net ET summaries and surface and groundwater modeling workflows. The satellite surface energy balance (SEB) model Mapping EvapoTranspiration at high Resolution with Internalized Calibration (METRIC) (Allen et al., 2007) was used to estimate 30-meter resolution maps of monthly ET from 1985–2020 for agricultural and wetland areas. More specifically, monthly ET estimates were produced using the OpenET platform (Melton et al., 2022) which runs an implementation of METRIC (eeMETRIC) with automated calibration (Allen et al., 2013; Morton et al., 2013) within the Google Earth Engine (GEE) cloud computing platform (Gorelick et al., 2017). Because satellite-based ET includes ET derived from precipitation, the portion of precipitation that is "effective" or contributes to ET must be subtracted to estimate net ET or depletion (Bos et al., 2009). Net ET estimates ultimately serve as the foundational data for estimating irrigation application rates, irrigation withdrawals, and Net Irrigation Water Requirements (NIWR) (Jensen and Allen, 2016; Allen et al., 1998). In agricultural areas, net ET is equivalent to the consumptive use of irrigation water (CU_{irr}), while in groundwater dependent ecosystems,

such as phreatophyte shrublands and wetlands, net ET is equivalent to groundwater ET (ET_g). For this work, researchers used the crop consumptive use model, ET Demands, to estimate effective precipitation in areas of irrigated agriculture. ET Demands effective precipitation was then subtracted from eeMETRIC ET_a to estimate agricultural net ET (i.e., CU_{irr}).Similar combinations of satellite-based ET and ET Demands effective precipitation have been used in the Upper Colorado River Basin and the State of Oregon in support of agricultural consumptive uses and losses modeling and reporting (Huntington et al., 2022; Huntington et al., 2024, in review). Unlike agricultural areas, nearly all precipitation in both phreatophyte shrubland and wetlands areas is effective and consumed by ET (i.e., no losses to runoff or deep percolation). Wetland net ET estimates were developed as eeMETRIC monthly ET_a less total precipitation. Last, to avoid known issues with SEB modeling in lower ET, sparsely vegetated areas, ET_g from phreatophyte shrublands was estimated directly using the Beamer-Minor method (BMM) based on satellite imagery, vegetation indices, precipitation, reference ET, and micrometeorological-based ET estimates. Databases, summaries ET, net ET, precipitation, effective precipitation, and metadata from this work are documented and available for use in the KRRNFS but may be applicable to related studies. The combined outputs from study modeling and databases are intended to be used as input to surface water and groundwater modeling efforts to simulate and assess pre-development natural streamflow estimates for the Klamath River.

METHODS

Boundary Digitizing and Attribution

To meet project requirements, agricultural field boundaries depicting the maximum irrigated extent of all agricultural lands within the Klamath River Basin were developed to produce field-level monthly and annual spatial summaries ET, net ET, and related attribution for all irrigated lands within the KRRNFS area for the entire period of study. Areas of wetland and phreatophytic vegetation were similarly digitized to create summaries of ET for these areas of natural landcover.

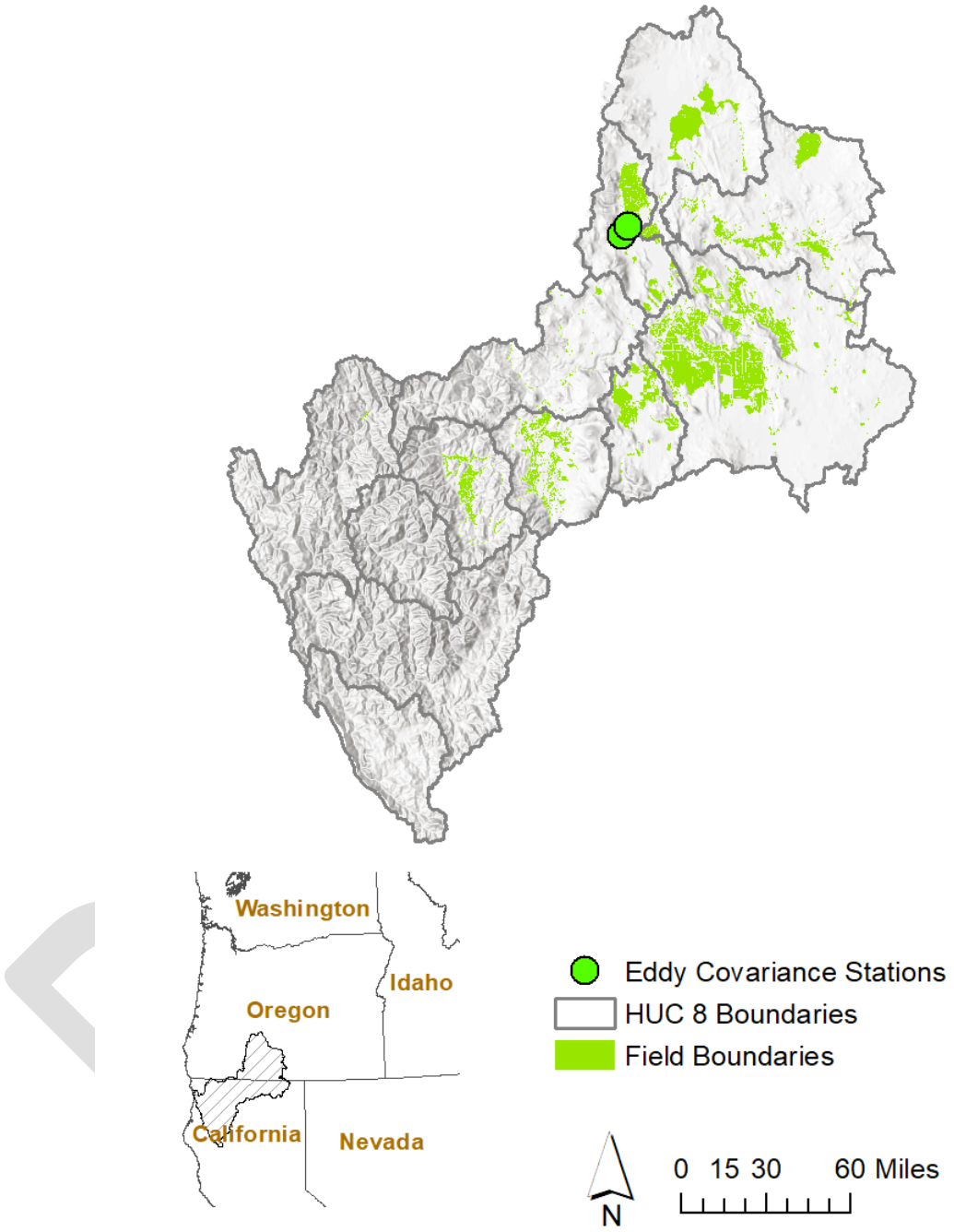

Figure 4. Study area of KRRNFS, Hydrologic Unit Code (HUC)-8 basins, agricultural field boundaries, and eddy covariance stations used for assessing remote sensing data.

Field Boundary Digitizing

A single dataset of field boundaries for all agricultural lands within the Klamath River Basin was developed and digitized at the 1:2,500 scale within Geographic Information Systems (GIS) software in collaboration with TSC and Oregon Water Resources Department

(OWRD). Field boundaries were developed to represent the maximum extent of actively irrigated areas for the period of 1985–2020 (Figure 4). A compilation of existing field boundaries from California and Oregon were assembled, and aerial imagery, satellite data, and water right places of use spatial data were used to inform the extensive manual editing and creation of field boundary linework to represent the maximum irrigated extent of agriculture within the KRRNFS area. Extensive collaboration with USBR and Oregon Water Resources Department (OWRD) aided in the development and review of the field boundary dataset. Changes in field shapes, such as a square wheel-line irrigated field having changed to a center pivot irrigated circular field, were accounted for by digitizing adjoining change areas as separate features (e.g. circular area as one feature, and corners as separate features) so that individual field feature attributes could be summarized and assigned through time. Field boundaries were used to develop spatial summaries related to ET, effective precipitation, net ET, irrigated acres, and crop type, and were the primary dataset for calculating volumes of net ET.

Existing field boundary datasets adopted or modified for this study included the 2019 Crop Mapping Dataset developed by the California Department of Water Resources (CDWR) (California Natural Resources Agency, n.d.) and U.S. Department of Agriculture (USDA) Common Land Unit (CLU) dataset (USDA, 2008). While these datasets met spatial extent and scale requirements for this effort, neither dataset was developed to account for field boundary changes through time (annually), and boundaries did not sufficiently correspond to field extents observed in aerial and satellite imagery. Modifications were made by merging CDWR and CLU at 1:2,500 scale and manually editing using aerial imagery as reference. Imagery products were comprised of the National Agriculture Imagery Program (NAIP) (National Agriculture Imagery Program (NAIP), 2019) acquired from 1995 to 2018, USGS Digital Orthophoto Quadrangle (DOQ) (Earth Resources Observation and Science (EROS) Center, 2017) acquired from 1993 to 2000, and Oregon Statewide Imagery Program (OSIP) (*State of Oregon: Oregon Geospatial Enterprise Office – Oregon Statewide Imagery Program*, n.d.) acquired in 2018. Landsat derived Normalized Difference Vegetation Index (NDVI) images produced with GEE were used to visualize per-pixel maximum NDVI values for the period of July through October for 1985–2020 to identify areas that were irrigated for any portion of this period. This approach of using a combination of historical aerial and satellite imagery spanning multiple decades was important for accurately identifying irrigated lands that had been fully or partially irrigated, developed, or fallowed at different points in time over the study period.

Agricultural Field Attribution

The agricultural field geometries developed by DRI and TSC were populated with attributes relevant to analysis, using a variety of data sources. Attributes describing crop type were essential to the estimation of net ET, while irrigation system type attribution are necessary for assigning annual field scale irrigation efficiency which are used in the KRRNFS to model applied water. The data described below were attributed at the annual timestep, based on the data available.

Irrigation System Type

The irrigation system type for each agricultural field was defined to inform estimates of irrigation efficiency over time. Workflows used to identify irrigation system type and attribute to the individual agricultural field boundaries were developed with significant input and direction from the USBR Klamath Basin Area Office (KBAO), which applied local knowledge to develop a classification scheme, produce example images of typical system configurations, and provide a review of irrigation system attribution for select areas in the Klamath River Basin. GIS technicians from TSC were valuable in augmenting DRI staff in the attribution of irrigation system type.

The irrigation system type was attributed based on high spatial resolution aerial images and expert knowledge of agricultural practices within the Klamath River Basin. Initial training provided by USBR in identifying irrigation system type was followed by the creation of internal training products and the organization of group-led training sessions; these efforts were subject to review and input by USBR staff. OSIP, NAIP and DOQ imagery were used as the primary input for this work, which resulted in all agricultural fields in the Klamath River Basin attributed using the irrigation system types described in Table 1.

Table 1. Classifications used to describe agricultural irrigation system type.

Irrigation Type	Description
0	Developed/No longer irrigated
1	Sprinkler-Pivot-Linear
2	Sprinkler-Other (Wheel Line, Hand Line, Solid Set, Big Gun, Travelling Gun, Pods)
3	Flood-Uncontrolled (Wild Flood) and No Apparent Irrigation Equipment
4	Flood-Controlled (Land Leveling, Borders, Basins, Furrows)
5	Micro (Micro Sprinklers, Drip Lines, Subsurface Drip)

Due to the limited availability of high-quality aerial images for years prior to 1995, irrigation system type was attributed at an annual timestep for the period of 1995–2020. For the purposes of the KRRNFS, irrigation system types were assumed to be static for the period of 1980–1995, and represented with the 1995 classification. This assumption was made with support by KBAO based on its observations that most sprinkler systems on the Project were installed post-1995.

Aerial imagery was not available for many years; therefore, changes in irrigation system type were attributed based on expert judgment. This judgment was most often applied when a change was observed between two images acquired in non-consecutive years. In these instances, the change in irrigation system type was assumed to occur approximately halfway between image dates (e.g., a field that was “2 – Sprinkler-Other” in 2005 but appeared as “1 – Sprinkler-Pivot-Linear” in 2009 was assigned a change in status in 2007).

Crop Type

Agricultural field boundaries were attributed with annual crop type classifications based on the USDA Cropland Data Layer (CDL) (Boryan et al., 2011). The CDL dataset is generally considered to be the most accurate crop type product available for field-scale annual crop type mapping for the contiguous United States (CONUS), with the most recent years of data achieving ~95% accuracy crop classification for major crop types (Zhang et al., 2020). The CDL dataset is based on statistical classification using crop type training data combined with Landsat imagery data, which results in a dataset that covers the CONUS at 30 m spatial resolution. Due to limitations in spectral and temporal resolution of Landsat data for some regions and time periods, it is common to have multiple crop type classifications within a single agricultural field of uniform crop type. Single crop type classifications for agricultural field boundaries were estimated and attributed based on the majority crop type within individual respective field boundaries. The attribution of crop type to the individual agricultural field boundaries is primarily used to specify crop type and parameters (e.g., rooting depth, maximum allowable depletion, crop coefficient curve) in the ET Demands model (refer to the ET Demands methods section below for additional details). Annual crop type information from CDL for the Klamath River Basin is provided by USDA from 2008-2020. For years prior to continuous data availability, the majority crop type classification between 2008 and 2020 was used.

Irrigation Status

Irrigation status rasters and field boundary summaries were derived from version 1.2 of the open-source IrrMapper model (Ketchum et al., 2020). IrrMapper uses a Random Forest (RF) modeling approach to predict four classes of "irrigated agriculture," "dryland agriculture," "uncultivated lands," and "wetlands" at annual time steps and at 30m spatial resolution across the Western U.S. IrrMapper was used in this study to produce annual rasters of irrigation classes from 1985–2020. Irrigation classes were simplified into two class values of "1," representing the irrigated class, and "0," representing the three intermediate non-irrigated classes. Field boundaries were attributed with spatially averaged binary irrigation class values at annual time steps and range from 0 to 1. A value of =>0.5 would indicate that more than half of the land contained within the field boundary was classified as irrigated.

IrrMapper irrigation status was not used to develop estimates of ET or net ET represented in this work, however these data were provided to TSC to assist in the analysis of annual patterns of irrigation activity. These data could be used to aggregate summaries of net ET at basin scale and serve as a reference in identifying agricultural fields which benefit from irrigation or shallow groundwater.

Phreatophyte and Wetland Mapping

Pre-development potential area of groundwater discharge boundaries (i.e. phreatophyte and wetland boundaries), were digitized in a GIS using a combination of georeferenced maps delineating the spatial extent of historical wetlands and phreatophyte vegetation (Figure 5) (Gannett et al., 1887; Lippincott et al., 1905; Humphreys & Reaburn,

1905; Bureau of Reclamation, 1908). Pre-development phreatophyte and wetland boundaries were then modified using a suite of datasets to account for contemporary land cover changes from agricultural development, water diversions, depth to groundwater, drainage of natural wetlands, and climate variability. Datasets that were used to develop the delineation of contemporary phreatophyte extents include groundwater level measurements acquired from the OWRD Groundwater Information System (GWIS) (https://apps.wrd.state.or.us/apps/gw/gw_info/gw_map/Default.aspx) and the USGS National Water Information System (NWIS) (https://waterdata.usgs.gov/nwis), digital elevation model (DEM), soils data from the Soil Survey Geographic Database (SSURGO)(USDA, 2017), high resolution aerial imagery from NAIP, Landsat-derived land surface temperature (LST) and vegetation indices, maximum surface water extent (MSWE) rasters for the Klamath Marsh (Kennedy, 2021), irrigated agriculture field boundaries, and a subirrigation potential map for the Sprague basin (Snyder et al., 2012). Depth to groundwater information was combined with NAIP and Landsat imagery to constrain the phreatophyte extents to lowland areas where the depth to groundwater was less than the phreatophyte limit of 50 to 60 feet below the ground surface (Robinson, 1958; Nichols, 1994) and areas that exhibited relatively cool surface temperature and higher vegetation vigor compared to adjacent xerophytic vegetation that commonly occupy piedmont slope areas. Landsat LST data is a primary dataset for mapping ET due to evaporative cooling effects that result from the conversion of liquid to vapor (Allen et al., 2007; Anderson et al., 2012). Agricultural fields and wetland polygons within pre-development and contemporary phreatophyte areas were masked and removed from VI-based ET_g estimation (Figure 6), with wetland ET estimated separately using eeMETRIC.

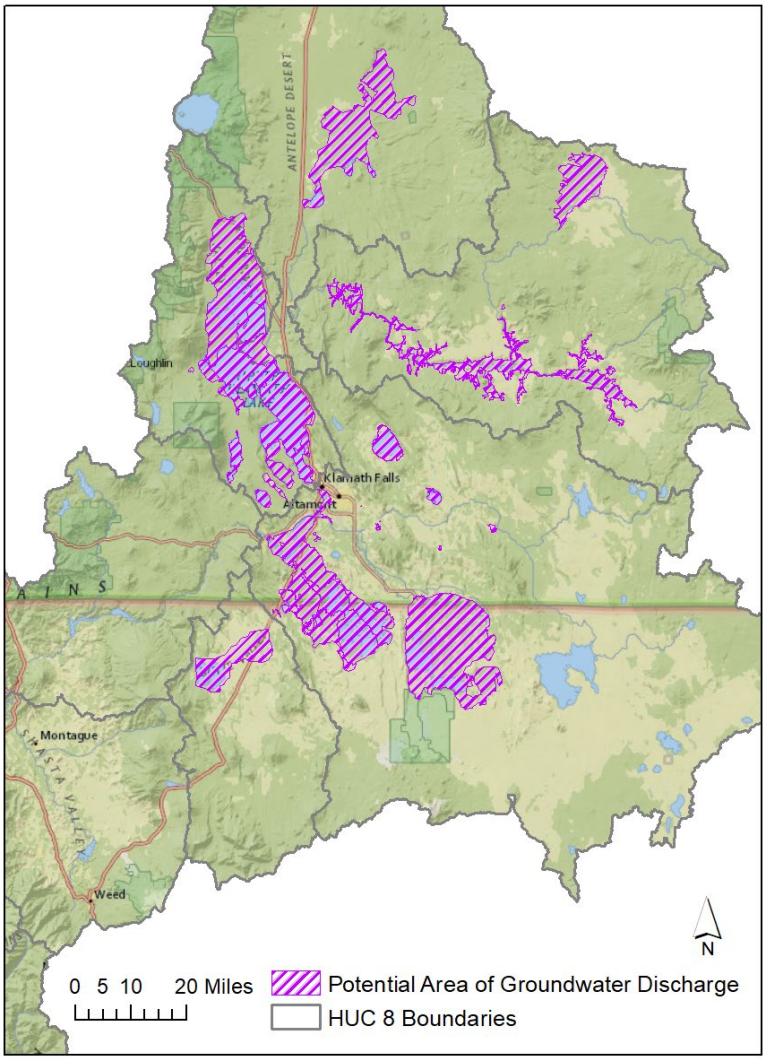

Figure 5. Pre-development potential area of groundwater discharge boundaries (includes phreatophyte vegetation, wetlands, and open water bodies within the KRRNFS area).

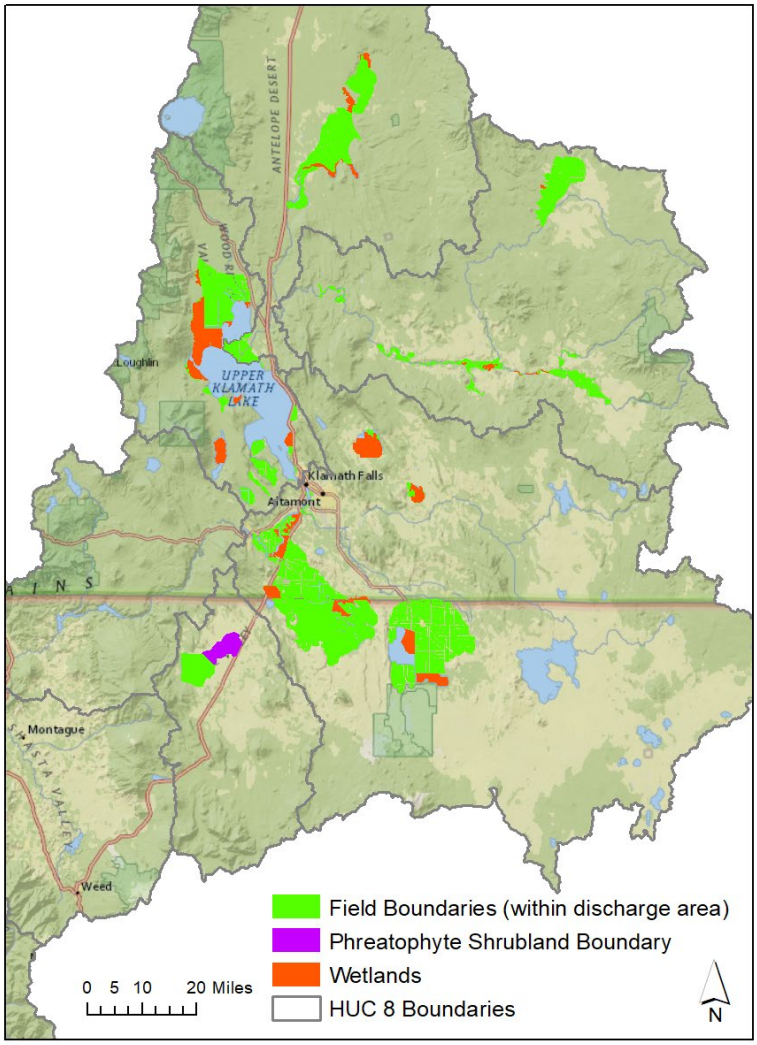

Figure 6. Contemporary phreatophyte shrubland boundary, wetlands, and agricultural field boundaries within the potential area of groundwater discharge. Note: some wetland areas are included in the field boundary dataset (e.g., Klamath Marsh, Lower Klamath Wildlife Refuge, and Sycan Marsh).

Weather Data and Reference ET

Historical weather and reference ET data used in this study were derived from the gridMET gridded weather dataset (Abatzoglou, 2013). gridMET is a daily ~4 km spatial resolution dataset providing estimates of near surface weather conditions for the contiguous United States (CONUS) from 1979 to present. gridMET combines spatial information from the Parameter-elevation Regressions on Independent Slopes Model (PRISM; Daly et al., 2008) with regional reanalysis data from North American Land Data Assimilation System (NLDAS-2) (Mitchell et al., 2004, Xia et a., 2021) to provide continuous, high-resolution estimates of minimum and maximum air temperature, relative humidity, solar radiation, wind

speed, and precipitation. The American Society of Civil Engineers (ASCE) Standardized Penman-Monteith (PM) equation (ASCE-PM) for a grass reference surface (ET_o) (Walter et al., 2000; ASCE-EWRI, 2005) served as a primary input for all ET estimates including actual ET (ET_a) from eeMETRIC, crop potential ET (ET_c) from ET Demands, and ET_g from the BMM (described in detail later).

The primary input data source for the gridMET dataset, NLDAS, does not account for irrigated areas and associated ET within land surface – boundary layer coupling processes (Ozdogan & Rodell, 2010). Even in highly advective arid environments, field-scale land surface-atmospheric feedbacks and boundary layer conditioning have been well documented in irrigated areas surrounded by water-limited areas; therefore, ET_o estimates based on ambient non-irrigated weather data (e.g., gridMET) require adjustment (Allen et al., 1983; Temesgen et al., 1999; Szilagyi & Schepers, 2014; Huntington et al., 2015). Both eeMETRIC and ET Demands models use gridded ET_o that was bias-corrected to local agricultural weather station calculations to account for known over-estimation of ET_o in irrigated areas by gridMET (Allen et al., 2021; Melton et al., 2022; Huntington et al., 2022). Unlike eeMETRIC and ET Demands, BMM empirical relationships rely on native gridMET ET_o estimates and therefore used non-bias-corrected ET_o directly from gridMET.

Data from agricultural weather stations used in the bias correction workflow were acquired from the USBR AgriMet program, California Irrigation Management Information System (CIMIS), and the Natural Resources Conservation Service (NRCS) Soil Climate Analysis Network (SCAN) (Figure 7; Supplemental Table 1). Extensive data quality assurance and quality control (QA/QC) was performed prior to processing and calculation of ET_o. Agricultural weather data were evaluated, filtered, and corrected using agweather-qaqc (Dunkerly et al., 2024), an open-source software developed DRI that processes and corrects data according to the recommendations of Allen (1996; 2008), ASCE-EWRI, and the Food and Agriculture Organization of the United Nations (FAO) guidelines (Allen et al., 1998; ASCE-EWRI, 2005). For example, solar radiation measurements were compared to theoretical limits of clear-sky solar radiation, and corrections were performed to ensure erroneous measurements due to dust or debris on the pyranometer window, non-level base plate, sensor miscalibration or drift, or obstructions were minimized (Allen, 1996).

The gridded bias correction factors were developed using QA/QC-ed agricultural station data across the western U.S., including those shown in Figure 7. The process for developing and spatially interpolating bias correction factors is briefly described below, and is similar to the approach of Pearson et al. (2021). Post-processed agricultural station data were used to calculate ET_o for each station, which was then compared with gridMET calculated ET_o using an open-source software package, gridwxcomp, developed by DRI (Volk et al., 2023a). Ratios of mean monthly station ET_o to gridMET ET_o were computed for respective stations to estimate mean monthly bias factors for each station. Station to gridMET ET_o bias ratios of mean monthly ET_o were then used to create monthly bias correction surfaces by interpolating between stations using a kriging approach. The resulting mean monthly bias correction surfaces were multiplied by respective daily gridMET ET_o estimates, resulting in bias-corrected ET_o estimates that are representative of irrigated agricultural weather conditions. Supplemental Table 1 lists agricultural weather stations used, with metadata, and mean monthly ratios developed using the gridwxcomp software and used for spatial interpolation within and surrounding the Klamath River Basin.

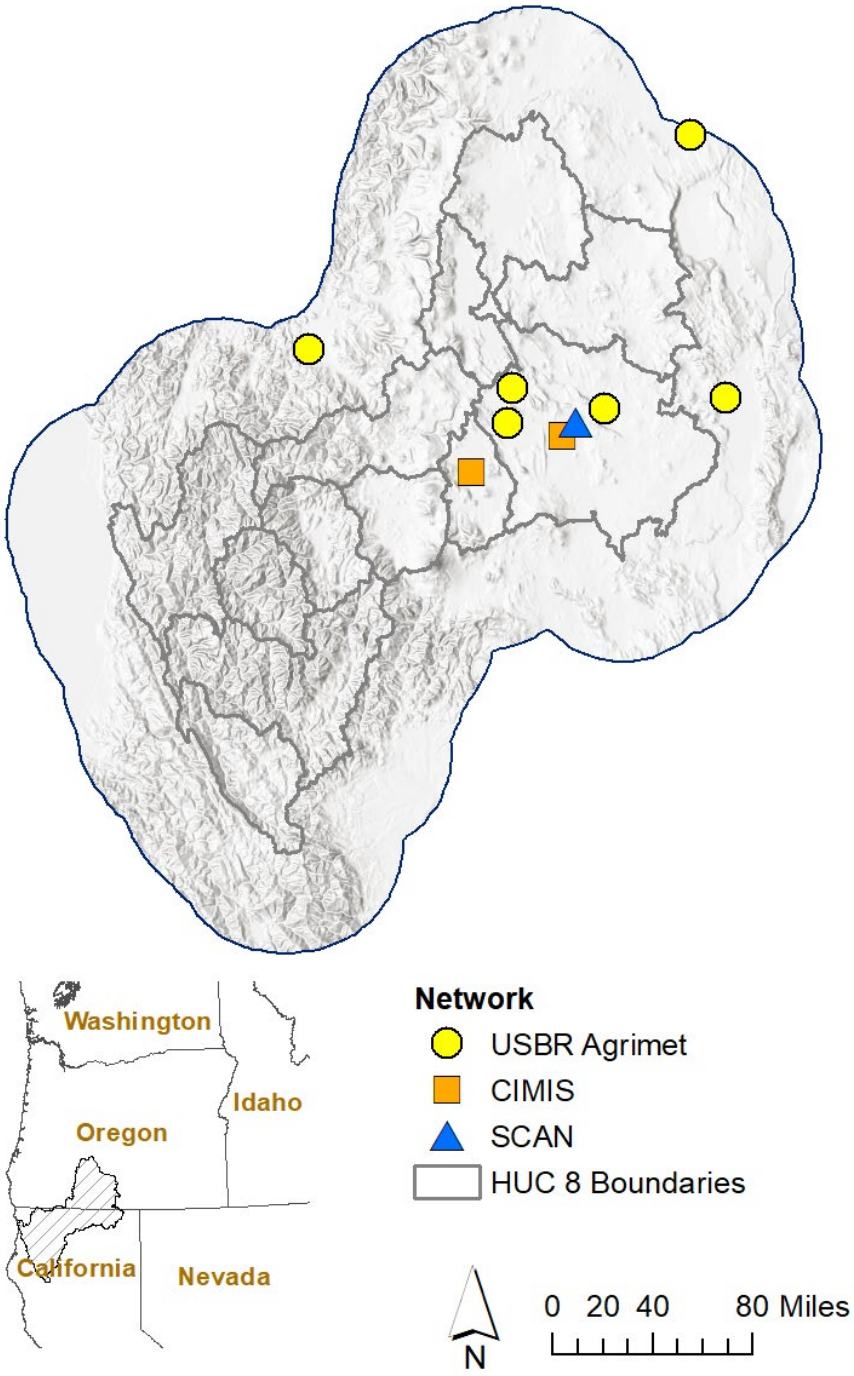

Figure 7. Distribution of agricultural weather stations within and near the Klamath River Basin that were used to produce OpenET reference ET bias correction surfaces used for bias correction of gridMET ET_o.

Non-reference ET variables used by ET Demands including temperature, wind speed, and precipitation were not adjusted to station observations. The ET Demands calibration routine internally compensates for bias in individual variables such as air temperature

impacts on phenology, while the reference ET bias correction compensates for overestimation of atmospheric water demand and ET estimates. Furthermore, gridMET precipitation was used directly for BMM ET_g, ET Demands effective precipitation, and wetland net ET estimates due to large uncertainty and known inconsistencies in station precipitation observations (Yang et al., 1998; Hanson et al., 2004). In support, Lundquist et al. (2019) found high-resolution atmospheric models such as PRISM (a primary input to gridMET) can better represent total precipitation across mountainous watersheds than observational gage networks.

ET Demands

The following text provides a brief overview of the ET Demands potential crop ET and daily soil water balance model used to estimate root zone effective precipitation (P_{rz}) for agricultural areas throughout the Klamath Basin. P_{rz} is the amount of gross reported precipitation less any surface runoff or deep percolation that resides in the soil and is available for consumption by evaporation or transpiration (Allen et al., 1998). While the primary variable of interest from ET Demands is P_{rz}, supporting variables (internal to ET Demands) such as ET_c, surface runoff, deep percolation, and NIWR are also discussed to provide additional information on model set-up, processing, and accuracy. KRRNFS ET Demands modeling supports irrigated agricultural net ET estimation. Non-irrigated, non-agricultural simulations produced by the ET Demands modeling workflow such as rain-fed agriculture, wetlands, and open water were not used in additional KRRNFS modeling tasks. Detailed documentation of the ET Demands model and previous applications are described in Allen et al. (2005), Allen and Robison (2009), and Huntington et al. (2015). Specifics related to the Python ET Demands software and application can be found at: https://github.com/usbr/et-demands.

At the core of the ET Demands model is the FAO-56 dual crop coefficient model (Allen et al., 1998) (Figure 8). The ET_c for each crop type was estimated at each gridMET cell (i.e., ET cell) using the FAO-56 dual crop coefficient equation:

$$ET_c = (K_s K_{cb} + K_e) ET_o \quad (1)$$

where ET_o is bias-corrected gridMET ASCE-PM grass reference ET, K_{cb} is the basal crop coefficient, and K_e is the soil surface evaporation coefficient. K_{cb} and K_e are dimensionless and range from 0 to 1.2 when used with ET_o. Daily K_{cb} values over a season, commonly referred to as the crop coefficient curve, represent the ratio of actual crop ET to reference ET as a function of vegetation phenology and growth stages through time. K_{cb} values can vary from year to year depending on the start, duration, and termination of the growing season, all of which are dependent on temperature during spring, summer, and fall periods. The stress coefficient (K_s) ranges from 0 to 1, where 1 equates to no water stress, which is generally the case for fully irrigated crops during the irrigation season as opposed to rain fed crops or native vegetation that commonly experience some water stress. A daily soil water balance is used for simulating available water within the root zone and to estimate K_s within ET Demands. K_s is generally 1 when computing ET_c for irrigated crops but can be less than 1 during winter when precipitation is low. ET Demands estimates of K_s during winter, for dormant covers of mulch and grass, can often be less than 1 since there is no irrigation specified for dormant non-growing season periods. A second daily soil water balance for the

upper 0.1 m of soil is used in ET Demands to estimate K_e. The upper 0.1 m zone is assumed to be the only layer supplying water for direct evaporation from the soil surface.

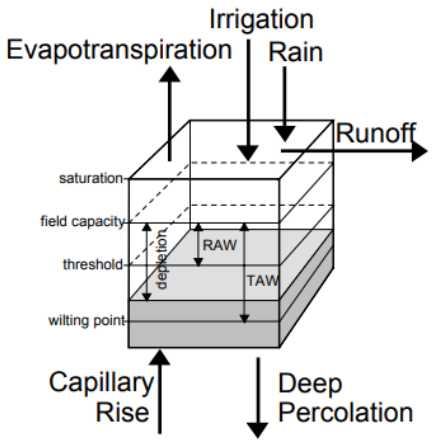

Figure 8. Conceptual diagram of the FAO-56 daily soil water balance used within ET Demands (modified from Allen et al., 2006).

The dual crop coefficient approach allows for separate accounting of transpiration and evaporation to better quantify evaporation from precipitation and simulated irrigation events. Separate accounting of evaporation and transpiration also allows for year-round simulation of wintertime soil moisture gains that often offsets irrigation requirements during the beginning of the growing season. Accounting for wintertime soil moisture gains and losses is important for accurate estimation of P_{rz} and the NIWR. The NIWR is defined as the amount of water needed in addition to precipitation to grow a non-water limited crop, otherwise known as the precipitation deficit, and is estimated within ET Demands as ET_c minus P_{rz}. Although P_{rz} includes precipitation that is later evaporated and possibly not transpired by the crop, ET_c includes evaporation of precipitation, therefore ET_c minus P_{rz} represents the NIWR rather than ET_c minus the P_{rz} portion that is effective toward transpiration only.

ET Demands Model Discretization

The KRRNFS area was divided into 4km grid cells (i.e., ET Cells) based on the gridMET weather dataset (Figure 9) (Abatzoglou, 2013). ET Cells included in this work were limited to those that contain irrigated croplands as defined by the field boundary dataset discussed in the "Methods" section. A total of 760 cells in the KRRNFS study area were used for extracting gridMET weather data, assigning crop types and soil properties, and parameterizing the ET Demands model across the KRRNFS area. 51 unique crop types were identified based on USDA CDL within agricultural areas of the KRRNFS from 2008–2020. For efficiency and model simplification, these 51 unique CDL classes were grouped into 8 common and unique crop types supported by ET Demands (Supplemental Table 2). Only those 8 common crop types contained in each individual ET Cell were simulated within the ET Demands model. Each ET Demands crop type is assigned crop specific parameters

related to ET and soil water balance modeling such as rooting depth, growing season timing, K_{cb} phenology, water consumption, maximum allowable depletion, and runoff curve number.

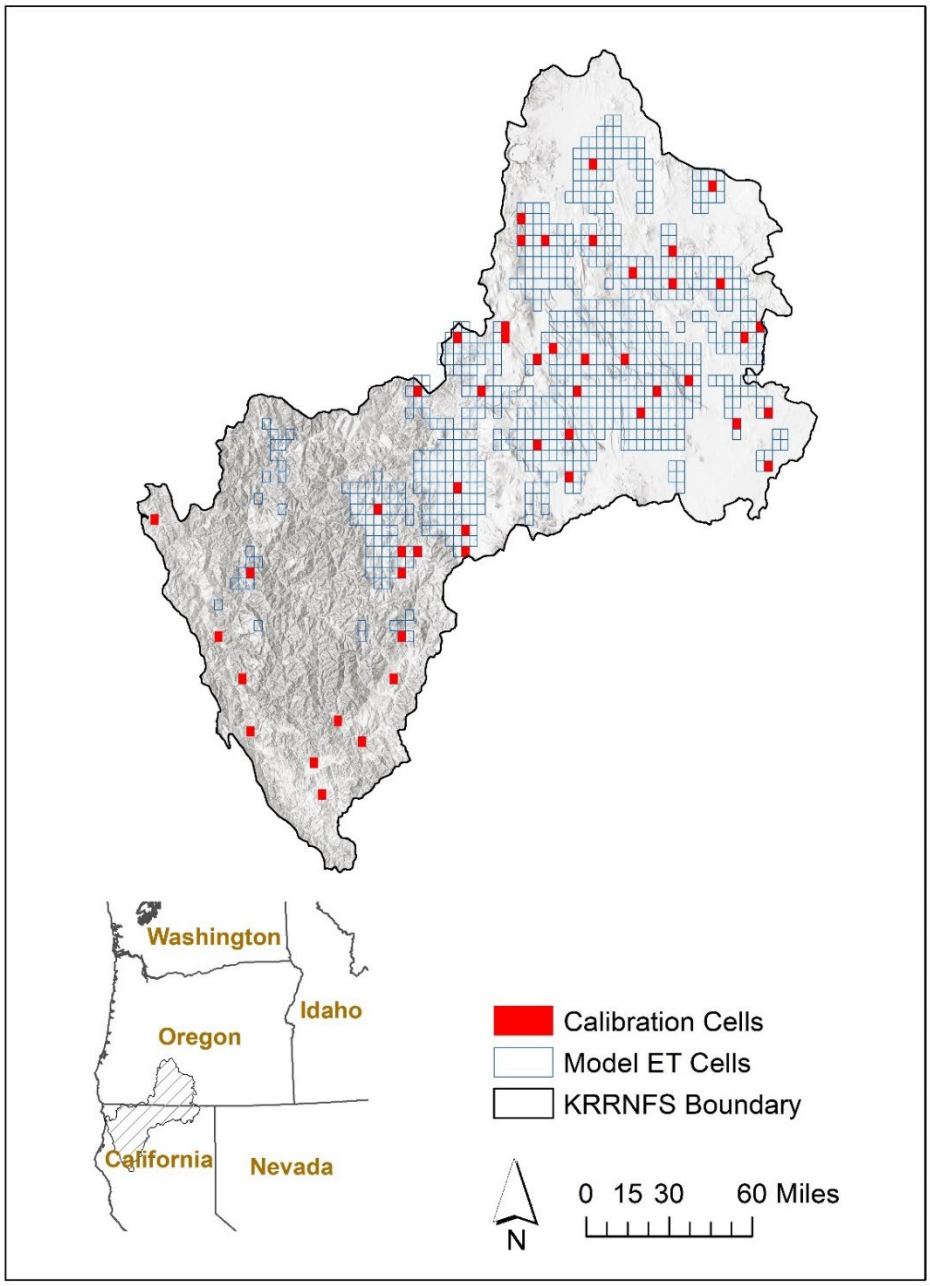

Figure 9. Distribution of ET Demands model grid and cells used to calibrate ET Demands crop parameters throughout the KRRNFS area.

Calibration cells distributed throughout the study area were used to control spatially varying crop parameters within ET Demands related to start, end, seasonal advancement of K_{cb} curves (discussed below), harvest, and senescence (Figure 9). Specific ET Demands crop parameters including 30-day average temperature (T_{30}), cumulative growing degree day (CGDD), timing to effective full cover (EFC) or termination, and killing frost were adjusted at each calibration cell to simulate observed and documented crop phenology. Calibrated crop parameters were then spatially interpolated throughout the study area using an inverse distance weighting approach. Calibration cells were selected throughout the study area to control for spatial differences related to climate, topography, and management. The use of spatially distributed climate time series data is an advancement over previous irrigation water requirement and ET Demands studies and enables more accurate representation of spatially varying crop phenology and water use than is possible using point weather station or coarse scale climate distributions.

ET Demands Soils Data and Simulated Runoff

Soil attributes required for ET Demands parameterization were obtained from the NRCS State Soil Geographic (STATSGO) database (USDA-NRCS, 1991). STATSGO is a spatial soils GIS database and contains physical soil attributes required to estimate soil water holding and infiltration parameters of the ET Demands dual soil zone and root zone water balance and runoff modules. STATSGO attributes of available water capacity (AWC) and sand, silt, and clay fractions were used to estimate spatial distributions of total evaporable water and readily evaporable water used in the surface soil layer water balance, and total available water and readily available water were used in the root zone water balance. These parameters affect the simulation of irrigation timing and depth, evaporation losses from soil, deep percolation from root zones, antecedent soil moisture, and simulated runoff from precipitation. Soil attributes for AWC and sand, silt, and clay fractions were averaged over 152-cm depths and were then intersected with irrigated crop land areas and spatially averaged and attributed for each ET Cell (Figure 10).

Runoff is simulated within ET Demands based on a modified version of the USDA-NRCS curve number (CN) approach (USDA-NRCS, 1998). The modified CN approach within ET Demands uses soil properties, crop type, daily precipitation depth, and soil water balance and antecedent soil moisture conditions within ET Demands. The CN hydrologic soil groupings were determined from spatially averaged percent sand, silt, and clay fractions over agricultural areas within each model grid cell in the study area. The CN hydrologic groupings of A, B, and C were estimated based on common percent composition thresholds: if sand is greater than 50% then the type is A, if clay is greater than 40% then the type is C, otherwise the type is B. Antecedent soil water content impacts the CN value due to the dependency of soil water content on unsaturated hydraulic conductivity and infiltration. To approximate soil water content effects, the CN value is adjusted according to the estimated soil water content prior to any precipitation. Adjustment of CN values is based on the approach of USDA-NRCS (1998) and Allen (1998) for dry (ASC I) and wet (ASC III) conditions. Expressions by Hawkins et al. (1985) are utilized within ET Demands to scale CN values in between dry and wet conditions according to antecedent soil water contents.

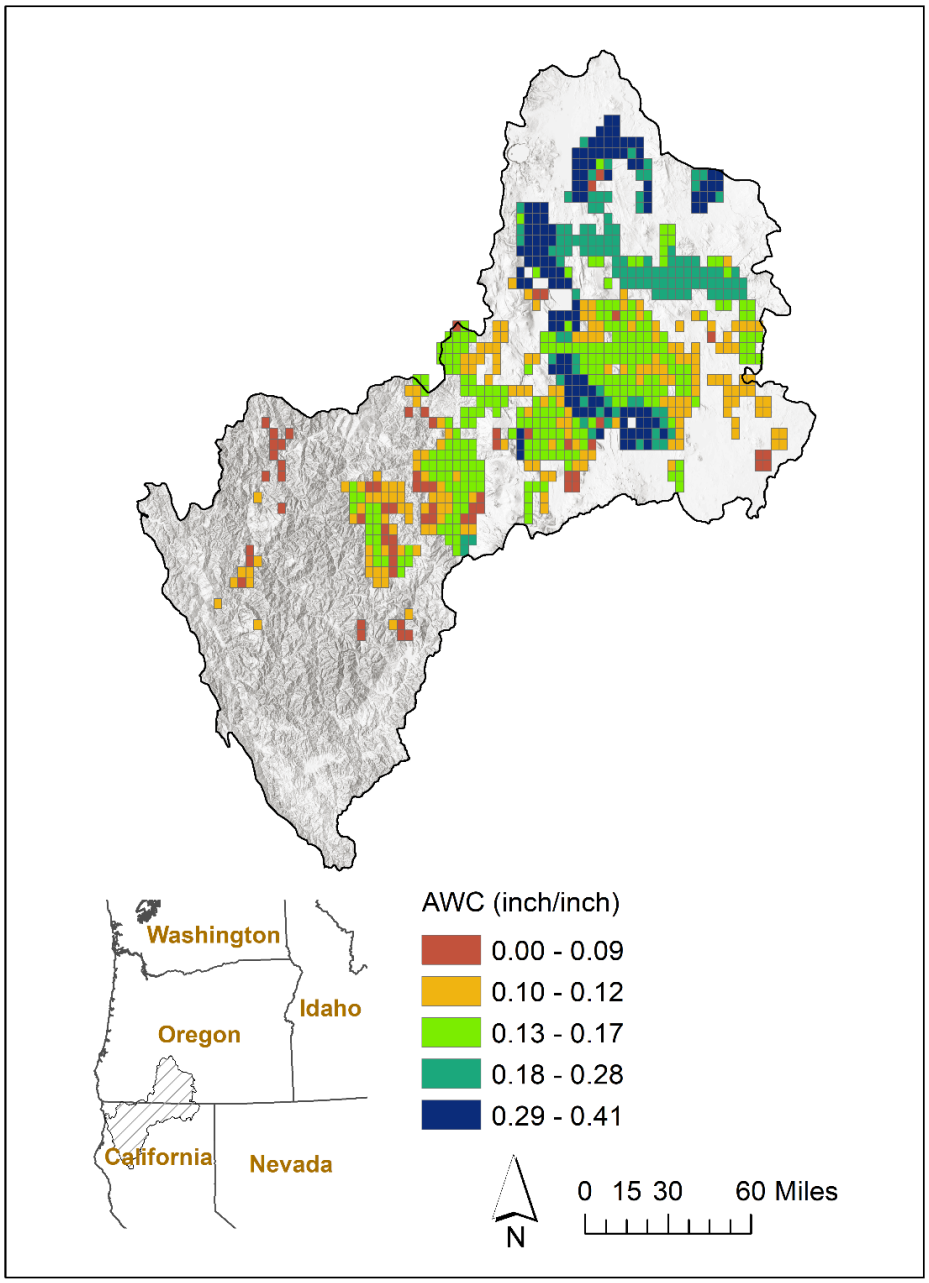

Figure 10. Distribution of KRRNFS area soil AWC from the STATSGO dataset.

ET Demands Crop Coefficients

For this study, K_{cb} curves outlined in Allen and Robison (2009) and Huntington et al. (2015) were adopted for the application of ET Demands. The Klamath NFS ET Demands model uses grass reference based K_{cb} curves congruent with ET_o values representative of irrigated areas and those used by eeMETRIC. The K_{cb} curves are primarily traceable to

lysimeter-based K_{cb} curves of Wright (1982, 2001) and Reclamation's AgriMet program. Three methods were used for simulating green-up, planting, EFC, harvest, and advancement of K_{cb} curves based on 1) normalized cumulative growing-degree-days (NCGDD) from planting or green-up to EFC, with this ratio extended until termination of the cropping period; 2) percent time from planting to EFC, with this ratio extended until termination; and 3) percent time from planting to EFC and then number of days after full cover to termination. These approaches allow for crop specific crop stage and temporal interpolation of K_{cb} curves to be a function of temperature, such as T_{30}, rather than specified or fixed calendar dates. Green-up and time to EFC is strongly impacted by short-term weather conditions, primarily by air temperature, soil temperature, and water availability. Planting dates for annual crops are affected by air temperature and soil temperature at seed depth. Because of these strong dependencies, thermal-based approaches such as CGDD are commonly used for defining planting and green-up dates, crop coefficient development and temporal interpolation, and transferring crop coefficients among regions (Sammis et al. 1985; Slack et al. 1996; Howell et al. 1997; Snyder et al. 1999; Wright 2001; DeTar 2004; Marek et al. 2006; Allen and Robison 2009). Functionality within ET Demands allows for variable timing of green-up, planting, EFC, harvest, and advancement of K_{cb} curves based on the weather and climate and offers increased accuracy in estimating potential crop water use given temporal and spatial climate variability. The simulation of temperature dependent growing season timing and crop development within ET Demands is a substantial improvement over traditional reference ET – crop coefficient applications and approaches that assume fixed dates and crop stages regardless of interannual climate variability.

ET Demands Model Calibration

The ET Demands model provides default crop coefficient and soil water balance parameters for each modeled crop type, however, calibration is needed to account for potential inaccuracies in climate and soils data, model components and assumptions (e.g., root depth and root growth functions, maximum allowable depletion (MAD) thresholds for simulated irrigations, antecedent soil moisture runoff CN function, etc.), and local management practices. Calibration of the 8 unique KRRNFS crop type parameters at 49 calibration cells located in agricultural areas throughout the basin (Figure 9) was primarily based on typical and documented dates of growing season start, full cover, harvest, and end of season information obtained from local sources and previous studies (USDA-NASS, 2010; Huntington et al., 2015; OSU-COAREC, 2023). In addition, Landsat derived NDVI time series were developed for select crops and fields across primary calibration cells using Climate Engine (Huntington et al., 2017), and were used to calibrate crop coefficient season length, phenology, and harvest parameters (Figure 11). NDVI provides a measure of vegetation vigor and is directly related to plant productivity (Cihlar, et al., 1991). Comparisons were performed between NDVI and ET Demands simulated K_{cb} curve phenology, and calibration parameters were adjusted to minimize differences in simulated crop phenology timing and stage. A comparison of NDVI and secondary calibration was not performed for all crop types and calibration cells and instead used to validate primary calibration based on typical and documented growing season and phenology dates and aid in calibration for areas where no information or local knowledge was available.

Crop specific parameters calibrated at defined calibration cells were spatially interpolated using inverse distance weighting throughout the model domain to account for spatial differences in temperature and crop phenology relationships as well as crop management. Spatially distributed calibration parameters were mapped to all ET Demands ET Cells and then used for calibrated ET Demands simulations. Figure 11 illustrates calibrated ET Demands model simulation of grass hay K_{cb} for a field near Copco Lake, CA, and shows generally good agreement between K_{cb} and Landsat NDVI. Green-up occurs in early April, reaching full cover in early June, and mid-season cutting occurs in early July, followed by grazing operations and reduced productivity for the remainder of the season. Similarly, Figure 12 shows Landsat NDVI and ET Demands simulated K_{cb} for an alfalfa hay field near Merrill, OR. ET Demands simulated K_{cb} growing season timing agrees well with Landsat NDVI, and observed alfalfa harvest dates are also simulated well.

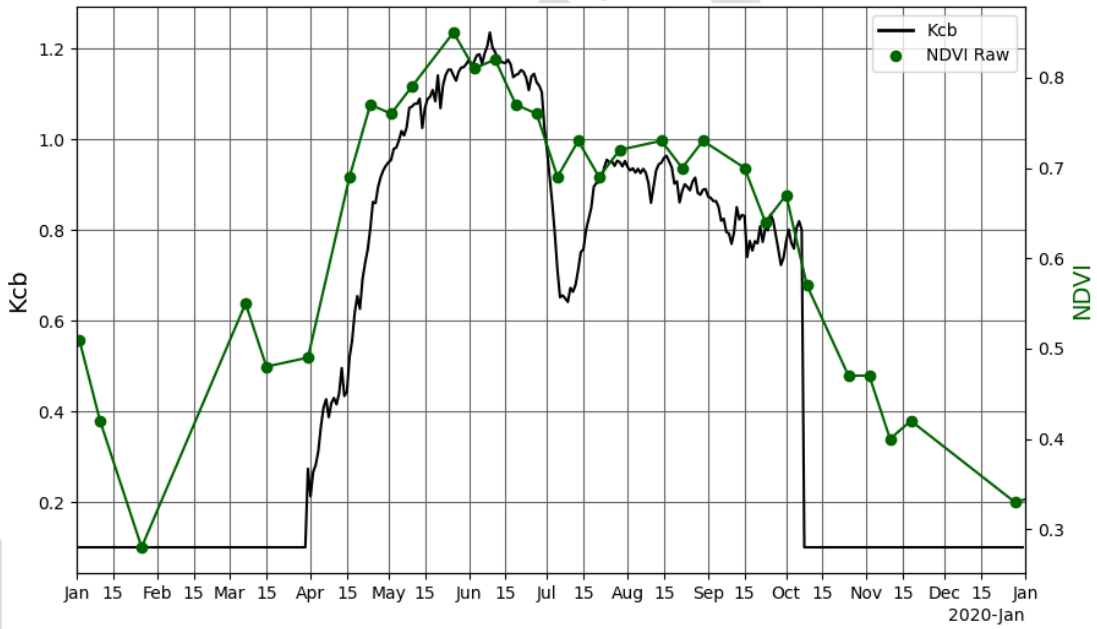

Figure 11. Time series comparison of Landsat derived NDVI and ET Demands simulated K_{cb} for grass hay crop in ET Cell 564161 near Copco Lake, CA.

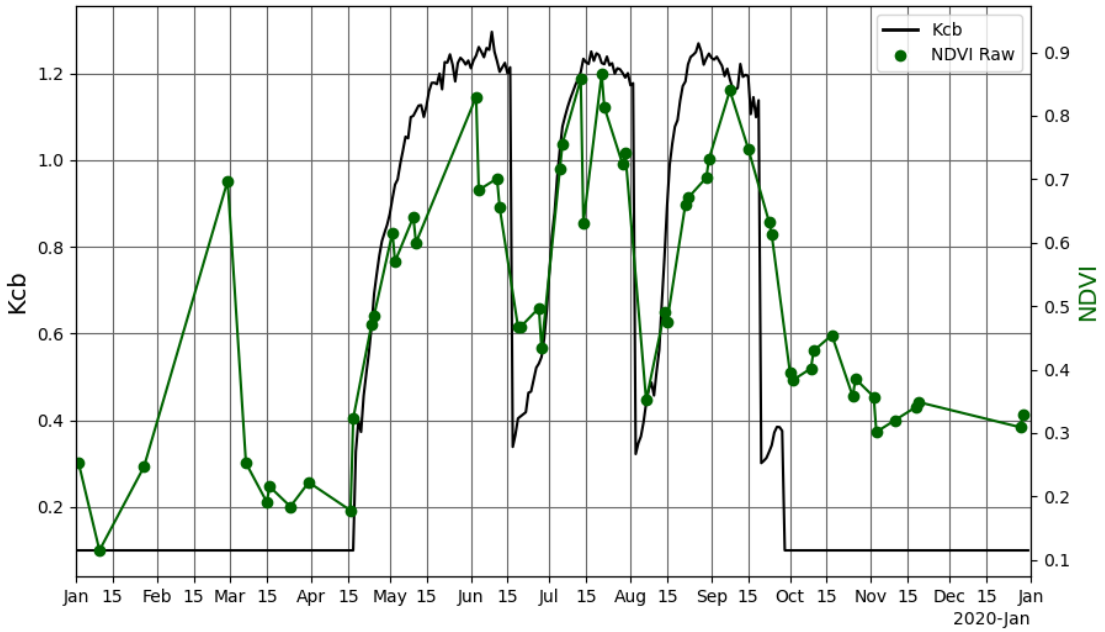

Figure 12. Time series comparison of Landsat derived NDVI and ET Demands simulated K_{cb} for alfalfa hay crop in ET Cell 565566 outside of Merrill, OR.

Variability in crop phenology within ET Demands is primarily a function of air temperature. For example, cooler spring temperatures will result in later green-up and slower crop development, while warmer temperatures will result in earlier green-up and more rapid progression to EFC and harvest. ET Demands calibration and simulated crop phenology patterns are weather and climate dependent and reflect general management practices, and therefore do not represent crop stages and phenology for all fields. Individual crops and fields will vary, sometimes to a large degree, due to crop management practices, weather, water shortage, crop stress and other factors. However, general agreement of simulated crop stage and phenology green-up and senescence timing improves accuracy of subsequent calculations such as P_{rz}, NIWR, and estimation of agricultural net ET through the combined use of ET Demands and satellite estimates of ET_a. Use of remote sensing ET models is needed to capture field scale spatial and temporal variability not obtainable with weather-based crop coefficient models such as ET Demands.

Agricultural and Wetland ET

eeMETRIC Produced with OpenET

ET_a for agricultural areas was estimated in this study using a combination of satellite data and reference ET. While traditional reference ET and crop coefficient approaches are useful for estimating ET_c under well-watered and stress-free conditions, satellite remote sensing approaches are currently the most feasible and accurate for estimating field-scale ET_a over large areas and time periods (Fisher et al., 2017; Anderson et al., 2012). OpenET is a cloud-based processing platform and web application developed to efficiently produce and access field-scale ET data over large areas using a combination of Landsat satellite and

gridded reference ET data (Melton et al., 2022). Landsat is ideal for field-scale ET_a estimation as it provides 30m resolution optical and thermal data at 8–16-day return intervals. Furthermore, Landsat's long-term data record since 1984 can observe spatial and temporal variations in crop phenology, water stress, and agricultural management practices (e.g., crop development and senescence, water shortage and deficit irrigation, harvests) (Tasumi et al., 2005; Cammalleri et al., 2014). OpenET estimates daily ET_a based on pixel-level temporal linear interpolation of ET_oF values for clear sky conditions, enabling time integration and summaries of monthly and annual ET_a estimates. More information on the background and methods of OpenET can be found at https://openetdata.org/methodologies/.

Detailed accuracy assessments of OpenET model ensembles at micrometeorological flux stations show good skill in predicting monthly ET_a for agricultural lands (slope=0.86-1.02, r^2=0.89-0.94, MAE=15.5-21.6 mm/mo, RMSE=20.9-27.4 mm/mo, n=1,307, stations=23) (Melton et al., 2022). Technical aspects of the OpenET initiative are being led by DRI, National Aeronautics and Space Administration (NASA), and university partners with in-kind support from GEE, and includes scientists and software engineers behind many of the most prominent and commonly used models for calculating ET from satellite and weather data. Given DRI's role in leading OpenET model integration, data production, and post-processing, use of the OpenET platform for historical ET_a data production was ideal for the 1985–2020 portion of the study period.

Of the 6 models included in OpenET, eeMETRIC was selected for estimating agricultural ET_a in this study for the following reasons: 1) local compute and cloud-based versions of METRIC have demonstrated consistent performance in estimating ET_a for croplands under well-watered and deficit irrigation conditions in similar semi-arid and arid environments (Huntington et al., 2018; Huntington et al., 2022; Volk et al., 2023c); 2) is widely used across CONUS and has been used in previous research and water management decisions in the Klamath River Basin (Allen et al., 2015; Cuenca, 2013; Snyder et al., 2012; Zhao et al., 2015); and 3) automated calibration and data production using GEE enables efficient, large scale assessment in space and time (Kilic et al., 2021; Allen et al., 2013).

The OpenET platform was used to execute eeMETRIC and daily time integration models across all Landsat images acquired over the study area for the period of 1985–2020. Monthly ET_a images at 30m spatial resolution were spatially averaged to all field boundary polygons to produce geodatabase attributes of field-scale ET_a. Monthly net ET was computed on an individual field level within the geodatabase by subtracting respective ET Demands monthly P_{rz} estimates from monthly ET_a estimates.

Deconfliction of Open Water Evaporation and Agricultural Evapotranspiration

Significant land use changes in the vicinity of Upper Klamath Lake took place during the period of July 2006 to November 2008 when agricultural lands on the Williamson River Delta were restored to wetland, thereby altering the configuration of the lake (Erdman, Hendrixson, and Rudd, 2011). This change in Upper Klamath Lake was accounted for by TSC in the open water tech memo (Mikkelson, 2023), which describes extents and rates of open water evaporation for the Klamath River Basin for the study period. The processes of ET and open water evaporation are similarly constrained by the atmospheric demand for water as described by reference ET (ET_o) and thus estimates of evaporation rates calculated with the Daily Lake Evaporation Model (DLEM) should be similar in magnitude to the ET

rates produced by eeMETRIC for these areas of wetland inundated with shallow water; however, it was necessary to minimize the spatial and temporal overlaps of calculated ET and open water evaporation.

Agricultural field boundaries developed for this study depict the maximum extent of agriculture within the basin for the period of study and were held static and fixed throughout the study period. These boundaries were frequently digitized using linear, manmade features such as roads, fence lines, and levies as reference. This use of levies in the creation of agricultural field boundary data resulted in the boundaries having good agreement with Upper Klamath Lake for the period of 1980–2006. To minimize the spatial and temporal overlap of estimates developed from the DLEM and eeMETRIC for the period following the restoration of the Williamson River Delta, field boundary summaries of eeMETRIC were post processed. Spatial statistics were performed to characterize the overlap in open water extents and individual agricultural field boundaries. For agricultural polygons that overlapped with TSC open water extents by ≥50% for a given period, ET and net ET for the associated periods were overwritten with zero values.

Pre-1985 ET_a

The modern archive of Landsat satellite data began in March of 1984, when the Landsat 5 satellite began acquiring regular optical and thermal observations of the Earth's surface. To estimate ET_a prior to the operation of Landsat 5, an analog approach was developed using monthly fractions of grass reference ET (ET_oF) (i.e., eeMETRIC derived crop coefficients) calculated for the period of 1985–2020, which were applied to year-specific ET_o. Bias-corrected gridMET ET_o data produced by DRI and OpenET from 1979–2020 provided consistent estimates of ET_o for the full study period. Monthly ET_a estimates for the pre-1985 period were calculated as follows:

$$ET_{a\ month\_of\_interest} = ET_oF_{analog\_month} * ET_{o\ month\_of\_interest} \quad (7)$$

where $ET_{a\ month\_of\_interest}$ is the analog estimated ET_a for the month of interest, $ET_oF_{analog\_month}$ is the month specific ET_oF from the analog water year, and $ET_{o\ month\_of\_interest}$ is the gridMET bias-corrected ET_o value for the pre-1985 month of interest. Analog ET estimates were computed at the field level within the geodatabase, based on spatially averaged ET_oF and ET_o values derived from eeMETRIC and bias-corrected gridMET data, respectively.

Analog months were identified and selected on a water year (Oct–Sept) basis using the Klamath Normalized Wetness Index (NWI) developed by Larry Dunsmoor of Confluence Resource Consulting (L. Dunsmoor, personal communication, August 17, 2022). The Klamath NWI provides information on relative water availability throughout the region using historical water level, streamflow, and precipitation information. Use of monthly ET_oF values from similarly wet years accounts for general patterns related to water availability for irrigation, while the use of monthly ET_o accounts for evaporative demands for the pre-1985 period. Table 2 provides a summary of the water year specific analog year assignments used to estimate monthly ET_a for the pre-1985 period. The monthly eeMETRIC data produced with OpenET begins in March 1984; however, spatial and temporal coverage of Landsat data

was limited from March through May of 1984 due to cloud cover and infrequent image acquisitions. To avoid data gaps during this period, a mix of analog and eeMETRIC field-level ET_a estimates were used. Similar to the post-1985 period, monthly net ET for the pre-1985 period was computed at the field level within the geodatabase by subtracting ET Demands monthly P_{rz} estimates from respective analog ET_a estimates.

Table 2. Water year and analog water year pairs identified based on the Klamath NWI and used for estimating field-level monthly ET_oF and ET_a for study years 1980–1985.

Water Year	Analog Water Year	Comment
1980	2001	Oct-Dec analog estimates; Jan-Sept 1980 not used in KNFS modeling
1981	2001	Oct-Sept analog estimates
1982	2006	Oct-Sept analog estimates
1983	1999	Oct-Sept analog estimates
1984	1999	Jan-Feb analog estimates; Mar-May 1984 (mix of analog and eeMETRIC due to cloud masking); Jun-Sep eeMETRIC
1985	OpenET	Oct-Sept OpenET data

Wetland ET_a and Net ET

Wetlands within the Klamath River Basin have demonstrated variability in composition, both spatially and temporally, with some areas subjected to reoccurring inundation of water. Due to standing water causing negative VI values and thereby confounding a regression-based approach relying on NDVI, the Beamer-Minor Method was deemed inappropriate for largescale use on wetland landcover within the Klamath River Basin. ET_a for wetlands was estimated using eeMETRIC, which has demonstrated good performance in wetlands within the region (Melton et al., 2022; Volk et al., 2023b) and compared well to eddy-covariance data collected by Stannard et al. (2013). Monthly net ET estimates for wetlands were calculated by subtracting the respective monthly total precipitation with the assumption that all precipitation discharges through ET (i.e., 100% of the total precipitation is effective) and none of the precipitation runs off or contributes to recharge.

Groundwater Discharge from Phreatophytes and Wetland ET

Groundwater discharge in the Klamath River Basin occurs primarily via ET_g from phreatophyte vegetation and bare soil evaporation within valley floor shrubland, wetlands, and spring discharge areas. Knowledge about pre-development (i.e., pre-Project) and contemporary extents of these areas is important for the development of representative ET_g

rates and volumes for different time periods of interest. The largest area of phreatophytes within the Klamath River Basin is comprised of shrublands, and while shrubland phreatophytes exhibit relatively low rates of ET_g, their large contributing areas equate to large groundwater discharge volumes (Nichols, 2000; Smith et al., 2007; Beamer et al., 2013). The summaries developed of groundwater discharge from phreatophytic and wetland ET are an input to the KRRNFS and were used by the TSC to develop ET rates of natural landcover for pre-development conditions.

Phreatophyte ET_g Rates

Researchers at DRI and the USGS have conducted extensive research and developed methodologies focused on estimating phreatophyte ET_g and groundwater discharge. The USGS has frequently implemented an "ET unit" approach for uniformly spatially distributing micrometeorological station-based estimates of ET_g rates across respective ET units to estimate volumes of groundwater discharge. The approach is based on uniformly applying average annual ET_g rates from previous studies to ET unit areas of similar vegetation and soil characteristics to estimate the volumes. ET units are estimated using ranges of average vegetation index (VI) values computed from mid-summer Landsat satellite imagery (Smith et al., 2007; Garcia et al., 2022). Alternatively, several studies led by DRI researchers have estimated phreatophyte ET_g rates by developing and applying statistical relationships between VI's and micrometeorological station-based water year ET_a, ET_g, PPT, and ET_o (Groeneveld et al., 2007; Beamer et al., 2013). Although these empirical statistical approaches enable transferability by accounting for local climate conditions and water supply and demand differences between station and study locations (i.e. PPT and ET_o), past studies have typically relied on custom and different atmospheric correction approaches, and only used one or two mid-summer Landsat images both in developing and applying empirical relationships between VI's and ET_g.

Phreatophyte ET_g was calculated for the study period using the Landsat Collection 2 archive (Crawford et al., 2023), gridMET weather data, and phreatophyte boundaries described in the previous section. Annual ET_g rates were estimated using a revised version of the approach described by Groeneveld et al. (2007), Beamer et al. (2013), and Minor (2019). The approach, referred to as the Beamer-Minor method (BMM), uses water year total ET_a observations derived from in situ micrometeorological and energy balance station data collected at 36 sites (54 site years; some sites with multiple years of ET data) from ten studies in the Great Basin (Reiner et al., 2002; Maurer et al., 2005; Moreo et al., 2007; DeMeo et al., 2008; Arnone et al., 2008; Allander et al., 2009; Garcia et al., 2015; Berger et al., 2016; Moreo et al, 2017; DeMeo, 2018) along with respective water year gridMET ET_o and PPT estimates for each site.

An energy balance closure (EBC) correction approach based on the energy balance ratio (EBR; ratio of the sum of turbulent fluxes to the sum of radiative fluxes), and similar to OpenET (Volk et al., 2023b) and FLUXNET (Pastorello et al., 2020) methodologies used for intercomparison and validation of satellite-based ET data, was used in the BMM approach to correct 39 site years of eddy covariance (EC) ET_a data at the daily time step. The remaining 15 site years of in situ ET_a data were collected using the Bowen ratio (BR) energy balance method, which inherently forces closure and doesn't require EBC corrections. The

application of EBC at daily time steps, as opposed to hourly or sub-hourly time steps, has been shown to reduce effects of soil-heat-flux measurement and storage inaccuracies (Leuning et al., 2012). Prior to EBC corrections, EBR values ranged from 0.62 to 1.18 with a mean EBR of 0.92 across all sites. Following EBC corrections, EBR values ranged from 0.98 to 1.02 with a mean EBR of 1.01 across all sites. More details on processing and gap-filling steps are outlined in Volk et al. (2023a) are provided in the open-source flux-data-qaqc GitHub repository (https://github.com/Open-ET/flux-data-qaqc) (Volk et al., 2021).

After EBC corrections and normalization of the in situ ET_a data for each site year (discussed below), normalized ET_a (ET*) was paired with respective Landsat Collection 2 surface reflection derived NDVI values for source areas around each micrometeorological station to develop a least-squares linear regression model (Figure 13). Source area NDVI values for each site year were computed as the spatial average (100-meter buffer) of the respective mid-summer median NDVI composite. The NDVI – ET* regression of the approach of BMM is advantageous given that variations in vegetation characteristics, evaporative demand, and precipitation are accounted for both in deriving and applying the regression, and therefore enables transferability without having to collect additional in situ ET_a data in the local area of application. With the ET Unit approach, in situ measurements of ET_g must be made for various ET Units in the local area of application, or assumed ET_g rates must be specified.

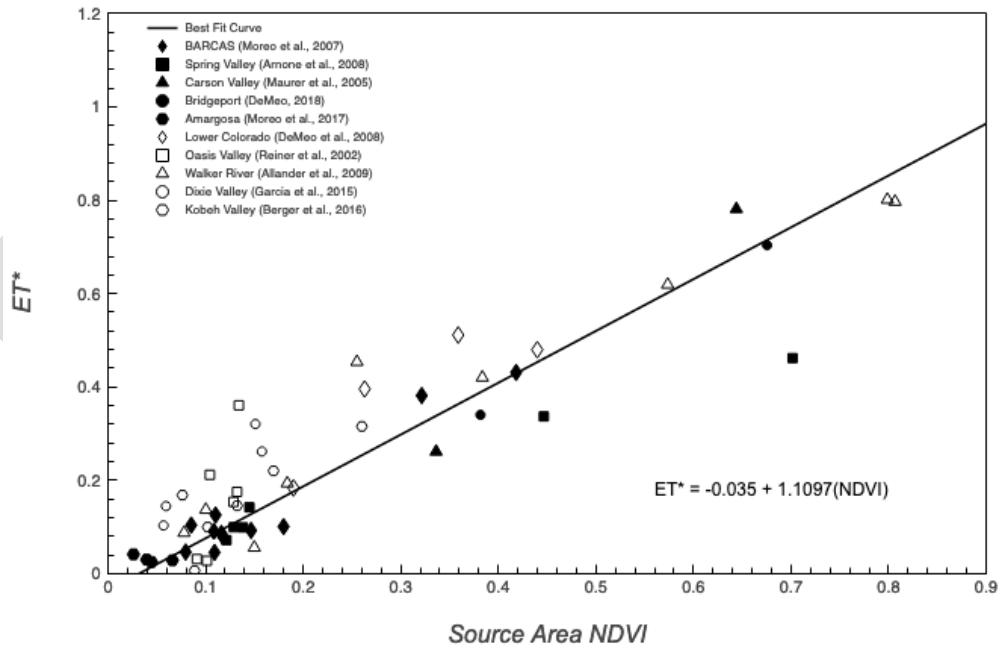

Figure 13. NDVI – ET* data pairs for 54 site years of eddy covariance and Bowen ratio flux tower stations used in the BMM. Symbols indicate which ET study the data point represents. The best-fit line and prediction equation are provided.

NDVI was chosen over other VI's (e.g., enhanced vegetation index, modified soil-adjusted vegetation index) because it is a relatively simple formulation, is frequently used among the scientific community, and has been shown to perform well for quantifying vegetation cover in semi-arid environments (McGwire et al., 2000; Wu, 2014). NDVI incorporates both red and near infrared (NIR) spectral bands and is defined as:

$$NDVI = \frac{(NIR - RED)}{(NIR + RED)} \quad (2)$$

where NIR is the near infrared surface reflectance and RED represents the red surface reflectance sourced from Landsat satellite data. The USGS converts the Landsat 5 Thematic Mapper (TM), the Landsat 7 Enhanced Thematic Mapper Plus (ETM+), and the Landsat 8 Operational Land Imager (OLI) top-of-atmosphere reflectance to surface reflectance using the Landsat ecosystem disturbance adaptive processing system (LEDAPS) (for Landsat TM and ETM+) and Landsat Surface Reflectance Code (LaSRC) (for Landsat 8 OLI) atmospheric correction algorithms (Landsat 8-9 Collection 2 Level 2 Science Product Guide | U.S. Geological Survey, 2022; Schmidt et al., 2013). Due to slight differences in the Landsat sensor bandwidths, cross-sensor calibration between Landsat TM, ETM+, and OLI was performed using equations developed by Huntington et al. (2016).

The mid-summer period from June 1st through September 15th was selected for temporally compositing Landsat NDVI imagery since precipitation and influences from non-phreatophytic vegetation are typically low and phreatophyte vegetation vigor is more pronounced during this period. Extensive cloud masking using Landsat CFmask products (Foga et al., 2017) and additional quality assurance and quality control (QA/QC) procedures were applied to ensure accurate Landsat imagery was considered in the analysis. The QA/QC steps involved computations of supplementary VI's, water indices (e.g., normalized difference water index), albedo, and LST to help identify and filter out poor quality images. After QA/QC steps were finished, normalized ET* for a given water year defined as:

$$ET^* = \frac{ET_a - PPT}{ET_o - PPT} \quad (3)$$

was estimated using the NDVI – ET* linear regression equation:

$$ET^* = \beta_0 + \beta_1 NDVI \quad (4)$$

where ET_a is the water year total actual ET in millimeters per year (mm/yr), PPT is the water year total precipitation (mm/yr), ET_o is the water year total grass reference ET (i.e., evaporative demand) (mm/yr), and β_0 and β_1 are the best-fit regression coefficients of -0.035 and 1.1097, respectively. Applying equation 4 to mid-summer NDVI resulted in estimates of mean ET* for phreatophyte vegetation with upper and lower 90th percentile confidence and prediction interval estimates included (Table 3). The confidence interval (CI) represents the degree of confidence in the mean ET* estimated for a given NDVI observation, whereas the prediction interval (PI) signifies the degree of confidence for a new NDVI and ET* data pair to fall within the interval at the 0.10 significance level (i.e., 90th percentile). The PI is wider than the CI since it accounts for the uncertainty in estimating the population mean ET*, plus the random variation of individual observations (Figure 14).

By rearranging equation 3, water year ET_a was estimated as:

$$ET_a = (ET_o - PPT)ET^* + PPT \quad (5)$$

where water year total PPT and ET_o was estimated using gridMET. Water year ET_g is then estimated by subtracting the water year PPT from the estimated water year ET_a:

$$ET_g = (ET_o - PPT)ET^* \quad (6)$$

Water year ET_g was estimated for phreatophyte vegetation for the 1985–2020 study period using the equations above with the following steps: 1) spatially average gridMET water year PPT and ET_o for phreatophyte boundaries, 2) compute spatially distributed NDVI using Landsat Collection 2 surface reflectance data, 3) compute spatially distributed ET*, ET_a, and ET_g rates, 4) export annual ET_g rate rasters at 30m resolution, 5) spatially average ET*, ET_a, and ET_g rates, and 6) multiply spatially averaged ET_g rates by the phreatophyte area to estimate ET_g volumes. All of the above steps were applied to each year of the study period using all QA/QC-ed June 1st through September 15th Landsat imagery. The annual ET_g rasters resulting from step 4 were further disaggregated to seasonal time steps by first computing the water year ET_g/ET_o ratios, and then multiplying the ET_g /ET_o ratio by the seasonal ET_o. For each water year, the four seasons are defined as October through December, January through March, April through June, and July through September.

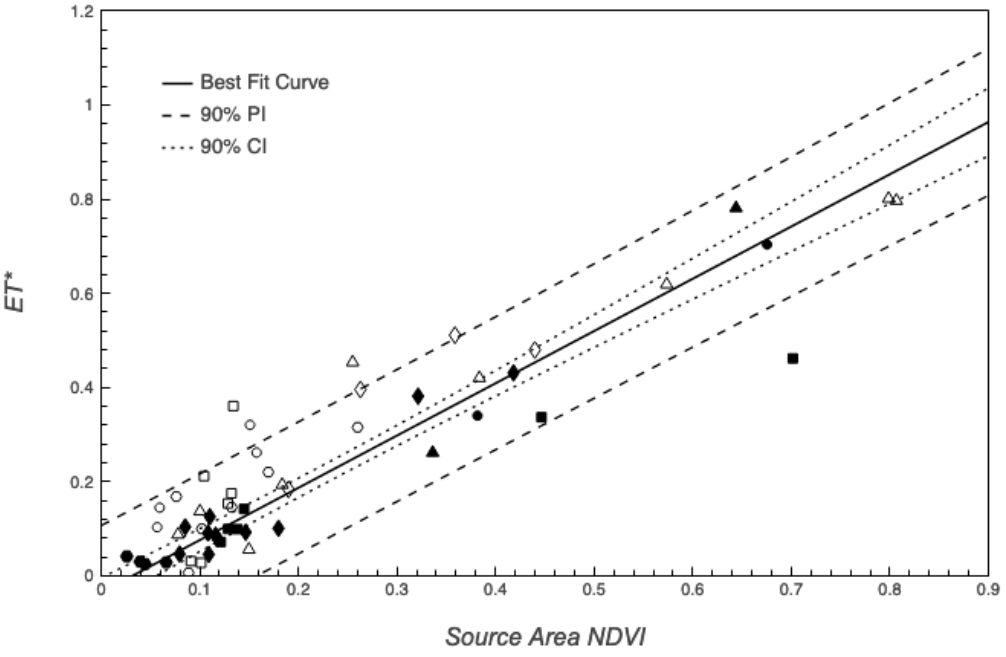

Figure 14. NDVI – ET* data pairs with the best-fit line and upper/lower 90th percentile CI and PI bands.

Annual ET_g rates were disaggregated to seasonal time steps so that ET_g rates for phreatophytes could be incorporated into the KRRNFS groundwater modeling framework and used for calibration. The period prior to 1985 was not estimated since the primary purpose for estimating ET_g was for groundwater model calibration, and the period of 1985–2020 is adequate for both calibration and validation.

Table 3. β-Coefficients of the NDVI – ET* predictive equation 90th percentile CI, and PI for estimating ET_g.

Equation	β_0	β_1
Linear (model)	-0.035	1.1097
Lower 90% CI band	-0.0477	1.0544
Upper 90% CI band	-0.0223	1.165
Lower 90% PI band	-0.172	1.0936
Upper 90% PI band	0.102	1.1258

RESULTS AND DISCUSSION

The following section describes and highlights results from the primary focus areas of the ET study, field boundary digitizing and irrigation system type attribution, irrigation status mapping and attribution, ET Demands modeling results, agricultural ET, wetland ET, phreatophyte ET, and field boundary summaries.

Field Boundary Digitizing and Irrigation System Type Attribution

The KRRNFS field boundary digitizing effort resulted in 12,930 unique and attributed features. Field boundary attributes associated with agricultural field boundaries and delineated wetlands are described in detail in Appendix 2, and include unique ID, military grid reference system ID, state, acres, year, irrigation system type, irrigation status, and growing season mean Landsat NDVI. The delineation of maximum irrigated extent for the 1985–2020 period resulted in the addition of features not present in field boundary datasets that were representative of current conditions. New polygons were most often digitized where irrigation occurred and since ceased, most often due to changes in land use as conversion from agricultural to municipal and residential uses. The inclusion of these previously irrigated lands in this dataset was necessary for the analysis of long-term consumptive use. Agricultural fields retired from agricultural production for the purposes of habitat restoration often maintain visual similarities with intermittently irrigated agricultural fields, and thus were retained in the dataset.

The attribution of irrigation system type for all agricultural field boundary features was an iterative, multi-agency effort, including geospatial analysts from both DRI and TSC. Irrigation type attribution (Table 1) was reviewed for completeness and quality, ensuring that multiple GIS technicians evaluated the attribution for each feature. The irrigation system type attribution effort resulted in per year attribution of irrigation system type for all fields for the period of 1995–2020.

IrrMapper

IrrMapper binary class values were attributed to field boundaries at annual time steps. Spatially averaging binary class values resulted in field boundary attribute values ranging from 0 to 1. Field boundary IrrMapper binary class fractions may be used to assess uncertainty and scale irrigation consumptive use volumes as additional post-processing analyses. Visual assessment of IrrMapper results indicated robust performance in areas of well-developed agriculture when compared to historical aerial imagery and growing season maximum Landsat NDVI, and field boundary delineations (Figure 15). This high degree of performance appears as irrigated pixels are predominantly constrained to field boundaries, with clear patterns of variation within geometries corresponding to likely patterns of intra-field partitioning combined with varied management or irrigation activity.

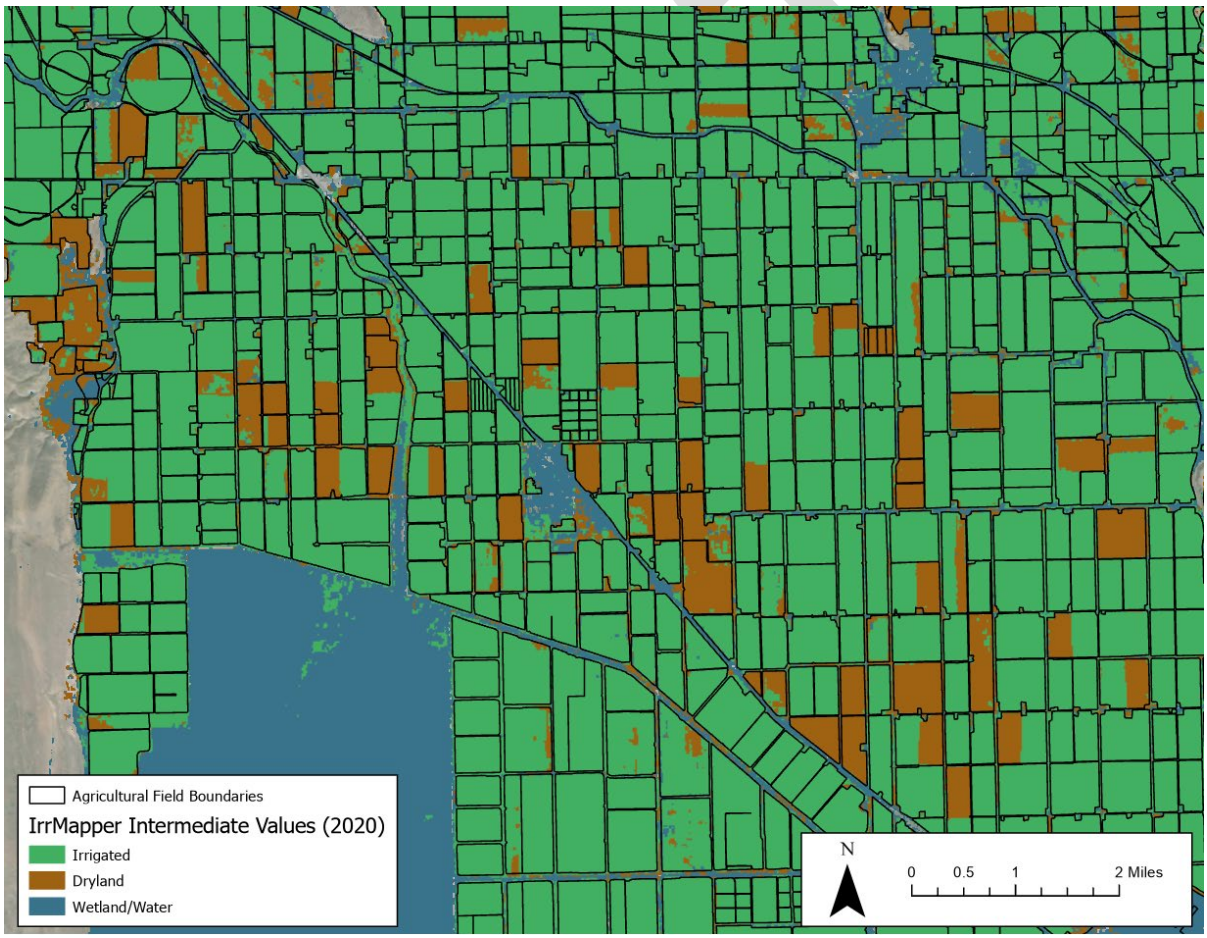

Figure 15. Overview of an agricultural area near Tulelake, CA where IrrMapper exhibits a high degree of accuracy.

Performance of IrrMapper was limited and less robust in agricultural areas of diversified pasture, where shallow groundwater, subirrigation, riparian corridors, and wetland areas are common (Figure 16). These areas are often classified as “herbaceous wetland” within the CDL product, yet are commonly cultivated and supplementally irrigated for

pasture grass and grazing. IrrMapper classes for these areas are commonly "wetland/water," which is considered an "unirrigated" class based on IrrMapper methodology. Additionally, these areas classified as "unirrigated" proved difficult for GIS analysts and project specialists to identify if lands were irrigated and cultivated due to lack of irrigation infrastructure and spatial water right information. Further investigation and refinement of IrrMapper wetland/water classifications based on local knowledge and water right information could be considered to refine irrigation consumptive use assessments and modeling activities.

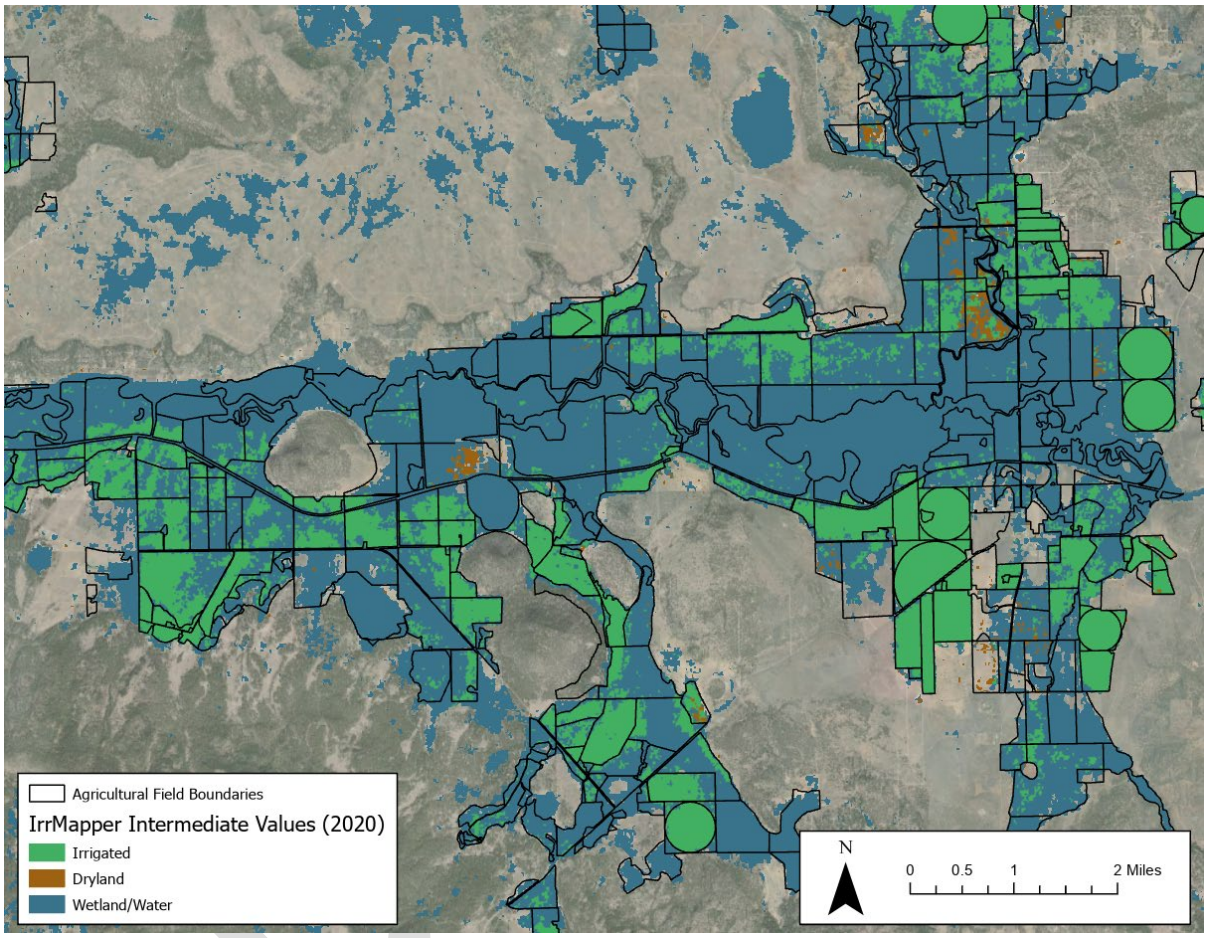

Figure 16. Overview of an agricultural area near the Sprague River in the vicinity of Beatty, OR where IrrMapper "wetland/water" classifications include agricultural fields that may be flood irrigated or subirrigated and cultivated for pasture grass or grazed.

ET Demands

The KRRNFS ET Demands model produces daily time series output of ET_c, NIWR, surface runoff, deep percolation, and P_{rz} assuming well-watered, potential crop conditions. While not used directly by the KRRNFS, accurate simulation of ET_c, NIWR, surface runoff, and deep percolation is required for accurate soil water balance modeling and P_{rz} estimation. Figure 17 illustrates an example time series of ET Demands output for a grass hay crop located south of Klamath Falls, OR. The grass hay simulation initiates the start and end of the

growing season in mid-April and mid-October, respectively. Irrigation events at the start and end of the season are typically small and spread out compared with mid-summer irrigation due to lower crop water demand, carry forward winter and spring soil moisture storage, and spring precipitation events. Elevated values of K_c and ET_c are simulated after wetting events due to soil evaporation losses (i.e., evaporation from soil beneath the canopy or in between plants following irrigation and precipitation) (Allen et al., 2009). Time series datasets shown in Figure 17 were produced for each unique grid cell and crop type combination.

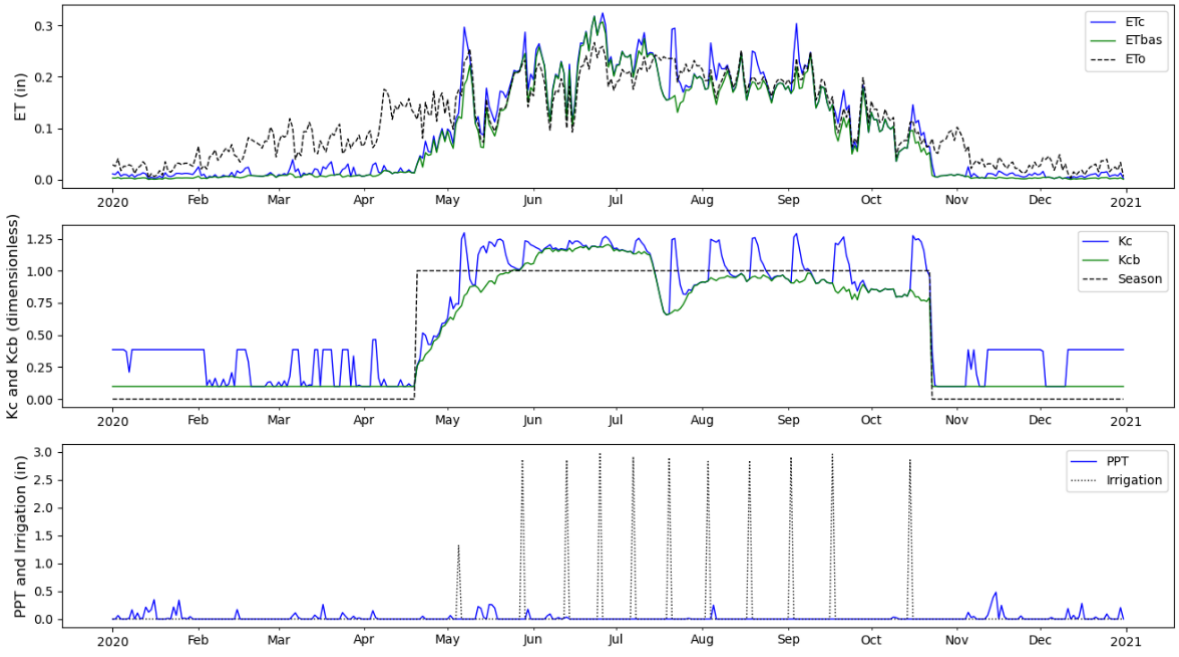

Figure 17. Example ET Demands simulation for a grass hay crop in cell 566947 south of Klamath Falls, OR.

For this work, the primary output variable of interest was P_{rz}. Estimates of P_{rz} were subtracted from OpenET eeMETRIC produced ET_a to estimate net ET for agricultural land. Figure 18 illustrates the spatial distribution of average annual ET Demands P_{rz} to total PPT fractions for the period of 1980 to 2020. The spatial distribution illustrates areas of high and low P_{rz} to PPT fractions, which is related to evaporative demand, and simulated partitioning of precipitation into runoff and deep percolation. Figure 19 illustrates the 1980–2020 average annual PPT distribution where lower P_{rz} to PPT fractions generally occur in areas of high elevation where larger annual PPT amounts correspond with less evaporative demand, and increased surface runoff and deep percolation. Higher P_{rz} to PPT fractions are simulated in areas with relatively low PPT and higher evaporative demand and correspond with valley floor areas along the California-Oregon border near Tule Lake.

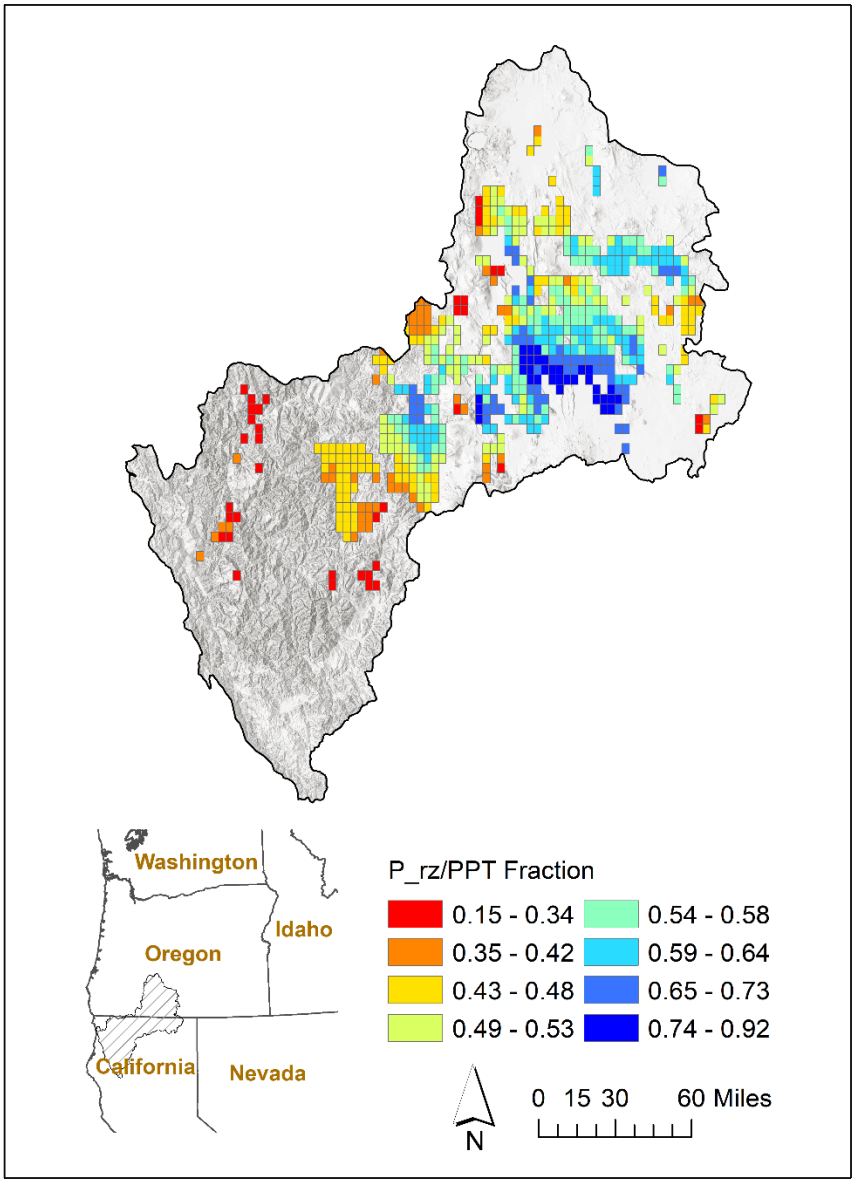

Figure 18. Average annual P_{rz} to PPT fraction for grass hay in estimated using ET Demands for the period of 1980–2020.

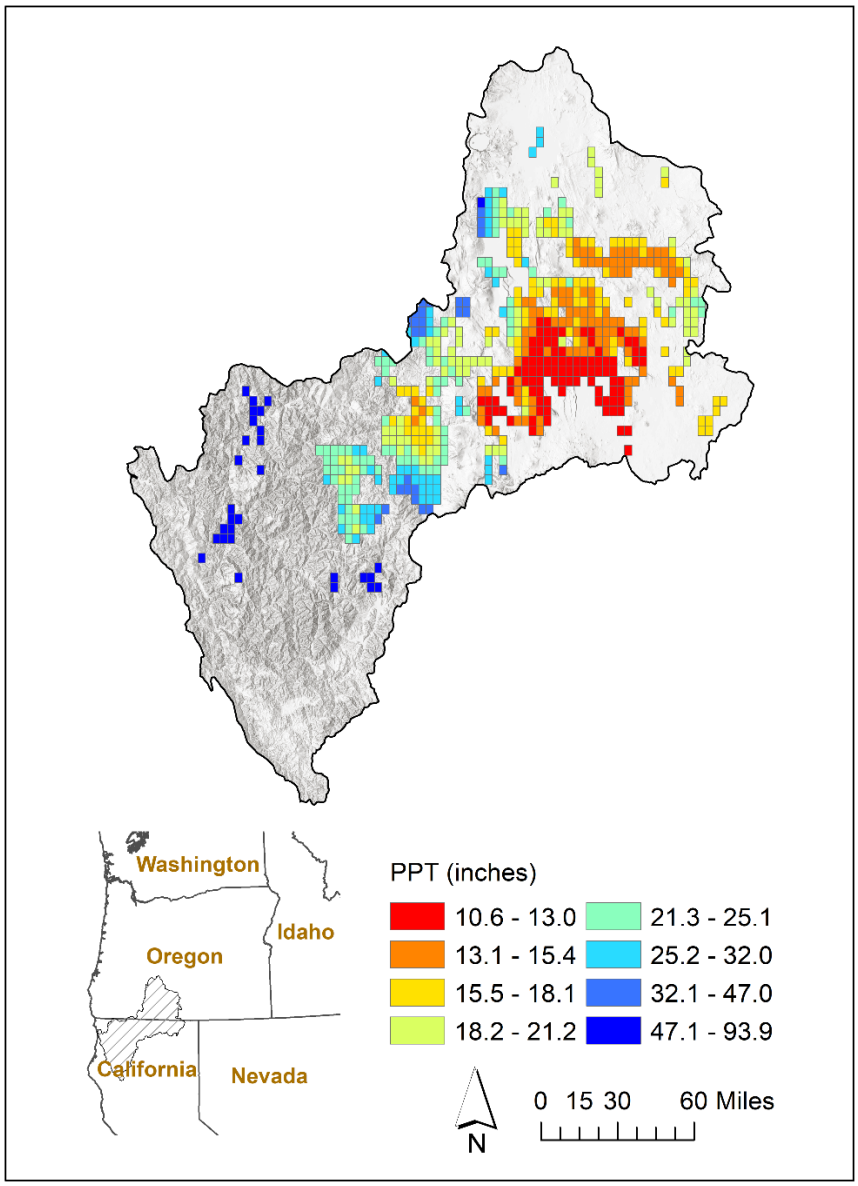

Figure 19. Average annual PPT for each ET Demands model grid cell for the period of 1980–2020.

Figure 20 illustrates cumulative daily ET_c, P_{rz}, NIWR, and irrigation simulated for grass hay for the year 2020. Cumulative ET_c and P_{rz} are similar from January until the start of the growing season until crop water demands increase and are met through irrigation. Irrigation events simulated within ET Demands fully saturate the soil profile with an

assumed 10% loss to deep percolation. Although the growing season starts in mid-April, the first irrigation is not simulated until early May due to carry forward soil moisture storage of wintertime precipitation. Also, note the decrease in NIWR after the end of the growing season, indicating storage of precipitation.

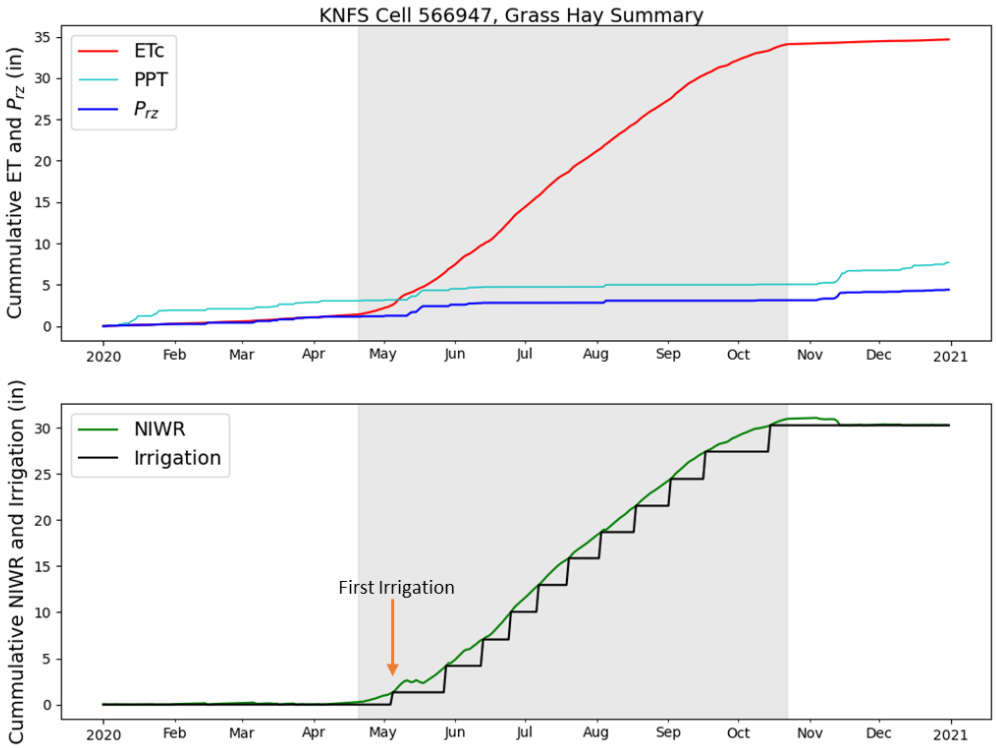

Figure 20. Time series plot of cumulative ET, P_{rz}, NIWR, and Irrigation for a grass hay crop in ET Cell 566947 south of Klamath Falls, OR. Gray shading represents the estimated growing season period with active irrigation.

ET Demand P_{rz} estimates are a function of crop type, water demand, precipitation timing and amount, and soil type. P_{rz} estimates developed in this study are intended to be used for estimating ET of applied irrigation water and ET from PPT. The complete ET Demands data package includes daily time series of all variables illustrated in Figure 20 for each unique agricultural crop–grid cell combination throughout the KRRNFS area from 1980–2020. ET Demands model daily time series output was aggregated to monthly totals for pairing with OpenET eeMETRIC ET_a estimates and estimation of agricultural net ET. Final P_{rz} results are summarized in the monthly field-level ET database which was provided to USBR and described in detail in Appendix 3. The ET Demands daily time series data package is described in detail in Appendix 5.

Agricultural and Wetland ET

For agricultural areas within the Klamath River Basin, calculations of monthly ET_a, ET_oF, ET_o, PPT, P_{rz}, and net ET rates and volumes were produced and summarized at field scale. Results were compiled into a data package that contains spatial and temporal data summaries for field boundaries. Appendix 3 details the file structure, variable definitions, units, and spatial and temporal extents of the data summaries.

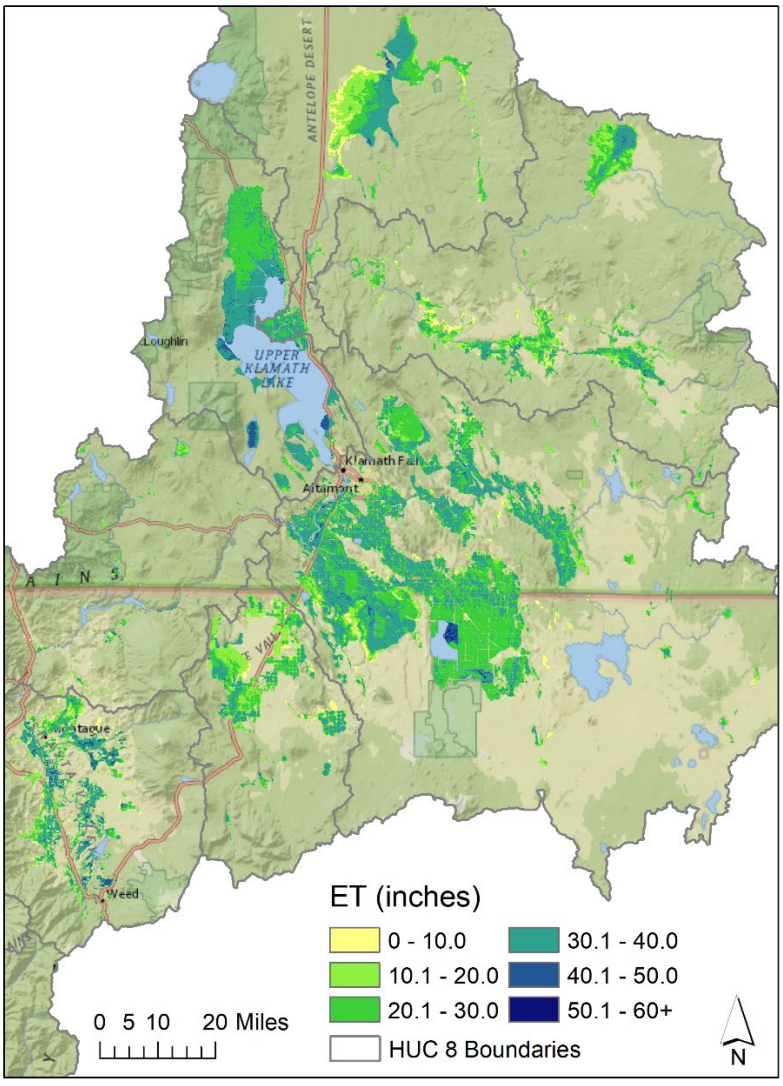

Figure 21. Spatial distribution of long-term (1985–2020) average annual ET for agriculture, wetlands, and pasturelands within the KRRNFS area.

Similarly, calculations of monthly ET_a, ET_oF, ET_o, PPT, P_{rz}, and net ET rates and volumes were produced and summarized for existing wetland areas around Upper and Lower Klamath Lakes, the Klamath Marsh, the Sycan Marsh, Tule Lake, and the Sprague river.

Results were compiled into a data package that contains spatial and temporal data summaries for delineated wetland polygons. Appendix 3 details the file structure, variable definitions, units, and spatial and temporal extents of the data summaries. Figure 21 illustrates the long-term average annual ET for the period of 1985–2020.

Comparison with Previous Estimates

To intercompare and validate ET data developed and summarized in this report, previous estimates of ET within the region were compiled and evaluated. Based on data quality and completeness, two comparison approaches were developed and described below.

Comparison to Stannard et al. (2013)

In a previous study conducted by the USGS, EC flux tower data were used to estimate ET for two wetland sites within the Upper Klamath Lake National Wildlife Refuge (NWR) during the period of May 2008 to September 2010 (Stannard et al., 2013). Landcover of these sites was comprised of a near monoculture of hardstem bulrush (*Schoenoplectus acutus*) for one site, while the other site consisted of a mix of vegetation characterized as 70% bulrush and 15% percent cattail (*Typha latifolia*). Daily estimates of ET produced by these two EC sites were compared against 29 days of eeMETRIC data produced on dates of Landsat scene acquisition, thereby minimizing error that could be introduced in the temporal interpolation of ET_oF in between Landsat images. Results of the intercomparison at the bulrush site are illustrated in Figure 22a and indicate good agreement between eeMETRIC and EC data (slope of 0.92, coefficient of determination (R^2) of 0.88, and root mean square error (RMSE) of 0.81). The comparison between eeMETRIC and EC data for the mixed vegetation was similar in agreement with slope of 0.95, R^2 of 0.87, and a RMSE of 0.83 (Figure 22b).

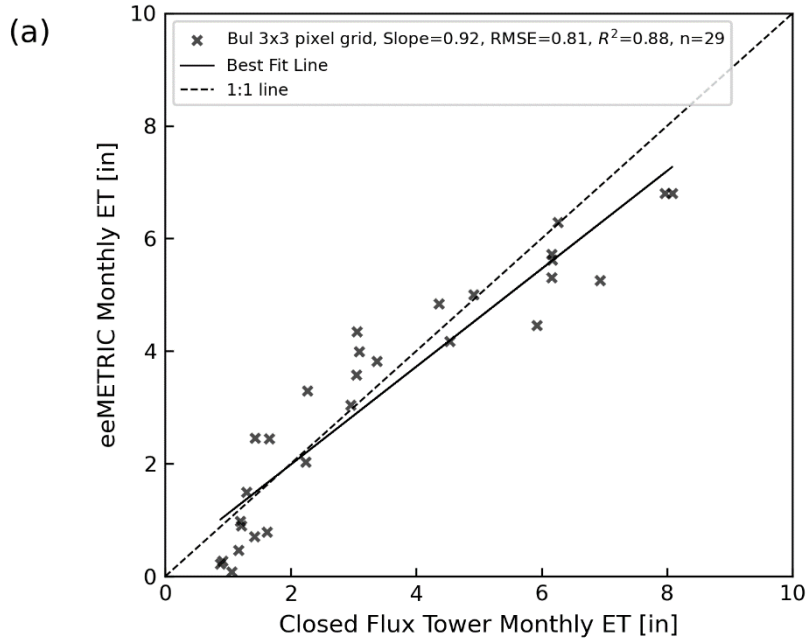

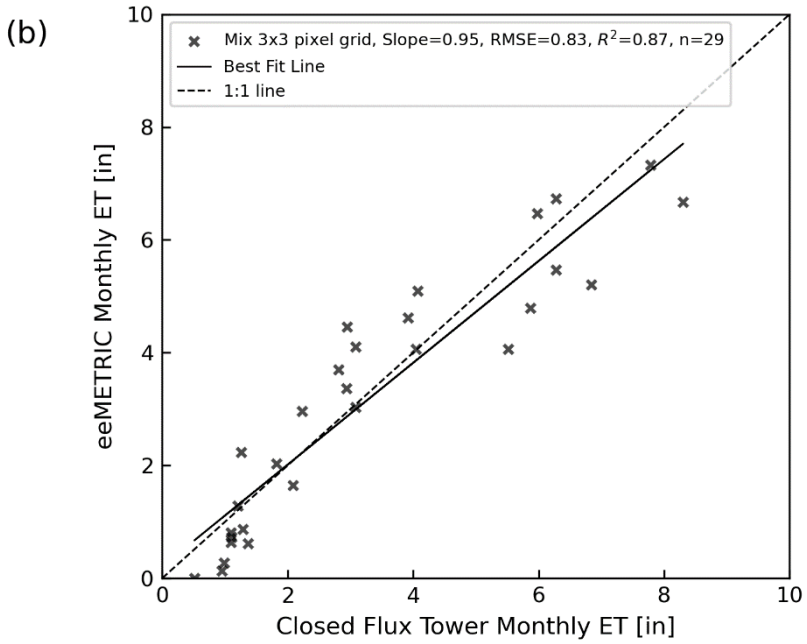

Figure 22. Comparison of OpenET eeMETRIC and EC flux tower station derived monthly ET from 2008-05-01 through 2010-09-01 for the bulrush (a) and mixed vegetation (b) sites north of Upper Klamath NWR.

ET+ METRIC

The METRIC model was previously applied within the Klamath River Basin in multiple studies in which ET data were developed by the consulting firm ET+ (R. Allen, personal communication, March 16th, 2022, Allen & Snyder, 2011; Snyder et al., 2012; Zhao et al., 2015). These applications of METRIC relied on an alfalfa reference ET (ET_r) dataset derived from ET_r calculated from nearby agricultural weather stations and interpolated into a spatially explicit ET_r surface. METRIC data were developed for the growing seasons (April–October) of the years 2004, 2006, 2010, 2013, and 2014. These estimates of ET were produced for two Landsat scenes, Worldwide Reference System (WRS) path/row p45/r30 and p45/r31.

Comparisons of ET+ METRIC to OpenET eeMETRIC, revealed that ET+ calculated rates of ET_a were greater than those produced by eeMETRIC. To isolate potential factors which could cause the disparity between calculated ET from the two models, an analysis of the three primary components of the ET calculation (ET_a, ET_o, and ET_oF) was performed. ET+ METRIC estimates of ET_a were derived from ET_r; therefore, it was necessary to create a common basis of comparison in the characterization of vegetation and land surface conditions represented in the term ET_oF. An ET_oF equivalent was produced by the following calculation:

$$ET_oF_{equivalent} = \frac{ET_oF_{OpenET\ eeMETRIC} * ET_{ET+METRIC}}{ET_{OpenET\ eeMETRIC}} \quad (8)$$

The creation of an ET_oF equivalent does not alter the calculations produced by ET+ but creates a metric useful for diagnostic purposes. Figure 23 "a","b", and "c" illustrate comparisons of ET_a, reference ET, and ET reference fraction respectively for a location in the Wood River, OR area. The comparison of ET+ METRIC to OpenET eeMETRIC in plot "a" indicates strong agreement between the two models when ET is least; however, divergence is more prominent at the highest rates of ET_a. Figure 23b illustrates a difference between calculations of reference ET used by the two models, which is consistent with two reference surfaces being used. Figure 23c illustrates a comparison between eeMETRIC ET_oF and METRIC ET_oF equivalent and indicates the primary source of divergence in values developed by eeMETRIC and METRIC. In this analysis, METRIC depicts much more robust vegetation vigor than is represented by eeMETRIC. These ET_oF equivalent values frequently exceeded 1.0 and reached a peak of 1.34 in May 2004. The R^2 for this comparison was calculated as 0.17, indicating a low degree correlation between ET_oF values.

The originator of both the METRIC and eeMETRIC models, Rick Allen, suggested in personal communication that an NDVI analysis could be applied to provide clarity on model disagreement (personal communication, March 23rd, 2022). For the site in Wood River, it was suggested that an NDVI consistently greater than 0.70–0.75 could support the ET+ METRIC results, whereas NDVI lower than the threshold may support the results produced by eeMETRIC.

An analysis was conducted of ET_a, ET_oF and ET_oF equivalents, and NDVI values for the years 2004, 2006, 2010, 2013, and 2014 (Figure 24). The years 2004, 2006, 2010, and 2014 were similar in pattern, with the repeated divergence in peak rates of ET calculated by METRIC and eeMETRIC. The area-weighted average of NDVI for these years peaked at or slightly above the 0.75 threshold. April–October average rates of NDVI for this agricultural unit were observed as 0.62. The comparison of ET data for 2013 is of particular note, as agreement between the two models during the growing seasons indicates that the calibrations used by ET+ METRIC model were very similar to the automated calibration used in eeMETRIC.

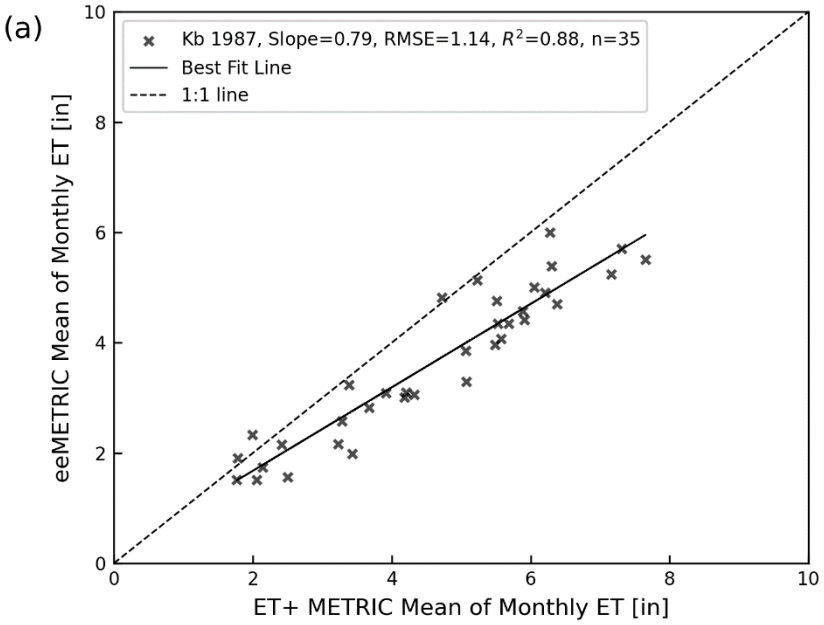
(a)
Kb 1987, Slope=0.79, RMSE=1.14, R^2=0.88, n=35
Best Fit Line
1:1 line
eeMETRIC Mean of Monthly ET [in]
ET+ METRIC Mean of Monthly ET [in]
0
2
4
6
8
10

1

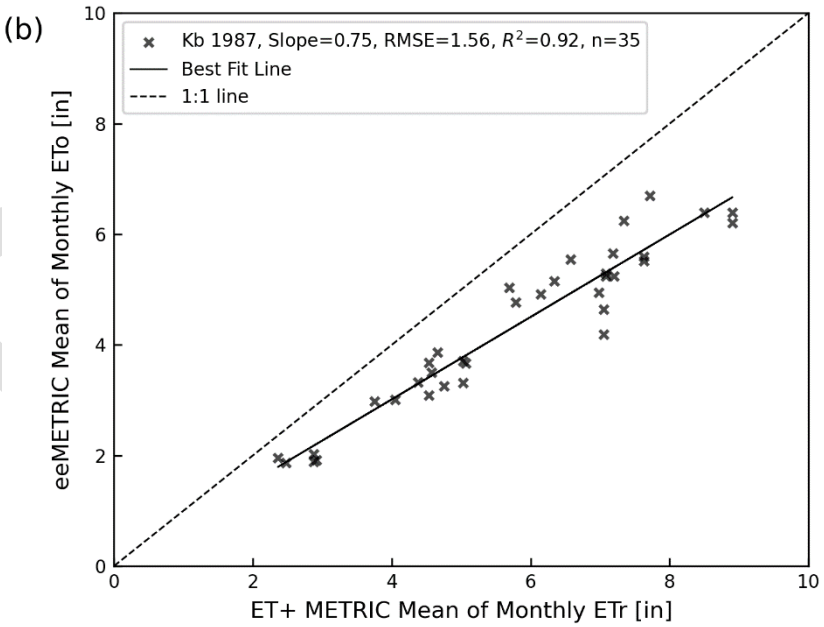
(b)
Kb 1987, Slope=0.75, RMSE=1.56, R^2=0.92, n=35
Best Fit Line
1:1 line
eeMETRIC Mean of Monthly ETo [in]
ET+ METRIC Mean of Monthly ETr [in]
0
2
4
6
8
10

2

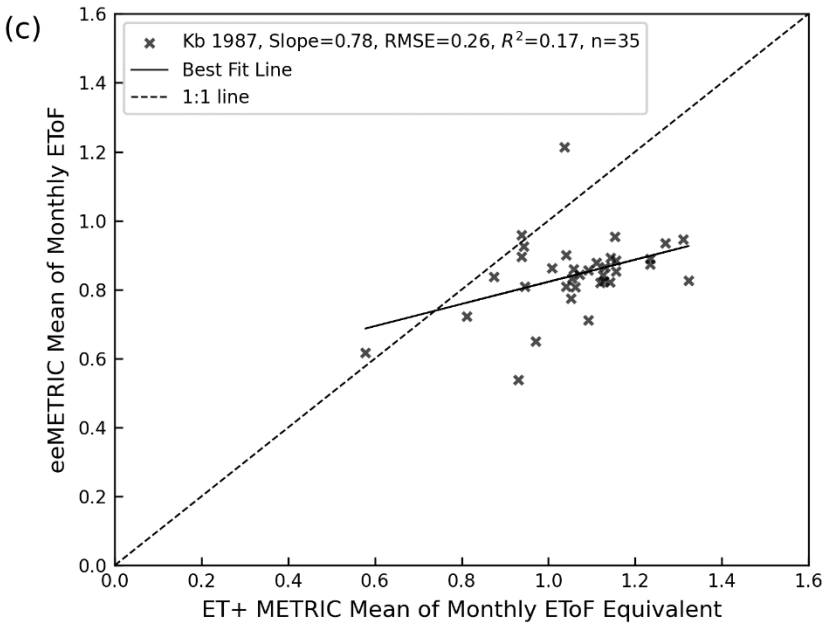

Figure 23. Comparison of OpenET eeMETRIC and ET+ derived monthly ET (a), reference ET (b), and fraction of reference ET (c) for the growing season months (Apr–Oct) of 2004, 2006, 2010, 2013, and 2014 at the actively irrigated KB_1987 field in the Wood River Valley north of Upper Klamath NWR.

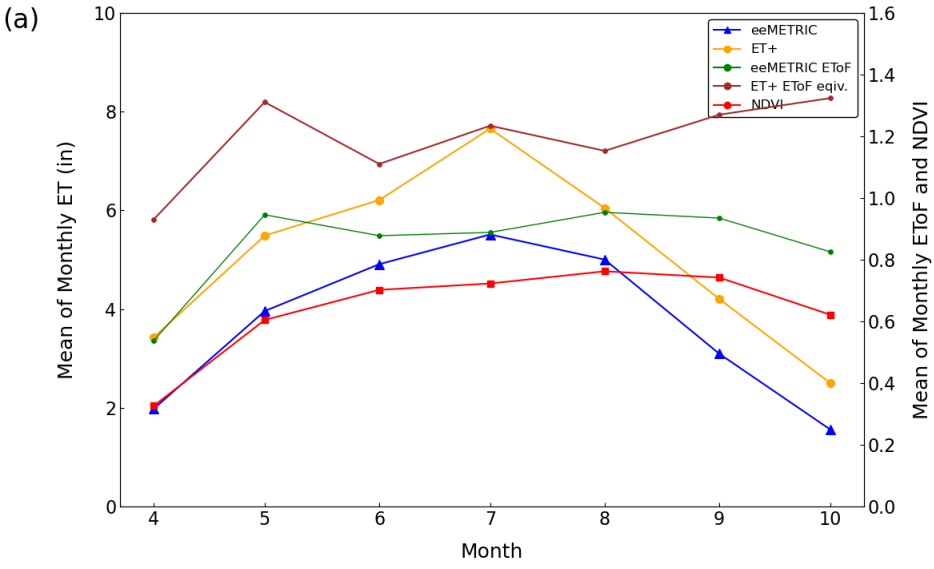

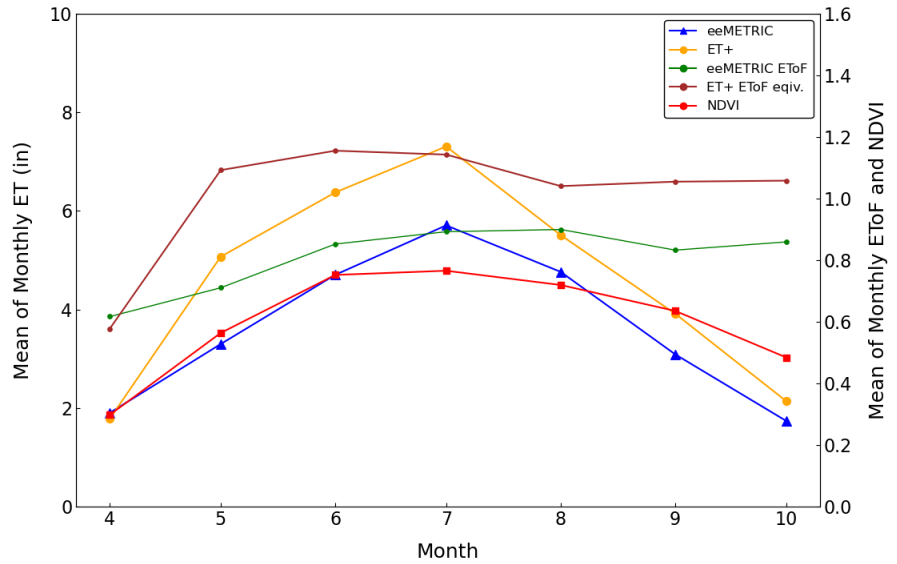
(b)
eeMETRIC
ET+
eeMETRIC EToF
ET+ EToF eqiv.
NDVI
Mean of Monthly ET (in)
Mean of Monthly EToF and NDVI
Month
0
2
4
6
8
10
0.0
0.2
0.4
0.6
0.8
1.0
1.2
1.4
1.6
4
5
6
7
8
9
10

1

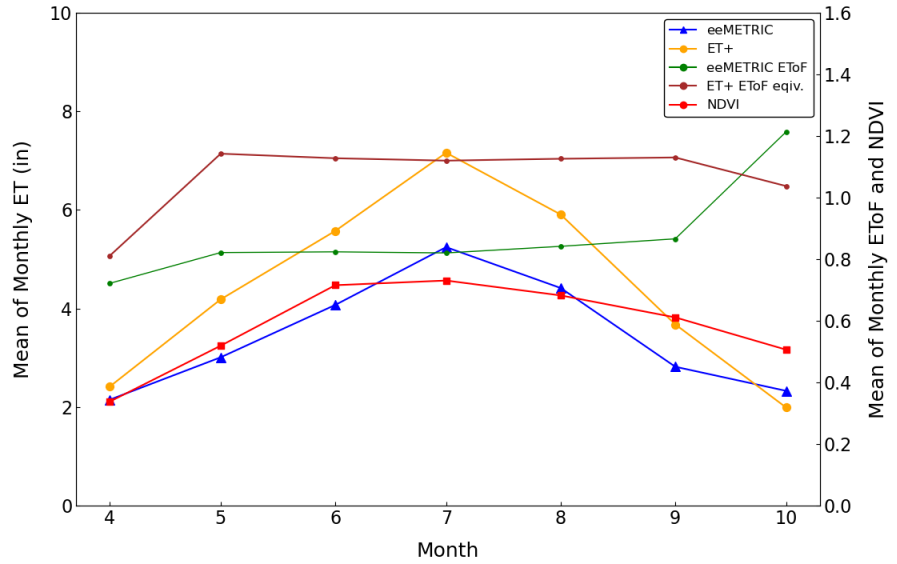
(c)
eeMETRIC
ET+
eeMETRIC EToF
ET+ EToF eqiv.
NDVI
Mean of Monthly ET (in)
Mean of Monthly EToF and NDVI
Month
0
2
4
6
8
10
0.0
0.2
0.4
0.6
0.8
1.0
1.2
1.4
1.6
4
5
6
7
8
9
10

2

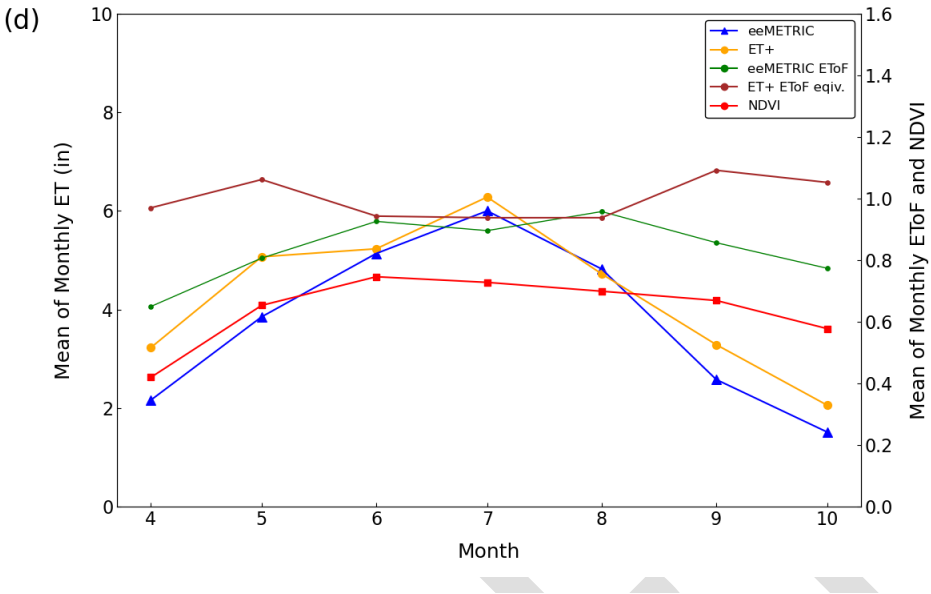

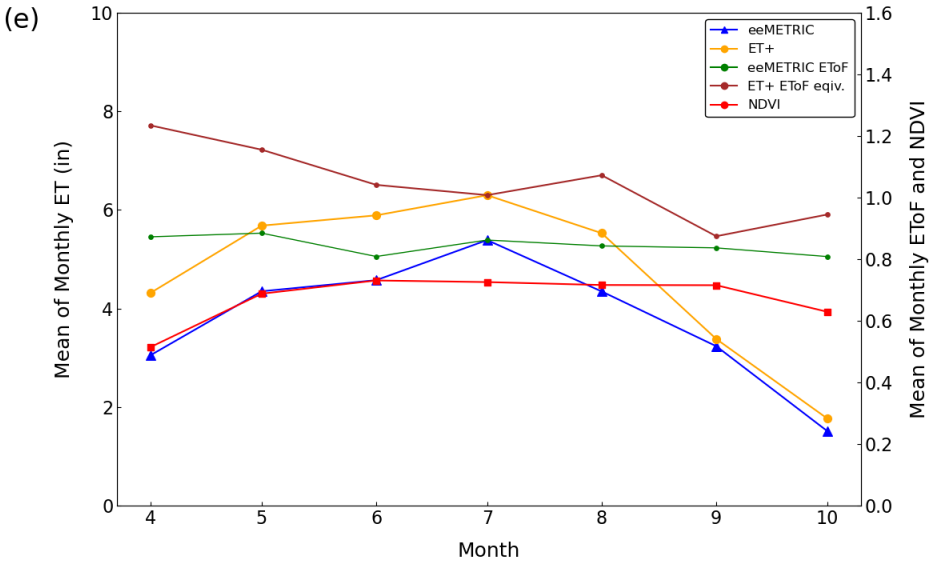

Figure 24. Time series of OpenET eeMETRIC and ET+ derived ET and fraction of reference ET, and Landsat derived NDVI for the growing season months (Apr-Oct) of 2004(a), 2006(b), 2010(c), 2013(d), and 2014(e) at the actively irrigated KB_1987 field in the Wood River Valley north of Upper Klamath NWR.

As the NDVI-based analysis does not conclusively support the ET estimates of either implementation of the METRIC model, this comparison serves to illustrate the results that have been developed with the two methodologies. The analysis of the geometry KB_1987 in Wood River, OR, illustrated the widest divergence of the two models, while stronger agreement was observed in well-managed agricultural areas. Fields which demonstrated this

agreement were documented near Lower Klamath Lake, OR where for the purposes of analysis the field boundary of KB_8328 was selected for comparison. Monthly ET_a rates from KB_8328 are illustrated in Figure 25a, where an R^2 of 0.91 was calculated between eeMETRIC and ET+ METRIC. The difference in reference ET values used by the two models is attributable to the use of grass and alfalfa reference surfaces by the two models, resulting in ET+ METRIC using consistently higher rates of reference ET (Figure 25b). Figure 25c illustrates eeMETRIC producing higher ET_oF values at the lowest range, whereas ET+ METRIC calculates higher ET_oF for time periods when ET is greatest. For this location of comparison, ET+ METRIC produced a peak monthly ET_oF of 1.44 for the month of April 2013, which was calculated as 1.04 by eeMETRIC. This observed difference is partly attributable to the use of ET_r by ET+ METRIC versus ET_o by eeMETRIC; however, variations in calibration methodologies may have exaggerated the difference in rats and volumes calculated by the two models.

For consistency, Figure 26 a, b, c, and d illustrate the annual time series of ET, ET_oF, and NDVI for months April–October for the years 2004, 2006, 2013, and 2014 in the same fashion as was illustrated for KB_1987 in Wood River, OR.

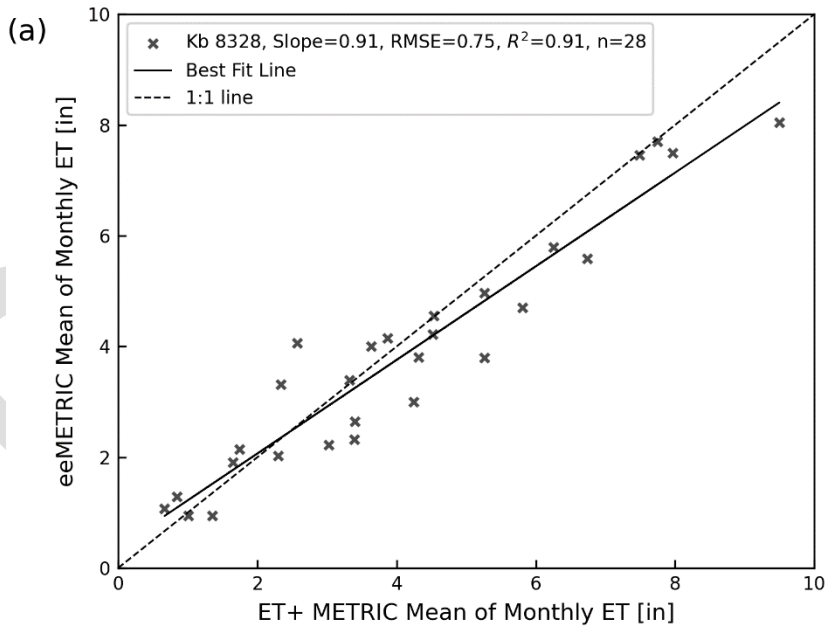

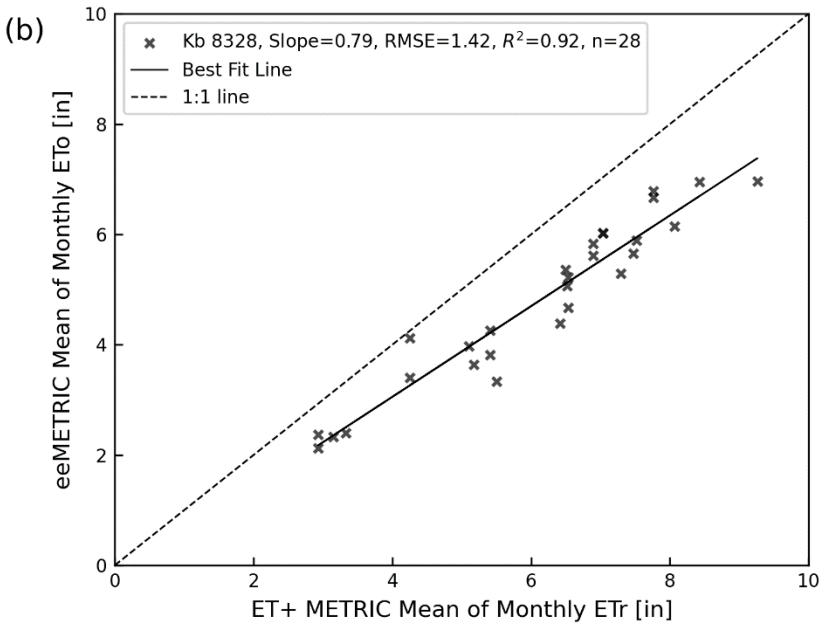

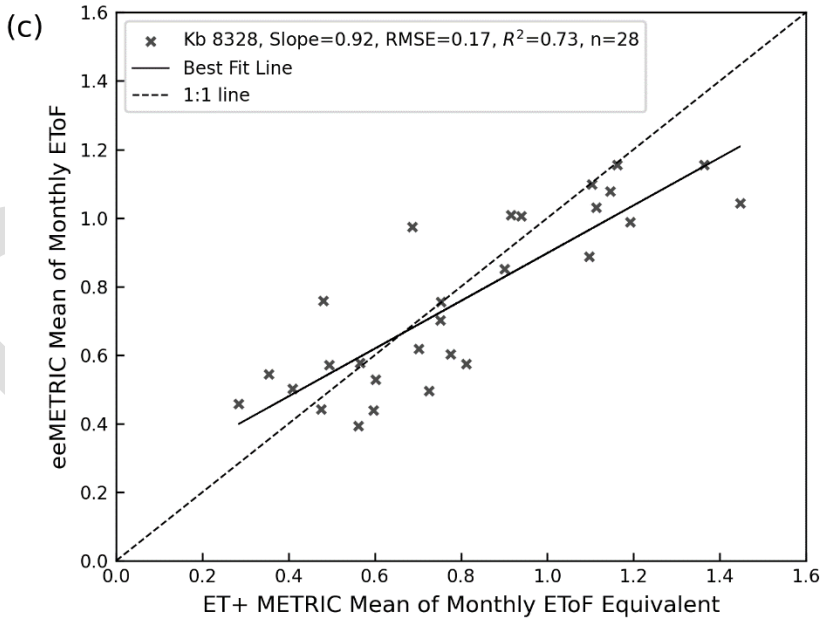

Figure 25. Comparison of OpenET eeMETRIC and ET+ derived monthly (a) ET, (b) reference ET, and (c) fraction of reference ET for the growing season months (Apr–Oct) of 2004, 2006, 2013, and 2014 at the actively irrigated KB_8328 field north of Lower Klamath Lake, OR.

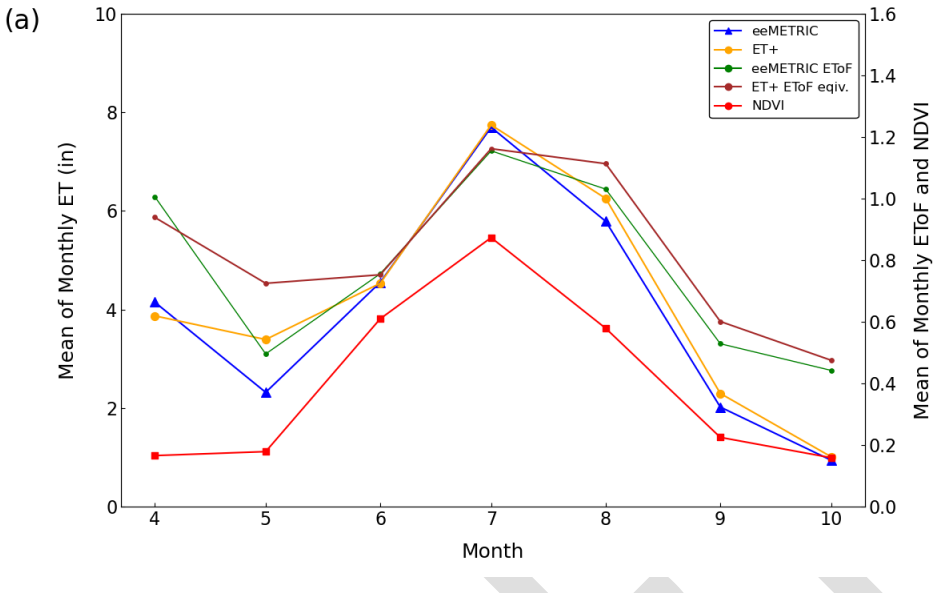
(a)
eeMETRIC
ET+
eeMETRIC EToF
ET+ EToF eqiv.
NDVI
Mean of Monthly ET (in)
Mean of Monthly EToF and NDVI
Month
0
2
4
6
8
10
0.0
0.2
0.4
0.6
0.8
1.0
1.2
1.4
1.6
4
5
6
7
8
9
10

1

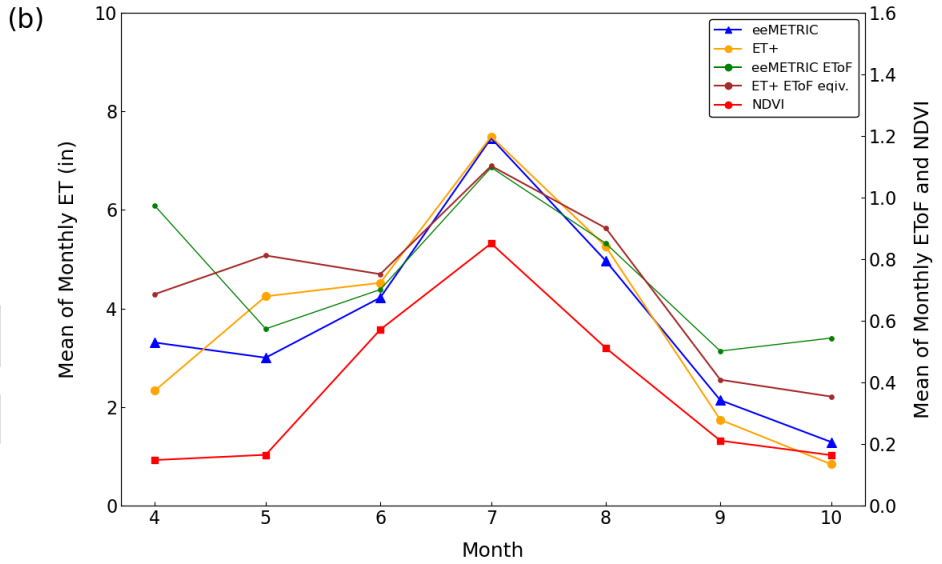
(b)
eeMETRIC
ET+
eeMETRIC EToF
ET+ EToF eqiv.
NDVI
Mean of Monthly ET (in)
Mean of Monthly EToF and NDVI
Month
0
2
4
6
8
10
0.0
0.2
0.4
0.6
0.8
1.0
1.2
1.4
1.6
4
5
6
7
8
9
10

2

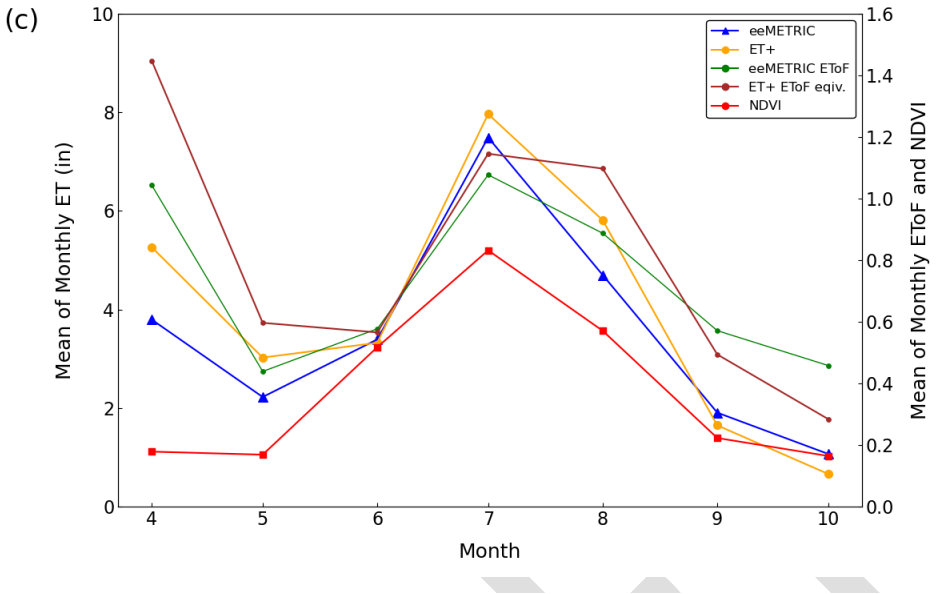

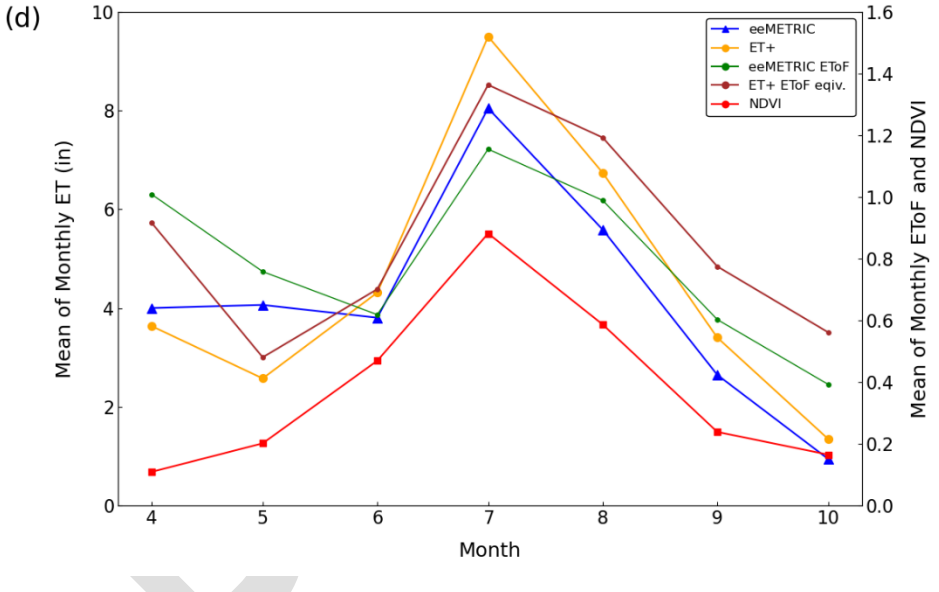

Figure 26. Time series of OpenET eeMETRIC and ET+ derived ET and fraction of reference ET, and Landsat derived NDVI for the growing season months (Apr–Oct) of (a) 2004, (b) 2006, (c) 2013, and (d) 2014 at the actively irrigated KB_8328 field north of Lower Klamath Lake, OR.

It is important to note that the underlying data produced by Landsat has changed as OpenET makes use of Landsat Collection 2 (*Landsat 8-9 Collection 2 Level 2 Science Product Guide | U.S. Geological Survey*, 2022), which offers numerous improvements to radiometric calibration and data processing. The creation of Landsat Collection 2 data supersedes previous Collection 1 data, as it was created by reprocessing both new and

historic Landsat data. At the time of this reporting, the underlying scene-images used by ET+ to develop monthly, seasonal, and annual summaries of ET are not available for direct 1:1 comparison. Discrepancies between eeMETRIC and the previous versions of the METRIC model may be attributed to the refinements of the METRIC model over the past decade, as well as the implementation and refinement of automated calibration methodologies which have been employed within eeMETRIC to produce reliable calibrations at scale.

Phreatophyte ET

Phreatophyte ET results from application of the BMM approach are summarized in tabular, raster, and GIS formats and are described in Appendix 4. Tabular summaries contain time series of spatially averaged annual ET_a, ET_g, ET_o, and PPT rates; 90th percentile CI and PI ET_a and ET_g rates; and supplementary VI's, water indices, LST, and albedo. Figure 27 illustrates time series of annual ET_g, ET_a, ET_o, and PPT rates for the Butte Valley estimated using the BMM approach from 1985–2020. Interannual variations in the annual ET_g and ET_a rates for phreatophyte shrublands in Butte Valley are largely controlled by variations in vegetation vigor, evaporative demand, and precipitation. Both annual and seasonal 30m resolution ET_g rasters were developed for the extent of phreatophyte shrublands within the Butte Valley HUC-8. Figure 28 illustrates the spatial distribution of the long-term (1985–2020) average annual ET_g for phreatophytes in Butte Valley where the BMM approach was applied. Dense shrubland areas exhibit higher ET_g rates (blue) than adjacent areas with more bare soil and sparse vegetation (light green, yellow).

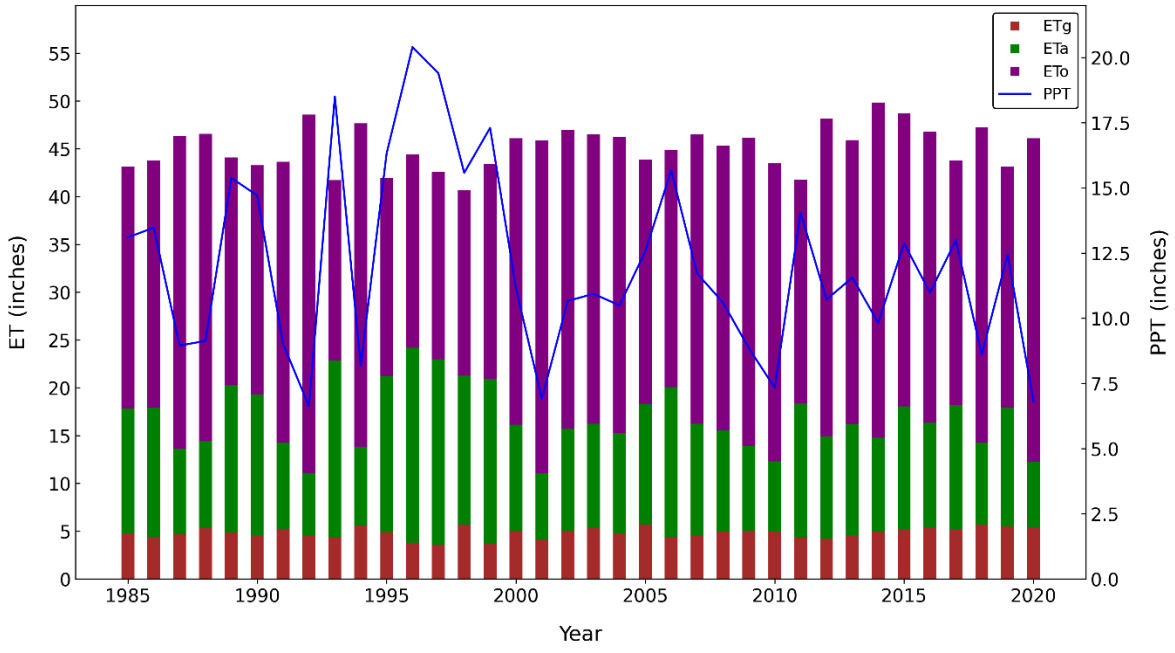

Figure 27. Annual ET_g, ET_a, ET_o, and PPT rate time series for phreatophyte shrublands in the Butte Valley HUC-8 from 1985–2020.

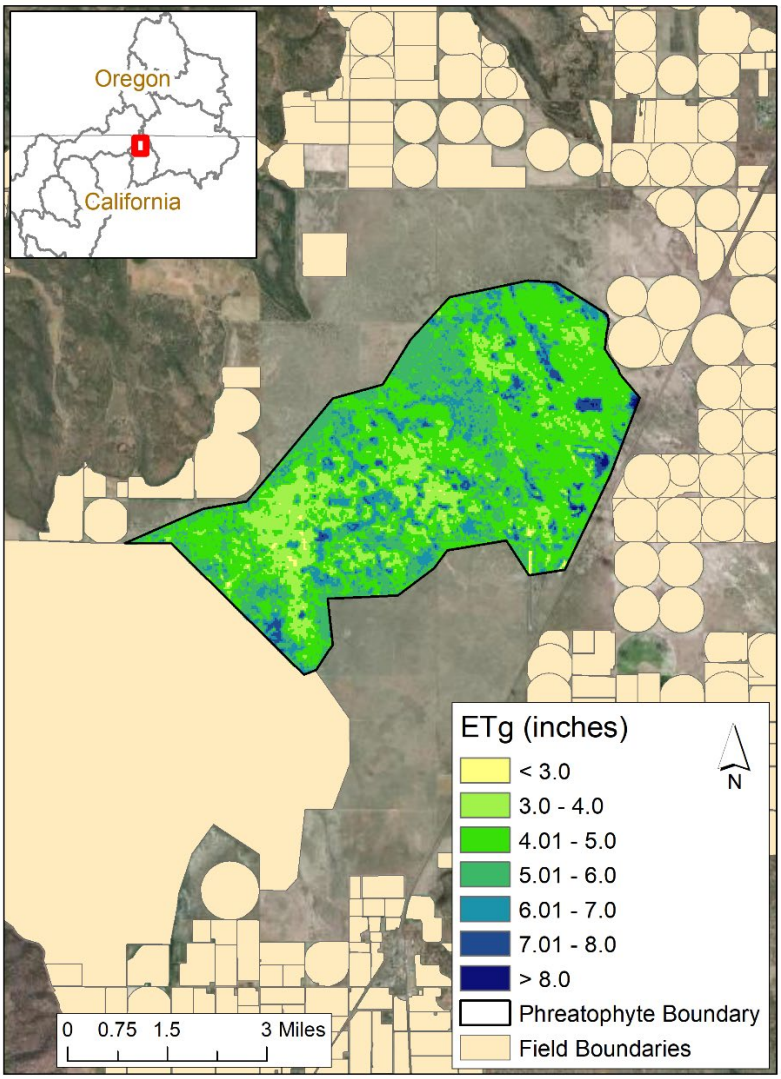

Figure 28. Spatial distribution of long-term (1985–2020) average annual ET_g rates for phreatophyte shrublands within the Butte Valley HUC-8.

LIMITATIONS AND UNCERTAINTY

Field Boundaries

The delineation and attribution of field boundaries within the KRRNFS area are susceptible to many errors and uncertainties. Inaccuracies may arise due to human error associated with the process of manually digitizing field boundary polygons as well as misclassification errors associated with the irrigation status, irrigation type, irrigation source type, and crop type attributes.

IrrMapper

The machine learning RF-based IrrMapper dataset used to determine annual irrigation status is in active development and will benefit from planned incremental improvements as the methodology and the training data are refined. The per-field irrigation status values represent the best available data for the study area. As of the time of this publishing, it is recognized that IrrMapper is most accurate for managed and engineered agricultural areas. For areas where natural wetlands or meadows were adapted for agricultural purposes, IrrMapper may often identify the areas as "wetland" in an intermediate step, and therefore classifies the areas as "unirrigated." These areas often are sub-irrigated where vegetation benefits from the shallow depth to water. These areas have been challenging for modeling efforts in the region, as these areas are difficult to clearly define as exclusively natural or agricultural.

ET Demands

ET Demands is a potential ET crop model designed to simulate NIWR under well-watered conditions with pristine management. Temperature-based thresholds are used to control growing season timing and crop development. Crop specific calibration parameters are calibrated for specific regions based on historical literature and comparison with NDVI time series derived from the Landsat satellite image archive. Manual calibration of CGDD, T_{30}, and other crop growth parameters ultimately relies on expert user opinion and judgement. Calibration is meant to capture average conditions and practices and may not accurately represent field level growth for all fields and scenarios during all years. It is important to note that beginning and ending season ET rates (i.e., April and October) are relatively low, minimizing the influence of slight mismatches in ET Demands simulated start and end dates.

The Klamath River Basin ET Demands model used a gridded approach based on the gridMET weather dataset 4km grid. Use of spatially varying weather data captures temperature and evaporative demand conditions not well resolved with coarser resolution implementations (e.g., HUC-6 or HUC-8). However, gridded application requires spatial interpolation of calibration parameters to account for spatial differences in management practices. Use of inverse distance weighting to interpolate calibration parameters may lead to inaccurate predictions in regions with abrupt spatial differences in crop development and timing. Additionally, field-level ET Demands crop assignments relied on year specific classifications from CDL from 2008 through 2020 and assumed a fixed crop type based on the 2008 to 2020 majority CDL classification for years prior. Discrepancies between CDL classifications and actual crop type will result in less accurate effective precipitation and subsequent net ET estimates.

The KRRNFS ET Demands model does not consider the influence of shallow groundwater on irrigation supply and assumes sprinkler-style irrigation to meet all crop water requirements. Irrigation events within ET Demands occur at set MAD thresholds. Higher MAD thresholds increase the time between irrigation events, while lower thresholds result in more frequent watering. Adjustment of irrigation frequency can result in higher (or lower)

ET and NIWR due to additional water losses to both bare soil evaporation and deep percolation. Large differences between simulated and actual practices will impact the accuracy of ET Demands effective precipitation estimates.

At the time of this work, the ET Demands model does not consider snowfall and accumulation when utilizing gridded weather datasets such as gridMET. All precipitation events within ET Demands occur as rain with immediate runoff and infiltration. Subsequently, ET Demands estimates of crop ET, P_{rz}, and NIWR in areas with significant snowfall may not align with actual conditions. Additional work is needed to understand how snowfall accumulation, drift, and melt processes impact water availability, P_{rz}, and NIWR in agricultural regions. Last, ET Demands crop growth simulations are based on typical northern-hemisphere April through October growth cycles. Non-standard management such as summer fallowing and or year-round growth may not be well represented in the model.

ET of Agriculture and Wetlands

The estimation of ET_a using eeMETRIC for agricultural areas and wetlands are subject to uncertainties and limitations. Possible factors contributing to these uncertainties include the individual accuracies of the eeMETRIC remote sensing model and the automated calibration and QA/QC procedures, observed meteorological data, estimated weather data and bias correction of gridMET ET_o, Landsat radiance and reflectance, spatial and temporal variability of cloud-free Landsat images, the interpolation of ET_oF values over time between Landsat images, additional gap-filling procedures, and previously mentioned uncertainties associated with field boundary dataset preparation. Nevertheless, previous studies have demonstrated that the eeMETRIC model used in this report generally provides accurate estimates within the range of 10 to 20 percent compared to measured crop ET in Oregon and other neighboring western states (Morton et al., 2013; Serbina and Miller, 2014; Liebert et al., 2015; Huntington et al., 2018; Huntington et al., 2022; Melton et al., 2022; Volk et al., 2023b).

Net ET of Agriculture and Wetlands

Net ET estimates for agricultural lands developed by this analysis are produced through a chained modeling workflow incorporating both bias and uncertainty in modeled meteorological, ET, and effective precipitation estimates. Individual components of the modeling workflow have been extensively validated through in situ and inter-model comparisons (Abatzoglou, 2013; Allen & Robinson, 2009; Huntington and Allen, 2009; Huntington and Allen, 2010; Melton et al., 2022; Volk et al., 2024); however, direct validation of Net ET estimates is difficult due to limited in situ observations and temporal and spatial discrepancies between measured and modeled estimates. This analysis reports net ET rates and volumes with no intermediate rounding of remotely sensed ET, modeled effective precipitation, or GIS acreage estimates. Estimated accuracy across the Klamath River Basin study domain varies and should be interpreted with respect to the spatial and temporal scale of subsequent data applications. For example, Allen et al. (2011) provides a detailed discussion of ET measurement accuracy and typical errors for EC (15-30 percent), soil water

balance (10-30 percent), and remotely sensed energy balance (10-20 percent) approaches. Additionally, Daly et al. (2008) reports average absolute errors of approximately 10 percent in the Western U.S. for PRISM annual precipitation normals that serve as the basis for gridMET downscaling. Despite the uncertainty of each modeling component, this effort overcomes weaknesses of historical approaches reliant on empirical or theoretical estimates by leveraging gridded weather data and remote sensing to capture on the ground conditions and variability in climate and irrigation status over a long historical period.

Monthly net ET estimates for wetlands assume that all precipitation discharges through ET (i.e., 100% of the total precipitation is effective) and none of the precipitation runs off or contributes to recharge.

Phreatophyte ET

ET_g estimates from phreatophyte shrublands produced in this study have numerous uncertainties and limitations. The NDVI – ET* predictive equation used in the BMM approach is empirical and relies on EC, BR, Landsat surface reflectance, and relatively coarse resolution gridded weather datasets, all of which are known to have inaccuracies and errors. Uncertainty in the 54 site years of in situ ET estimates derived from micrometeorological flux towers has been characterized as being +/- 10 to 12 percent (Maurer et al., 2005; Meyers & Baldocchi, 2005; Allander et al., 2009). EBC corrections were applied in this study to reduce some of this uncertainty prior to the formulation of the NDVI – ET* predictive equation; however, these corrections do not account for measurement errors associated with the EC and BR systems themselves.

The 4km gridded meteorological data from gridMET, air temperature, wind speed, solar radiation, humidity, and precipitation were used to develop estimates of ET_o, PPT, and ET* in the BMM approach. Although ET_o from gridMET was bias-corrected for improved estimation of ET over agricultural lands, no formal analysis was carried out to estimate similar biases over non-irrigated areas, such as the phreatophyte shrublands of Butte Valley, because of the absence of meteorological stations in shrubland environments within the study area.

The BMM approach used in this study relies on Landsat surface reflectance data products and recently standardized atmospheric correction techniques developed by the USGS (Schmidt et al., 2013; USGS, 2022). Factors such as aerosols, clouds, haze, and water vapor are recognized to impact atmospheric correction, and our approach in this research utilizes state-of-the-art weather model results and additional satellite data to address these complexities. The Landsat images used in this study, which underwent QA/QC, were acquired during the period spanning June 1st to September 15th (corresponding to days of year 152 through 258 in a non-leap year). For each year of the study period, a single estimate of NDVI, ET*, and ET_g were produced to characterize the vigor of phreatophyte vegetation. While the use of a single composite value may not fully capture conditions throughout the entire year, several studies have demonstrated the utility of both single and composite satellite-based ET approaches in estimating ET_a and ET_g from areas potentially influenced by groundwater discharge (Groeneveld et al., 2007; Beamer et al., 2013; Minor, 2019). These estimates have shown good agreement with riparian ET assessments based on advanced SEB and time integration models that involve iterative processing (Khand et al., 2017).

Considering the numerous assumptions and intricacies involved in estimating and upscaling ET_g rates from flux towers to a larger basin scale, the use of the NDVI – ET* regression model in this study is appealing. This is primarily because the model relies on 54 site years of in situ ET estimates and Landsat vegetation indices specifically tailored to phreatophyte areas. Furthermore, this approach takes into account the temporal and spatial fluctuations in evaporative demand and precipitation, which are the two primary drivers of ET. When we take into consideration all these factors and the associated limitations, single-scene or composite approaches emerge as more robust and likely to be more accurate compared to advanced SEB models or simple ET unit methods. In the latter approaches, ET rates from previous studies are assumed to be constant across time and space, and they are applied uniformly across similar ET units within the study areas of interest. However, it's important to acknowledge that the NDVI – ET* approach used in this study does have limitations that are common to empirical regression models. Additionally, the approach exhibits limited accuracy in estimating low ET_g rates in regions with sparse vegetation. These limitations become particularly noticeable due to challenges related to low signal-to-noise ratios and uncertainties associated with bare soil contributions to ET_g.

Lastly, inaccuracies in the delineation of potential groundwater discharge areas (i.e., phreatophyte areas) are a potential source of error (Zhu and Young, 2009). The phreatophyte areas defined in this study were identified using datasets which included aerial imagery, multispectral satellite imagery (including LST data), groundwater level measurements, and GIS datasets containing information on topography, vegetation, and previous phreatophyte delineations. Previous and historical delineations of groundwater discharge boundaries may have been less precise, primarily due to limitations in the availability of representative data, in particular access to high-resolution aerial imagery. While it's possible that the actual areas of ET_g could be smaller than those delineated in this study, areas with minimal ET_g typically exhibit very low NDVI values. Consequently, the BMM approach predicts negligible ET_g for these areas, as these low NDVI values indicate minimal vegetation cover.

SUMMARY

The primary objective of the ET Task of the Klamath River Revised Natural Flow Study was to develop field-scale estimates of ET_a using the eeMETRIC model, estimates of ET_g for phreatophyte shrublands using the BMM, estimates of wetlands ET using eeMETRIC, and develop estimates of effective precipitation, and net ET using the ET Demands model. eeMETRIC and ET Demands results were produced at the monthly, seasonal, and annual time steps, whereas BMM results were produced at the annual and seasonal time steps. The results from this effort are compiled into a series of field-specific .csv files, based on the delineated agricultural field boundaries, and are formatted for use in modeling and analysis using computer scripting languages which may be aggregated to irrigation districts or to hydrologic units as suitable for analysis and production of data. Calculations of ET_g are produced in both tabular form and spatially explicit raster images. These results are intended to guide and inform modeling efforts currently underway by USBR and USGS.

Combining ET estimates with effective precipitation from ET Demands allows for the partitioning of NIWR, runoff, infiltration, and evaporative losses. This work improves on

previous studies that relied on assumed or static rates of ET and effective precipitation, through the development and use of manually digitized agricultural field boundaries that represent maximum irrigated extents; use of long-term Landsat satellite data (1985–2020) and daily gridded weather data from gridMET (1979–2020); and state of the art land surface energy balance, machine learning, and soil water balance models. Datasets produced from this work are documented and intended for use within surface and groundwater modeling efforts of the KRRNFS, and other hydrologic studies.

ACKNOWLEDGMENTS

This work was funded by the U.S. Bureau of Reclamation as a component of the ongoing Klamath River Revised Natural Flow Study. This effort has been guided by ongoing collaboration with USBR TSC. USBR staff were instrumental in guiding the applications of ET models, in the development of methodologies for irrigation system type classification, and performed a comprehensive peer review of this report. TSC GIS staff provided support in the development and refinement of geospatial datasets necessary for this study. We would especially like to thank Mark Spears (USBR TSC) and Caroline Ubing (USBR TSC) for their efforts in project management, as well as Larry Dunsmoor (Confluence Resource Consulting) and Bill Cronin (USBR KBAO) for their in-depth knowledge of the Klamath River Basin. Dr. Jordan Beamer (OWRD) and Mellony Hoskinson (OWRD) supplied input on field boundaries, identified literature for review, and provided feedback on methods and approaches used in this study. The DRI team is grateful for the thoughtful review of Dr. Rick Allen and acknowledges his career which has advanced the application of remote sensing to address water resource issues.

REFERENCES

Abatzoglou, J. T. (2013). Development of gridded surface meteorological data for ecological applications and modelling. *International Journal of Climatology*, 33(1): 121-131. https://doi.org/10.1002/joc.3413

Allander, K. K., Smith, J. L., & Johnson, M. J. (2009). Evapotranspiration from the Lower Walker River Basin, West-Central Nevada, Water Years 2005-07: U.S. Geological Survey Scientific Investigations Report 2009-5079, 62 p. http://pubs.usgs.gov/sir/2009/5079/.

Allen, R. G., Brockway, C. E., & Wright, J. L. (1983). Weather station siting and consumptive use estimates. *Journal of Water Resources Planning and Management*, 109(2): 134-136. https://doi.org/10.1061/(ASCE)0733-9496(1983)109:2(134)

Allen, R. G. (1996). Assessing integrity of weather data for reference evapotranspiration estimation. *Journal of Irrigation and Drainage Engineering*, 122(2): 97-106. https://doi.org/10.1061/(ASCE)0733-9437(1996)122:2(97)

Allen, R. G., Pereira, L. S., Raes, D., & Smith, M. (1998). Crop Evapotranspiration - Guidelines for Computing Crop Water Requirements. *FAO Irrigation and Drainage Paper 56*, FAO: Rome, Italy, 1998. https://www.fao.org/3/x0490e/x0490e00.htm

Allen, R. G., Pereira, L. S., Smith, M., Raes, D., & Wright, J. L. (2005). FAO-56 Dual Crop Coefficient Method for Estimating Evaporation from Soil and Application Extensions. *Journal of Irrigation and Drainage Engineering*, 131(1): 2-13. https://doi.org/10.1061/(ASCE)0733-9437(2005)131:1(2)

Allen, R. G., Tasumi, M., & Trezza, R. (2007). Satellite-Based Energy Balance for Mapping Evapotranspiration with Internalized Calibration (METRIC)—Model. *Journal of Irrigation and Drainage Engineering*, 133(4): 380-394. https://doi.org/10.1061/(ASCE)0733-9437(2007)133:4(380)

Allen, R. G. (2008). Quality Assessment of Weather Data and Micrometeorological Flux-Impacts on Evapotranspiration Calculation. 農業気象, *Journal Agricultural Meteorology*, 64(4): 191-204, https://doi.org/10.2480/agrmet.64.4.5.

Allen, R.G., & Robison, C.W. (2009). Evapotranspiration and Consumptive Irrigation Water Requirements for Idaho, University of Idaho Report, 222 p. Available at http://www.kimberly.uidaho.edu/ETIdaho/

Allen, R. G. & D.T. Snyder. (2011). Completion Report on the Production of Evapotranspiration Maps for Year 2004 for the Upper Klamath and Sprague area of Oregon using Landsat Images and the METRIC™ Model. https://water.usgs.gov/GIS/dsdl/Report_KBRA_OPWP_ET_2004_ETplus.pdf

Allen, R. G., Pereira, L. S., Howell, T. A., & Jensen, M. E. (2011). Evapotranspiration Information Reporting: I. Factors Governing Measurement Accuracy. *Agricultural Water Management*, 98(6): 899-920. https://doi.org/10.1016/j.agwat.2010.12.015

Allen, R. G., Burnett, B., Kramber, W., Huntington, J., Kjaersgaard, J., Kilic, A. & Trezza, R. (2013). Automated calibration of the metric-landsat evapotranspiration process. JAWRA Journal of the American Water Resources Association, 49(3), 563-576.

Allen, R. G., & Huntington, J. L. (2015). Oregon Statewide Long-Term Water Demand Forecast—Appendix F: Comparison of Evapotranspiration Methods for the Klamath River Basin. State of Oregon Water Resources Department. https://www.oregon.gov/owrd/programs/Planning/IWRS/Documents/Appendix_F_Comparison_of_ET_methods_for_Klamath_basin.pdf

Allen, R. G., Dhungel, R., Dhungana, B., Huntington, J., Kilic, A., & Morton, C. (2021). Conditioning point and gridded weather data under aridity conditions for calculation of reference evapotranspiration. Agricultural Water Management, 245, 106531.

Anderson, M.C., Allen, R.G., Morse, A., & Kustas, W.P. (2012). Use of Landsat thermal imagery in monitoring evapotranspiration and managing water resources. *Remote Sensing of Environment*, doi:10.1016/j.rse.2011.08.025.

Arnone, J., Jasoni, R., Larsen, J., Fenstermaker, L., Wolfahrt, G., Kraftt, C., Lyles, B., Healey, J. Young, M., & Thomas, J. (2008). Variable evapotranspiration water losses from lowland agricultural and native shrubland ecosystems in the Great Basin of Nevada. DRI Publication Number: 655.7520.

ASCE-EWRI. (2005). The ASCE Standardized Reference Evapotranspiration Equation. In ASCE–EWRI Standardization of Reference Evapotranspiration Task Committee Report, ASCE, Reston, VA.

Beamer, J.P., Huntington, J.L., Morton, C.G., & Pohll, G. (2013). Estimating Annual Groundwater Evapotranspiration from Phreatophytes in the Great Basin Using Landsat and Flux Tower Measurements. *Journal of American Water Resources Association (JAWRA)*, 49(3): 518-533. DOI:10.1111/jawr.12058.

Beckham, S.D. 2006. Historical Landscape Overview of the Upper Klamath River Canyon of Oregon and California. Cultural Resource Series No. 13.

Berger, D.L., Mayers, C.J., Garcia, C.A., Buto, S.G., & Huntington, J.M. (2016). Budgets and chemical characterization of groundwater for the Diamond Valley flow system, central Nevada, 2011-12: U.S. Geological Survey Scientific Investigations Report 2016-5055, 83 p., http://dx.doi.org/10.3133/sir20165055.

Boryan, C., Yang, Z., Mueller, R., & Craig, M. (2011). Monitoring US Agriculture: The US Department of Agriculture, National Agricultural Statistics Service, Cropland Data Layer Program. *Geocarto International*, 26(5): 341-58. https://doi.org/10.1080/10106049.2011.562309

Bos, M. G., Kselik, R. A., Allen, R. G., & Molden, D. J. (2009). Effective precipitation. Water Requirements for Irrigation and the Environment, 81-101.

Bureau of Reclamation. (1908). Klamath Project: General Map. Map No. 10676.

Bureau of Land Management. 1990. Final Eligibility and Suitability Report for the Upper Klamath Wild and Scenic River Study.

Cammalleri, C., M. C. Anderson, and W. P. Kustas (2014). Upscaling of evapotranspiration fluxes from instantaneous to daytime scales for thermal remote sensing applications, Hydrol. Earth Syst. Sci., 18(5), 1885–1894, doi:10.5194/hess-18-1885-2014

Cihlar, J., L. St Laurent, and J. A. Dyer. "Relation between the normalized difference vegetation index and ecological variables." Remote sensing of Environment 35.2-3 (1991): 279-298.

Crawford, C. J., Roy, D. P., Arab, S., Barnes, C., Vermote, E., Hulley, G., ... & Zahn, S. (2023). The 50-year Landsat Collection 2 Archive. *Science of Remote Sensing*, 100103.

Cuenca, R. H., Ciotti, S. P., & Hagimoto, Y. (2013). Application of Landsat to evaluate effects of irrigation forbearance. Remote Sensing, 5(8), 3776-3802.

DeMeo, G.A., Smith, J.L., Damar, N.A., & Darnell, J. (2008). Quantifying Groundwater and Surface-Water Discharge from Evapotranspiration processes in 12 Hydrographic Areas of the Colorado Regional Groundwater Flow System, Nevad, Utah, and Arizona: U.S. Geological Survey Scientific Investigations Report 2006-5145, 36 p. http://pubs.usgs.gov/sir/2008/5116.

DeMeo, G.A. (2018). Evapotranspiration data from two sites at the head of the East Walker River near Bridgeport, CA, June 2012 through September 2013: U.S. Geological Survey, https://doi.org/10.5066/F79C6WM9.

DeTar, W. R. (2004). Using a Subsurface Drip Irrigation System to Measure Crop Water Use. *Irrigation Science*, 23(3): 111-122. https://doi.org/10.1007/s00271-004-0099-5

Dunkerly, C., Huntington, J. L., McEvoy, D., Morway, A., & Allen, R. G. (2024). agweather-qaqc: An Interactive Python Package for Quality Assurance and Quality Control of Daily Agricultural Weather Data and Calculation of Reference Evapotranspiration. Journal of Open Source Software, 9(97), 6368

Earth Resources Observation and Science (EROS) Center. (2017). Digital Orthophoto Quadrangle (DOQ) [Tiff]. U.S. Geological Survey. https://doi.org/10.5066/F7125QVD

Erdman, C. S., H. A. Hendrixson, and N. T. Rudd. 2011. 'Larval Sucker Distribution and Condition before and after Large-Scale Restoration at the Williamson River Delta, Upper Klamath Lake, Oregon.' Western North American Naturalist 71: 472–80. https://www.researchgate.net/publication/262088272

Fisher, J. B., Melton, F., Middleton, E., Hain, C., Anderson, M., Allen, R., ... & Wood, E. F. (2017). The future of evapotranspiration: Global requirements for ecosystem functioning, carbon and climate feedbacks, agricultural management, and water resources. *Water Resources Research*, *53*(4), 2618-2626.

Foga, S., Scaramuzza, P. L., Guo, S., Zhu, Z., Dilley Jr, R. D., Beckmann, T., ... & Laue, B. (2017). Cloud detection algorithm comparison and validation for operational Landsat data products. *Remote Sensing of Environment*, 194, 379-390.

Gannett, H., Leiberg, J. B., Thompson, A. H., Karr, M. B., & E. Ricksecker. (1887). Land Classification and Density of Standing Timber (Plate LXXII, Twenty-First Annual Report Part V). Plates 071 and 072.

Garcia, C.A., Huntington, J.M., Buto, S.G., Moreo, M.T., Smith, J.L., & Andraski, B.J. (2015). Groundwater discharge by evapotranspiration, Dixie Valley, west-central Nevada, March 2009-September 2011 (ver. 1.1, April 2015): U.S. Geological Survey Professional Paper 1805, 90 p. http://dx.doi.org/10.3133/pp1805.

Garcia, C.A., Corson-Dosch, N.T., Beamer, J.P., Gingerich, S.B., Grondin, G.H., Overstreet, B.T., Haynes, J.V., and Hoskinson, M.D. (2021). Hydrologic budget of the Harney Basin groundwater system, southeastern Oregon (ver. 1.1, November 2022): U.S. Geological Survey Scientific Investigations Report 2021–5128, 144 p., https://doi.org/10.3133/ sir20215128

Gorelick, N., Hancher, M., Dixon, M., Ilyushchenko, S., Thau, D., & Moore, R. (2017). Google Earth Engine: Planetary-scale geospatial analysis for everyone. Remote sensing of Environment, 202, 18-27.

Groeneveld, D.P., Baugh, W.M., Sanderson, J.S., & Cooper, D.J. (2007). Annual groundwater evapotranspiration mapped from single satellite scenes. *Journal of Hydrology*, v. 344, p. 146-156.

Hanson, C. L., Pierson, F. B., and Johnson, G L. "Dual-gauge system for measuring precipitation: Historical development and use." *Journal of Hydrologic Engineering* 9.5 (2004): 350-359.

Hardy, T.B., & Addley, R.C., 2001. Evaluation of Interim Instream Flow Needs in the Klamath River, Phase III, Final Report. Prepared for U.S. Department of Interior by Instiute for Natural Systems Engineering, Utah Water Research Laboratory, Utah State University, Logan, Utah: November 21, 2001. 315 p.

Hawkins, R. H., Hjelmfelt, A. T., Jr., & Zevenbergen, A. W. (1985). Runoff probability, storm depth, and curve numbers. *Journal of Irrigation and Drainage Engineering*, 111(4): 330-340. https://doi.org/10.1061/(ASCE)0733-9437(1985)111:4(330)

Howell, T. A., Steiner, J. L., Schneider, A. D., Evett, S. R., & Tolk, J. A. (1997). Seasonal and Maximum Daily Evapotranspiration of Irrigated Winter Wheat, Sorghum, and Corn-Southern High Plains. *Transactions of the American Society of Agricultural Engineers*, 40(3): 623-634. http://dx.doi.org/10.13031/2013.21321

Humphreys, T.H., & Reaburn, D.L. (1905). Topographic Survey of Irrigable Lands. Map No. 7655, Drawer No. 497-A.

Huntington, J. L., & R. G. Allen. "Evapotranspiration and net irrigation water requirements for Nevada." World Environmental and Water Resources Congress 2009: Great Rivers. 2009.

Huntington, J. L., & R. G. Allen. (2010). Evapotranspiration and net irrigation water requirements for Nevada. Nevada State Engineer's Office Publication, 266 pp.

Huntington, J. L., Gangopadhyay, S., Spears, M., Allen, R. King, D., Morton, C., Harrison, A., McEvoy, D., Joros, A., & Pruitt, T. (2015). West-Wide Climate Risk Assessments: Irrigation Demand and Reservoir Evaporation Projections. U.S. Bureau of Reclamation, Technical memorandum No. 86-68210-2014-01, 196p., 841 app. https://www.usbr.gov/watersmart/baseline/docs/irrigationdemand/irrigationdemands.pdf

Huntington, J. L., McGwire, K. C., Morton, C. G., Snyder, K., Peterson, S., Erickson, T., Niswonger, R., Carroll, R. W., Smith, G. T., Allen, R. (2016). Assessing the Role of Climate and Resource Management on Groundwater Dependent Ecosystem Changes in Arid Environments with the Landsat Archive, Remote Sensing of Environment, 185, 186-197, 10.1016/j.rse.2016.07.004

Huntington, J. L., Hegewisch, K. C., Daudert, B., Morton, C. G., Abatzoglou, J. T., McEvoy, D. J., & Erickson, T. (2017). Climate engine: Cloud computing and visualization of climate and remote sensing data for advanced natural resource monitoring and process understanding. Bulletin of the American Meteorological Society, 98(11), 2397-2410.

Huntington, J. L., Bromley, M., Morton, C. G., & Minor, T. B. (2018). Remote Sensing Estimates of Evapotranspiration from Irrigated Agriculture, Northwestern Nevada and Northeastern California, 38, 41275. https://www.dri.edu/metric-et

Huntington, J. L., Pearson, C., Minor, B. A., Volk, J. M., Morton, C. G., Melton, F. S., & Allen, R. (2022). Appendix G: Upper Colorado River Basin OpenET Intercomparison Summary, Technical Report prepared for U.S. Bureau of Reclamation. http://dx.doi.org/10.13140/RG.2.2.21605.88808

Huntington, J.L., Minor, B.A., Bromley, M., Pearson, C., Beamer, J., Ingwersen, K., Carrara, K., Hoskinson, M., Atkin, J., Brito, J., Dunkerly, C., Ott., T.(2024). Crop Evapotranspiration, Consumptive Use, Irrigation Water Requirements, and Reservoir Evaporation for Oregon. Desert Research Institute Report, prepared for the Oregon Water Resources Department. In Review.

Jensen, M. E. & Allen, R. G. (2016). Evaporation, evapotranspiration, and irrigation water requirements. American Society of Civil Engineers: Reston, VA, USA.

Kennedy, J.J. (2021). Klamath Marsh January Through May Maximum Surface Water Extent, 1985-2021 (ver. 2.0, March 2022): U.S. Geological Survey data release, https://doi.org/10.5066/P9CRB511.

Ketchum, D., Jencso, K., Maneta, M. P., Melton, F., Jones, M. O., & Huntington, J. L. (2020). IrrMapper: A Machine Learning Approach for High Resolution Mapping of Irrigated Agriculture Across the Western US. *Remote Sensing*, 12(14), 2328. https://doi.org/10.3390/rs12142328

Khand, K., Taghvaeian, S., & Hassan-Esfahani, L. (2017). Mapping Annual Riparian Water Use Based on the Single-Satellite-Scene Approach. *Remote Sensing*, 9(8), 832.

Kilic, A., Allen, R. G., Blankenau, P., Revelle, P., Ozturk, D., & Huntington, J. (2021). Global production and free access to Landsat-scale Evapotranspiration with EEFlux and eeMETRIC. In *6th Decennial National Irrigation Symposium, 6-8, December 2021, San Diego, California*. American Society of Agricultural and Biological Engineers, pp. 9.

Landsat 8-9 Collection 2 Level 2 Science Product Guide | U.S. Geological Survey. (2022). https://www.usgs.gov/media/files/landsat-8-9-collection-2-level-2-science-product-guide

Leuning, R., Gorsela, E. van, Massman, W. J., & Isaac, P. R. (2012). Reflections on the surface energy imbalance problem. Agricultural and Forest Meteorology. 156: 65-74., 65-74. https://doi.org/10.1016/j.agrformet.2011.12.002

Liebert, R., Huntington, J., Morton, C., Sueki, S., & Acharya, K. (2015). Reduced evapotranspiration from leaf beetle induced tamarisk defoliation in the Lower Virgin River using satellite-based energy balance. *Ecohydrology*, 9(1): 179-193. https://doi.org/10.1002/eco.1623

Lippincott, J. B., Murphy, D. W., & T. H. Humphreys. (1905). Topographic and Irrigation Map, Upper and Lower Klamath Projects. Sheet 1 Map No. 7855.

Lundquist, J., Hughes, M., Gutmann, E., & Kapnick, S. (2019). Our skill in modeling mountain rain and snow is bypassing the skill of our observational networks. Bulletin of the American Meteorological Society, 100(12), 2473-2490.

Marek, T., Colaizzi, P., Howell, T. A., Dusek, D., & Porter, D. (2006). Estimating Seasonal Crop ET Using Calendar and Heat Unit Based Crop Coefficients in the Texas High Plains Evapotranspiration Network. ASABE Paper No: 062206, 2006 ASABE Annual International Meeting, Portland, Oregon, July 9-12, 2006, 11 p. http://dx.doi.org/10.13031/2013.21437

Maurer, D.K., Berger, D.L., Tumbusch, M.L., & Johnson, M.J. (2005). Rates of evapotranspiration, recharge from precipitation beneath selected areas of native vegetation, and streamflow gain and loss in Carson Valley, Douglas County, Nevada, and Alpine County, California: U.S. Geological Survey Scientific Investigations Report 2005-5288, 70 p. http://pubs.usgs.gov/sir/2005/5288.

McGwire, K., Minor, T., & Fenstermaker, L. (2000). Hyperspectral Mixture Modeling for Quantifying Sparse Vegetation Cover in Arid Environments. Remote Sensing of Environment, 72(3), 360-374. https://doi.org/10.1016/S0034-4257(99)00112-1

Melton, F. S., Huntington, J. L., Grimm, R., Herring, J., Rollison, D., Erickson, T., Allen, R., Anderson, M., Fisher, J. B., Kilic, A., Senay, G. B., Volk, J., Hain, C., Johnson, L., Ruhoff, A., Blankenau, P., Bromley, M., Carrara, W., Daudert, B., Doherty, C., Dunkerly, C., Friedrichs, M., Guzman, A., Halverson, G., Hansen, J., Harding, J., Kang, Y., Ketchum, D., Minor, B., Morton, C., Ortega-Salazar, S., Ott, T., Ozdogan, M., ReVelle, P. M., Schull, M., Wang, C., Yang, Y., & Anderson, R. G. (2022). OpenET: Filling a critical data gap in water management for the western United States. *JAWRA Journal of the American Water Resources Association*, 58(6): 971-994. https://doi.org/10.1111/1752-1688.12956

Meyers, T.P. & Baldocchi, D.D. (2005). Current Micrometeorological Flux Methodologies with Applications in Agriculture. Micrometeorology in Agricultural Systems (Agronomy), J.L. Hatfield (Editor). American Society of Agronomy Inc., Madison, Wisconsin, pp. 381-396.

Minor, B. (2019). Estimating Annual Groundwater Evapotranspiration from Hydrographic Areas in the Great Basin using Remote Sensing and Evapotranspiration Data Measured by Flux Tower Systems (unpublished master's thesis). University of Nevada, Reno.

Mitchell, K. E., Lohmann, D., Houser, P. R., Wood, E. F., Shaake, J. C., Robock, A., Cosgrove, B. A., Sheffield, J., Duan, Q., Luo, L., Higgins, R. W., Pinker, R. T., Tarpley, J. D., Lettenmaier, D. P., Marshall, C. H., Entin, J. K., Pan, M., Shi, W., Koren, V., Meng, J., Ramsay, B. H., & Bailey, A. A. (2004). The multi-institution North American Land Data Assimilation System (NLDAS): Utilizing multiple GCIP products and partners in a continental distributed hydrological modeling system. *Journal of Geophysical Research*, 109, D07S90. https://doi.org/10.1029/2003JD003823

Mikkelson, K., PE, PhD. (2023). Klamath River Basin Revised Natural Flow Study Phase 1 & 2 Open Water Evaporation Modeling (Technical Memorandum ENV-2024-006). Bureau of Reclamation Technical Service Center.

Moreo, M.T., Laczniak, R.J., & Stannard, D.I. (2007). Evapotranspiration rate measurements of vegetation typical of groundwater discharge areas in the Basin and Range carbonate-rock aquifer system, White Pine County, Nevada, and adjacent areas in Nevada and Utah, September 2005-August 2006: U.S. Geological Survey Scientific Investigations Report 2017-5079, 55 p. http://doi.org/10.3133/sir2017079.

Moreo, M.T., Andraski, B.J., & Garcia, C.A. (2017). Groundwater discharge by evapotranspiration, flow of water in unsaturated soil, and stable isotope water sourcing in areas of sparse vegetation, Amargosa Desert, Nye County, Nevada: U.S. Geological Survey Scientific Investigations Report 2017-5079, 55 p. http://doi.org/10.3133/sir2017079.

Morton, C. G., Huntington, J. L., Pohll, G. M., Allen, R. G., Mcgwire, K. C., & Bassett, S. D. (2013). Assessing Calibration Uncertainty and Automation for Estimating Evapotranspiration from Agricultural Areas Using METRIC. *Journal of American Water Resources Association*, 49(3): 549-562. https://doi.org/10.1111/jawr.12054

National Agriculture Imagery Program (NAIP). (2019). [Data set]. DOI/USGS/EROS. https://catalog.data.gov/dataset/national-agriculture-imagery-program-naip

National Research Council (NRC), 2008. Hydrology, Ecology, and Fishes of the Klamath River Basin. National Research Council of the National Academies, Committee on Hydrology, Ecology, and Fishes of the Klamath River, Board on Environmental Studies and Toxicology, Water Science and Technology Board, Division on Earth and Life Studies, Washington, D.C.

Nichols, W. D. (1994). Groundwater discharge by phreatophyte shrubs in the Great Basin as related to depth to groundwater. Water Resources Research, 30(12), 3265-3274.

Nichols, W.D. (2000). Regional Ground-Water Evapotranspiration and Ground-Water Budgets, Great Basin, Nevada: U.S. Geological Survey Professional Paper 1628, 82 pp.

Ozdogan, M. & Rodell, M. (2010). Simulating the effects of irrigation over the United States in a land surface model based on satellite-derived agricultural data. *Journal of Hydrometeorology*, 11(1): 171-184.

OSU-COAREC (Oregon State University – Central Oregon Agricultural Research and Extension Center). Crops. Available at Crops | College of Agricultural Sciences (oregonstate.edu)

Pastorello, G., Trotta, C., Canfora, E., Chu, H., Christianson, D., Cheah, Y. W., ... & Law, B. (2020). The FLUXNET2015 dataset and the ONEFlux processing pipeline for eddy covariance data. Scientific data, 7(1), 1-27.

Pearson, C., Huntington, J., and C. Dunkerly, (2021). Agricultural Evapotranspiration and Net Irrigation Water Requirements for the Upper Colorado River Basin: 2020 ET Demands Model Summary. Desert Research Institute Report, prepared for U.S. Bureau of Reclamation, pp. 49. http://www.ucrcommission.com/wp-content/uploads/2022/11/Assessing-Agricultural-Consumptive-Use-in-the-UCRB-Phase-III-Technical-Appendices-Nov-2022.zip

Reclamation, 2005. Natural Flow of the Upper Klamath River. Prepared by the Technical Service Center, Denver, Colorado, and Klamath Basin Area Office, Klamath Falls, Oregon, November 2005.

Reiner, S.R., Laczniak, R.J., DeMeo, G.A., Smith, J.L., Elliott, P.E., Nylund, W.E., & Fridrich, C.J. (2002). Groundwater Discharge Determined from Measurements of Evapotranspiration, Other Available Hydrologic Components, and Shallow Water-Level Changes, Oasis Valley, Nye County, Nevada: U.S. Geological Survey Water-Resources Investigations Report 01-4239, 65 p. http://pubs.usgs.gov/wri/wri014239.

Robinson, T.W. (1958). Phreatophytes: U.S. Geological Survey Water-Supply Paper 1423, https://pubs.usgs.gov/wsp/1423/report.pdf.

Sammis, T. W., Mapel, C. L., Lugg, D. G., Lansford, R. R., & McGuckin, J. T. (1985). Evapotranspiration Crop Coefficients Predicted Using Growing Degree Days. *Transactions American Society of Agricultural Engineers*, 28(3): 773-780. https://doi.org/10.13031/2013.32336

Schmidt, G., Jenkerson, C., Masek, J., Vermote, E., & Gao, F. (2013). Landsat ecosystem disturbance adaptive processing system (LEDAPS) algorithm description: U.S. Geological Survey Open-File Report 2013-1057, 17 p.

Serbina, L. O., & Miller, H. M. (2014). Landsat and water: case studies of the uses and benefits of landsat imagery in water resources, U.S. Geological Survey Open-File Report 2017-1034. https://doi.org/10.3133/ofr20141108

Slack, D. C., Martin, E. D., Sheta, A. E., Fox, F. A., Jr., Clark, L. J., & Ashley, R. O. (1996). Crop Coefficients Normalized for Climatic Variability with Growing-degree-days. Proc., International Conf., Evapotranspiration and Irrigation Scheduling, San Antonio, Texas, C.R. Camp, E.J. Sadler, and R. E. Yoder (eds.). American Society of Agricultural Engineers, St. Joseph, Michigan, pp. 892-898.

Smith, J.L., Laczniak, R.J., Moreo, M.T., & Welborn, T.L. (2007). Mapping evapotranspiration units in the Basin and Range carbonate-rock aquifer system, White Pine County, Nevada, and adjacent parts of Nevada and Utah: U.S. Geological Survey Scientific Investigations Report 2007-5087, 20p.

Snyder, R. L., Spano, D., Cesaraccio, C., & Duce, P. (1999). Determining degree-day thresholds from field observations. *International Journal of Biometeorology*, 42: 177-182. https://doi.org/10.1007/s004840050102

Snyder, D.T., Risley, J.C., & Haynes, J.V. (2012). Hydrological information products for the Off-Project Water Program of the Klamath Basin Restoration Agreement: U.S. Geological Survey Open-File Report 2012-1199, 20 p., http://pubs.usgs.gov/of/2012/1199.

Stannard, D.I., Gannett, M. W., Polette, D. J., Cameron, J. M., Waibel, M. S., & Spears, J. M. (2013). Evapotranspiration from marsh and open-water sites at Upper Klamath Lake, Oregon, 2008–2010: U.S. Geological Survey Scientific Investigations Report 2013–5014, 66 p. https://doi.org/10.3133/sir20135014

State of Oregon: Oregon Geospatial Enterprise Office - Oregon Statewide Imagery Program. (n.d.). https://www.oregon.gov/geo/Pages/imagery.aspx

Stene, 1994. The Klamath Project. U.S. Department of the Interior, Bureau of Reclamation, History Program, Denver, Colorado.

Szilagyi, J. & Schepers, A. (2014). Coupled heat and vapor transport: The thermostat effect of a freely evaporating land surface. *Geophysical Research Letters*, 41(2): 435-441. https://doi.org/10.1002/2013GL058979

Tasumi, M., R. G. Allen, R. Trezza, and J. L. Wright (2005), Satellite-based energy balance to assess within-population variance of crop coefficient curves, J. Irrig. Drain. Eng., 131(1), 94–109.

Temesgen, B., Allen, R. G., & Jensen, D. T. (1999), Adjusting temperature parameters to reflect well-watered conditions. *Journal of Irrigation and Drainage Engineering*, 125(1): 26-33. https://doi.org/10.1061/(ASCE)0733-9437(1999)125:1(26)

USDA, F. (2008). Common Land Unit (CLU). Retrieved February 10, 2009.

USDA. (2017). The Gridded Soil Survey Geographic (gSSURGO) Database for Oregon. United States Department of Agriculture, Natural Resources Conservation Service. Available online at https://gdg.sc.egov.usda.gov/.

USDA-NASS (United States Department of Agriculture, National Agricultural Statistics Service). 2010. Field Crops – Usual Planting and Harvesting Dates. October 2010, 50p. Available at nass.usda.gov/Publications/Todays_Reports/reports/fcdate10.pdf

USDA-NRCS. (1991). State Soil Geographic (STATSGO) Data Base Data use information. United States Department of Agriculture Natural resources Conservation Service, National Soil Survey Center, Miscellaneous Publication number 1492.

USDA-NRCS. (1998). Estimation of Direct Runoff from Storm Rainfall. Part 630 Hydrology, National Engineering Handbook. Chapter 10. https://directives.sc.egov.usda.gov/OpenNonWebContent.aspx?content=17752.wba

U.S. Geological Survey (2022). Landsat 8 Surface Reflectance Code (LaSRC) Product, version 4.0, March 2022, 37 p.

Volk, J., Huntington, J., Allen, R., Melton, F., Anderson, M., & Kilic, A. (2021). flux-data-qaqc: A Python Package for Energy Balance Closure and Post-Processing of Eddy Flux Data. *Journal of Open Source Softw.*, 6(66), 3418. https://doi.org/10.21105/joss.03418

Volk, J., Pearson, C., Huntington, J., Dunkerly, C., & Morton, C. (2023a). WSWUP/gridwxcomp: Comparison of Weather Station and Gridded Climate Datasets, n.d., https://github.com/WSWUP/gridwxcomp

Volk, J. M., Huntington, J. L., Melton, F. S., Allen, R., Anderson, M. C., Fisher, J. B., Kilic, A., Senay, G., Halverson, G., Knipper, K., Minor, B., Pearson, C., Wang, T., Yang, Y., Evett, S., French, A. N., Jasoni, R., & Kustas, W. (2023b). Development of a Benchmark Eddy Flux Evapotranspiration Dataset for Evaluation of Satellite-Driven Evapotranspiration Models Over the CONUS. *Agricultural and Forest Meteorology*, 331, 109307. https://doi.org/10.1016/j.agrformet.2023.109307.

Volk, J. M., Huntington, J. L., Melton, F., Allen, R., Anderson, M., Fisher, J., Kilic, A., Senay, G., Halverson, G., Knipper, K., Minor, B. A., Pearson, C., Wang, T., Yang, Y., Evett, S., French, A. N., Jasoni, R. L., Kustas, W. (2023). Development of a benchmark Eddy flux evapotranspiration dataset for evaluation of satellite-driven evapotranspiration models over the CONUS, *Agricultural and Forest Meteorology*, 331, 109307. Elsevier

Volk, J. M., Huntington, J. L., Melton, F. S., Allen, R., Anderson, M., Fisher, J. B., Kilic, A., Ruhoff, A., Senay, G. B., Minor, B. A., Morton, C. G., Ott, T., Johnson, L., Comini de Andrade, B., Carrara, W., Doherty, C. T., Dunkerly, C. W., Friedrichs, M., Guzman, A., Hain, C., Halverson, G., Kang, Y., Knipper, K., Laipelt, L., Ortega-Salazar, S., Pearson, C., Parrish, G. E., Purdy, A., ReVelle, P., Wang, T., Yang, Y. (2024). Assessing the accuracy of OpenET satellite-based evapotranspiration data to support water resource and land management applications, *Nature Water*, 13 p. 10.1038/s44221-023-00181-7

Walter, I. A., Allen, R. G., Elliott, R., Jensen, M. E., Itenfisu, D., Mecham, B., Howell, T. A., Snyder, R., Eching, S., Spofford, T., Hattendorf, M., Martin, D., Cuenca, R. H., & Wright, J. L.; Task Committee on Standardization of Reference Evapotranspiration of the Environmental and Water Resources Institute of the American Society of Civil Engineers. (2000). ASCE's Standardized Reference Evapotranspiration Equation. *Watershed Management and Operations Management*, edited by R. G. Allen, A. Walter, R. Elliot, T. A. Howell, D. Itenfisu, & M. E. Jensen, 1-11. Reston, VA: American Society of Civil Engineers. https://doi.org/10.1061/40499(2000)126

Wright, J. L. (1982). New Evapotranspiration Crop Coefficients. *Journal of Irrigation and Drainage Division*, ASCE, 108(1): 57-74. https://doi.org/10.1061/JRCEA4.0001372

Wright, J. L. (2001). Growing degree day functions for use with evapotranspiration crop coefficients. CD-ROM, American Society of Agronomy, *Agronomy Abstracts*.

Wu, W. (2014). The Generalized Difference Vegetation Index (GDVI) for Dryland Characterization. Remote Sensing, 6(2), Article 2. https://doi.org/10.3390/rs6021211

Yang, D., Goodison, B. E., Metcalfe, J. R., Golubev, V. S., Bates, R., Pangburn, T., & Hanson, C. L. (1998). Accuracy of NWS 8" standard nonrecording precipitation gauge: Results and application of WMO intercomparison. Journal of atmospheric and oceanic technology, 15(1), 54-68.

Zhang, C., Yang, Z., Di, L., Lin, L., & Hao, P. (2020). Refinement of cropland data layer using machine learning. *Int. Arch. Photogramm. Remote Sens. Spatial Inf. Sci.,* 161-164. https://doi.org/10.5194/isprs-archives-XLII-3-W11-161-2020

Zhao, W., Allen, R.G., Trezza, R., and Robison, C.W., 2015, Evapotranspiration in the Upper Klamath Basin for the 2013 Growing Season (April - October): U.S. Geological Survey Data Release, http://dx.doi.org/10.5066/F72J68ZW.

Zhu, J., & Young, M. H. (2009). Sensitivity and Uncertainty of Ground-Water Discharge Estimates for Semiarid Shrublands 1. *JAWRA Journal of the American Water Resources Association*, 45(3), 641-653. https://doi.org/10.1111/j.1752-1688.2009.00312.x

SUPPLEMENTAL TABLES

Supplemental Table 1. Agricultural weather stations used in bias correction of ET_o, with mean monthly of station – GridMET ratios

Station Name	Source	Network ID	Station ID	GridMET ID	State	Latitude	Longitude	Elevation (meters)	Period of Record	Jan Mean Station ETo/GridMET ETo	Feb Mean Station ETo/GridMET ETo	Mar Mean Station ETo/GridMET ETo	Apr Mean Station ETo/GridMET ETo	May Mean Station ETo/GridMET ETo	Jun Mean Station ETo/GridMET ETo	Jul Mean Station ETo/GridMET ETo	Aug Mean Station ETo/GridMET ETo	Sep Mean Station ETo/GridMET ETo	Oct Mean Station ETo/GridMET ETo	Nov Mean Station ETo/GridMET ETo	Dec Mean Station ETo/GridMET ETo	Annual Mean Station ETo/GridMET ETo
Cedarville	Agrimet PN	cedc	031_CA	548966	CA	41.5853	-120.171	1402	6/23/1989 – 5/31/2019	0.86	0.96	0.99	0.97	0.95	0.95	0.96	0.94	0.91	0.89	0.87	0.86	0.94
McArthur	CIMIS	43	044_CA	532303	CA	41.0638	-121.456	1009	1/2/1994 – 12/31/2018	0.71	0.82	0.87	0.90	0.87	0.90	0.90	0.87	0.83	0.78	0.69	0.70	0.86
Alturas	CIMIS	90	066_CA	544801	CA	41.4382	-120.48	1343	1/2/1994 – 12/31/2018	0.89	0.91	0.91	0.85	0.84	0.87	0.91	0.91	0.91	0.89	0.94	0.91	0.89
Tulelake FS	CIMIS	91	067_CA	561409	CA	41.9589	-121.472	1230	1/2/1994 – 12/31/2018	0.83	0.94	0.95	0.92	0.92	0.94	0.91	0.91	0.92	0.86	0.86	0.87	0.91
Shasta College	CIMIS	224	162_CA	517037	CA	40.6255	-122.311	180	1/2/2013 – 12/31/2018	0.91	0.88	0.80	0.82	0.85	0.88	0.88	0.84	0.83	0.84	0.85	0.88	0.85
Scott Valley	CIMIS	225	163_CA	548902	CA	41.5778	-122.838	833	4/20/2015 – 12/31/2018	0.75	0.71	0.82	0.86	0.86	0.91	0.92	0.85	0.85	0.81	0.73	0.69	0.86
Macdoel II	CIMIS	236	174_CA	557238	CA	41.8025	-121.996	1300	4/18/2015 – 12/31/2018	0.99	0.93	0.94	0.88	0.87	0.97	0.99	0.94	0.94	0.96	0.96	0.92	0.94
Christmas Valley	Agrimet PN	chvo	765_OR	604393	OR	43.2414	-120.728	1312	7/13/1990 – 5/24/2019	0.93	0.96	0.97	0.98	0.94	0.97	0.95	0.94	0.91	0.90	0.92	0.94	0.95
Klamath Falls	Agrimet PN	kflo	776_OR	568332	OR	42.1647	-121.755	1250	3/31/1999 – 5/29/2019	0.72	0.84	0.90	0.92	0.92	0.95	0.90	0.87	0.84	0.78	0.74	0.74	0.88
Lakeview	Agrimet PN	lako	777_OR	566976	OR	42.1222	-120.523	1454	6/23/1989 – 5/29/2019	0.77	0.84	0.89	0.93	0.92	0.96	0.95	0.93	0.92	0.87	0.80	0.78	0.92
Lorella	Agrimet PN	loro	778_OR	565573	OR	42.0778	-121.224	1268	4/2/2001 – 5/29/2019	0.77	0.85	0.88	0.90	0.89	0.92	0.90	0.89	0.85	0.82	0.82	0.82	0.88
Medford	Agrimet PN	mdfo	779_OR	573848	OR	42.3311	-122.938	408	6/23/1989 – 5/25/2019	0.60	0.69	0.78	0.85	0.82	0.84	0.81	0.75	0.70	0.65	0.61	0.54	0.77
Worden	Agrimet PN	wrdo	788_OR	564173	OR	42.0125	-121.788	1244	4/20/2000 – 5/29/2019	0.74	0.88	0.94	0.96	0.93	0.93	0.88	0.88	0.87	0.84	0.84	0.82	0.90
Lynhart Ranch	SCAN	2074	1077_OR	564183	OR	42.0187	-121.389	1247	1/1/2010 – 10/5/2018	0.75	0.95	0.91	0.92	0.91	0.95	0.89	0.82	0.83	0.82	0.82	0.73	0.88

1 Supplemental Table 2. Crosswalk of CDL classes to crop types supported by ET Demands

CDL Crop Number	CDL Crop Type	ET Demands Crop Number	ET Demands Crop Assignment
0	Background	4	Grass Hay
1	Corn	7	Field Corn
12	Sweet Corn	9	Sweet Corn
14	Mint	4	Grass Hay
21	Barley	11	Spring Grain
23	Spring Wheat	11	Spring Grain
24	Winter Wheat	4	Grass Hay
25	Other small grains	11	Spring Grain
27	Rye	4	Grass Hay
28	Oats	4	Grass Hay
35	Mustard	4	Grass Hay
36	Alfalfa	3	Grass Hay
37	Other Hay/Non Alfalfa	4	Grass Hay
38	Camelina	4	Grass Hay
41	Sugarbeets	21	Garden Vegetables
42	Dry Beans	21	Garden Vegetables
43	Potatoes	29	Potatoes Early Season
44	Other Crops	4	Grass Hay
47	Misc Vegs & Fruits	21	Garden Vegetables
49	Onions	21	Garden Vegetables
53	Peas	21	Garden Vegetables
57	Herbs	21	Garden Vegetables
59	Sod/Grass Seed	4	Grass Hay
61	Fallow/Idle Cropland	4	Grass Hay
68	Apples	21	Garden Vegetables
69	Grapes	21	Garden Vegetables
71	Other Tree Crops	4	Grass Hay
77	Pears	21	Garden Vegetables
82	Developed	4	Grass Hay
87	Wetlands	51	Wetlands Large Stand
111	Open Water	51	Wetlands Large Stand
121	Developed/Open Space	4	Grass Hay
122	Developed/Low Intensity	4	Grass Hay
123	Developed Med Intensity	4	Grass Hay
131	Barren	4	Grass Hay
141	Deciduous Forest	4	Grass Hay
142	Evergreen Forest	4	Grass Hay
143	Mixed Forest	4	Grass Hay
152	Shrubland	4	Grass Hay
176	Grass/Pasture	4	Grass Hay
179	Error CDL code 179 = 176	4	Grass Hay
190	Woody Wetlands	4	Grass Hay
195	Herbaceous Wetlands	51	Wetlands Large Stand
205	Triticale	11	Spring Grain
206	Carrots	21	Garden Vegetables
208	Garlic	21	Garden Vegetables
221	Strawberries	21	Garden Vegetables
227	Lettuce	21	Garden Vegetables
241	Dbl Crop Corn/Soybeans	7	Field Corn
242	Blueberries	21	Garden Vegetables
247	Turnips	21	Garden Vegetables

APPENDICES

Appendix 1. Data products

Please note that these data products are for official use only and hosted by U.S. Bureau of Reclamation. To request access please contact Caroline Ubing (cubing@usbr.gov)

- Agricultural Field Boundaries
- Time series data for eeMETRIC ET_a and ET Demands
- Groundwater Component of ET (ET_g) for Phreatophytic Vegetation
- KNFS ET Demands model package

Appendix 2. Description of the agricultural field boundary dataset and feature attributes

Agricultural Field Boundaries

The agricultural field boundary dataset represents the maximum irrigated extent from 1985–2020. Basic feature attributes included in the dataset/shapefile include a unique identification name, positional information relative to state borders and the military grid reference system (MGRS) tiles, total feature/field acreage, crop type information through time (2008–2020), the data source of each annual crop type classification, the latest feature modification date, the irrigation system type (1995–2020), the irrigation water source, the irrigation status through time (1985–2020), and growing season average NDVI through time (1985–2020). The field names within the field boundary shapefile are as follows:

OPENET_ID – The OPENET_ID represents the unique field/feature identification code/name.

MGRS_TILE – The military grid reference system (MGRS) Grid Zone identifier the field is located within.

STATE – The state that the field is located within.

ACRES – The total area of field/feature in acres.

CROP_[YEAR] – The mode/majority classification of the USDA Cropland Data Layer codes within the field boundary for a given year.

CSRC_[YEAR] – The online data source for the crop type classification for a given year.

ITYP_[YEAR] – The irrigation system type classification (0, 1, 2, 3, 4, or 5) for a given year. "0" represents Developed/No longer irrigated, "1" represents Sprinkler-Pivot-Linear, "2" represents Sprinkler-Other (Wheel Line, Hand Line, Solid Set, Big Gun, Travelling Gun, Pods), "3" represents Flood-Uncontrolled (Wild Flood) and No Apparent Irrigation Equipment, "4" represents Flood Controlled (Land Leveling, Borders, Basins, Furrows), and "5" represents Micro (Micro Sprinklers, Drip Lines, Subsurface Drip).

IRR_[YEAR] – The irrigation status of the field/feature for a given year. A value of 1 represents irrigated conditions and a value of 0 represents non-irrigated conditions. Decimal values between 0 and 1 represent the spatial average of all the pixels within the field boundary.

GSNDVI_[YEAR] – The spatial average of the growing season (Apr–Oct) mean normalized difference vegetation index derived from Landsat for a given year.

Appendix 3. Description of monthly summaries of ET, ET_o, ET_oF, total precipitation, effective precipitation, and net ET

Monthly Time Series

The monthly net ET time series are assembled as one file per field boundary and contain information for the entire KNFS study period of 1980–2020. The monthly net ET time series has net ET information for up to 51 crops or land use conditions, which correspond to 8 simplified/generalized assignments used by ET Demands. Missing ET data for each time series during the time frame of March 1984–September 2020 was gap filled by first linearly interpolating monthly fraction of reference ET (ET_oF) and then multiplying the monthly ET_oF by the corresponding monthly reference ET (ET_o) to obtain actual monthly ET. Generally, missing ET data occurred in the winter months due to cloud contamination of the Landsat scene imagery. Because wintertime ET is often low, the total net ET is not impacted substantially by the gap filled data. For the October 1980–February 1984 time frame, Landsat and OpenET data is not available. To estimate ET prior to the Landsat and

OpenET data records, an analog approach was used that combines ET_oF from periods of similar wetness with the evaporative demand (i.e., ET_o) from pre-March 1984. Analog years that were selected for this analysis are listed in table 3. The monthly net ET files are under 100kb each but with over 12,000 fields the total size of the dataset is quite large. The size of this dataset necessitated the organization of output files into multiple folders for sharing purposes. The crop types that are included for the net ET time series are listed in Supplementary Table 2.

The names of the net ET files for the agricultural field boundaries contain a unique OPENET_ID name/code (e.g., "KB_5"), the irrigation district name (e.g., "KID") or the HUC-8 code (e.g., "18010201"), which represents the region where the field boundary is located, and the file extension ".csv." For example, the name for the field above is "KB_5_eemetric_etdemands_monthly_klamath_18010201_1980_2020.csv."

The time series for each field is from October 1980–December 2020. The monthly files contain rates of actual ET, reference ET, precipitation, and effective precipitation in units of mm/month, along with volumetric summaries of ET, reference ET, precipitation, effective precipitation, and net ET in units of acre-feet/month. The organization and definitions for the field names are as follows:

date – the date (start of month) in the format MM/DD/YYYY.

et (actual monthly ET) – the total estimated flux of ET as estimated by the OpenET eeMETRIC model in units of mm/month.

et_fraction (fraction of grass reference ET) – the ratio of the actual monthly ET as estimated by the OpenET eeMETRIC model to the monthly grass reference ET as estimated by gridMET.

et_reference (grass reference monthly ET) – the total estimated flux of ET from a hypothetical grass reference crop in units of mm/month.

ppt (total precipitation) – the total precipitation amounts as estimated by gridMET in units of mm/month.

ACRES (total field area) – the total field/feature area in units of acres.

P_rz (precipitation residing in the root zone) – the amount of gross reported precipitation less any surface runoff or deep percolation that resides in the soil and is available for consumption by evaporation or transpiration in units of mm/month. P_rz is computed as P – Runoff – DPerc in ET Demands where P is gross reported precipitation, Runoff is estimated surface runoff and DPerc is deep percolation of any precipitation below the maximum root zone for the crop or land cover type.

P_eft (precipitation residing in the root zone that is available for transpiration) – the amount of gross reported precipitation less any surface runoff or deep percolation that resides in the soil and is available for consumption by transpiration in units of mm/month. P_eft does not include the amount of infiltrated precipitation that evaporates from the surface evaporation layer (upper 100 mm of soil). The P_eft parameter is useful in estimating the amount of precipitation during the non-growing season that is stored and made available for transpiration requirements during the growing season. P_eft is always less than P_rz. When analyzed during the growing season, P_eft is useful for estimating how 'efficient' precipitation is in fulfilling transpiration requirements of crops, as opposed to simply 'burning off' as evaporation from the soil surface. P_eft was calculated as P – Runoff – Dperc – surface evaporation losses.

Irrigation – the irrigation timing and amount is simulated using a daily soil water balance in units of mm/month. Irrigation is simulated when the root zone dries to the specified threshold point (i.e., the maximum allowable depletion) where stress will begin to occur (listed in appendix 5). The simulated irrigation frequency and depth per irrigation is a function of the crop type and available water holding capacity.

Runoff (surface runoff from precipitation) – the surface runoff is estimated during precipitation events using the NRCS curve number as described in the main body of text. Units are in mm/month.

CDL Code (crop type classification) – the mode/majority crop type within the field that is used to crosswalk to the ET Demands classification for pairing with effective precipitation.

ET Demands Code (simplified crop type classification) – the crop assignment used by ET Demands for the daily soil water balance simulation.

GRIDMET_ID – the gridMET cell identification used to pair ET Demands with the eeMETRIC data.

OPENET_ID – the unique OpenET identification code/name for the field/feature.

ET Volume (ac-ft) – the total actual monthly ET volume in units of acre-feet/month. Calculated by multiplying the spatially averaged actual monthly ET rate by the field acreage.

ETo Volume (ac-ft) – the total monthly reference ET volume in units of acre-feet/month. Calculated by multiplying the spatially averaged monthly reference ET rate by the field acreage.

PPT Volume (ac-ft) – the total monthly precipitation volume in units of acre-feet/month. Calculated by multiplying the spatially averaged monthly precipitation rate by the field acreage.

Effec. PPT Volume (ac-ft) – the total monthly effective precipitation (equivalent to P_rz) volume in units of acre-feet/month. Calculated by multiplying the P_rz rate from ET Demands by the field acreage.

Net ET Volume (ac-ft) – the total monthly net ET volume in units of acre-feet/month. Calculated by subtracting the total monthly effective precipitation volume from the total actual monthly ET volume.

Appendix 4. Description of annual and seasonal summaries of groundwater ET

Annual Summaries

Annual summaries of ET_g as estimated by the Beamer-Minor Method (BMM) for Butte Valley are provided in both raster and tabular formats. The annual ET_g rasters (1985–2020) have 30-meter pixel resolution with a spatial extent limited to the extent of phreatophyte shrublands (i.e., area of potential groundwater discharge) within the Butte Valley basin. Each raster represents the total annual (Oct–Sept, water year timestep) ET_g in units of millimeters per year and are in GeoTIFF file format (e.g., butte_2015.etg_mean.tif). Complementing the annual ET_g rasters is a tabular summary ("klamath_etg_butte_only.xlsx"), which contains information about all Landsat satellite imagery and derived products that were produced by the BMM to estimate annual ET_g. Additional derived variables that were not directly used by the BMM but are useful for

QA/QC procedures include normalized difference water index (NDWI), soil-adjusted vegetation index (SAVI), albedo, land surface temperature (TS), and enhanced vegetation index (EVI). The "ET_g Volume" tab of the tabular summary lists all of the Landsat scenes and the spatial averages of numerous QA/QC variables and variables produced and used by the BMM. The field/column definitions are as follows:

ZONE_NAME – the zone/feature name used for zonal statistics.

ZONE_FID – the unique FID code of the zone/feature.

DATE – the Landsat scene overpass date in the format MM/DD/YYYY.

SCENE_ID – the Landsat scene identification text.

PLATFORM – the specific Landsat satellite code name.

PATH – the path of the Landsat satellite for the given overpass date.

ROW – the row of the Landsat satellite, which is the latitudinal center line of a frame of imagery for the given overpass date.

YEAR – the year of the overpass date.

MONTH – the month of the overpass date.

DAY – the day of the month for the overpass date.

DOY – the day of the year for the overpass date.

PIXEL_COUNT – the total number of pixels intersecting the zone/feature used in the BMM to estimate annual ET_g.

PIXEL_TOTAL – the total number of pixels intersecting the zone/feature that could nominally be used in the BMM to estimate annual ET_g.

FMASK_COUNT – the total number of pixels intersecting the zone/feature that were flagged by the FMask masking algorithm, which is used for clouds, cloud shadows, snow/ice, and water masking.

FMASK_TOTAL – the total number of pixels intersecting the zone/feature that could nominally be masked by the FMask algorithm.

FMASK_PCT – the percentage of the total pixels that were masked by the FMask algorithm.

ETSTAR_COUNT – the total number of pixels intersecting the zone/feature that fell below the BMM regression line that were assigned minimum ET* values.

CLOUD_SCORE – the simple cloud score for the image based on the pixels intersecting the zone/feature.

QA – Quality assessment flag used to identify poor quality scenes (unused, relied on manual filtering instead).

NDVI_SUR – the spatial average of the normalized difference vegetation index surface reflectance values for the zone/feature.

NDVI_TOA – the spatial average of the normalized difference vegetation index top-of-atmosphere values for the zone/feature.

SAVI_SUR – the spatial average of the soil-adjusted vegetation index surface reflectance values for the zone/feature.

ALBEDO_SUR – the spatial average of the albedo values for the zone/feature.

TS – the spatial average of the land surface temperature values for the zone/feature in units of kelvin.

EVI_SUR – the spatial average of the EVI surface reflectance values for the zone/feature.

ETSTAR_MEAN – the spatial average of the ET* values for the zone/feature as estimated by the BMM.

ETG_MEAN – the spatial average of the annual ET_g values for the zone/feature in units of mm/yr.

ETG_LPI – the lower 90th percentile prediction interval estimates of annual ET_g based on the BMM regression in units of mm/yr.

ETG_UPI – the upper 90th percentile prediction interval estimates of annual ET_g based on the BMM regression in units of mm/yr.

ETG_LCI – the lower 90th percentile confidence interval estimates of annual ET_g based on the BMM regression.

ETG_UCI – the upper 90th percentile confidence interval estimates of annual ET_g based on the BMM regression in units of mm/yr.

WY_ETO – the total water year ET_o as estimated by gridMET and used in the BMM in units of mm/yr.

WY_PPT – the total water precipitation as estimated by gridMET and used in the BMM in units of mm/yr.

Below the rows with the column values described above is the median annual groundwater ET rates from 1985-2020, total zone/feature acreage, and the median annual ET_g volume for the Butte Valley phreatophyte shrublands, which amount to 0.398 ft/yr, 7,435 acres, and 2,958 acre-ft/yr.

Seasonal Summaries

Seasonal summaries of ET_g as estimated by the Beamer-Minor Method (BMM) for Butte Valley are provided in raster format. The seasonal ET_g rasters (1985–2020) have 30-meter pixel resolution with a spatial extent limited to the extent of phreatophyte shrublands (i.e., area of potential groundwater discharge) within the Butte Valley basin. Each raster represents the total seasonal/quarterly (Oct–Dec, Jan–Mar, Apr–Jun, and Jul–Sept; water year timestep) ET_g in units of millimeters per quarter and are in GeoTIFF file format (e.g., butte_etg_Oct_Dec_wy_2015.tif). Seasonal summaries of ET_g for each water year were calculated by first computing the ratio of annual ET_g to annual ET_o and then multiplying the ET_g/ET_o ratio by the seasonal ET_o.

Appendix 5. Description of ET Demands model package and monthly output files

The ET Demands model package includes both input and output files used for execution of the model for the KNFS. Input datasets include grid cell location information (.shp), soils data (.shp), crop type (.cdl), and climate time series (.csv). Preprocessing routines reduce spatial datasets into formatted text files for input to ET Demands. Calibration files containing crop parameter values for each grid cell and crop type are stored in .shp format within the Calibration folder. Output files include daily monthly, and annual summary time series .csv files for each unique crop, grid cell combination. The following describes the monthly ET Demands output .csv files utilized for consumptive use estimation produced in the monthly Agricultural Field Boundary datasets described in Appendix 3. A full description of the ET Demands model and all required input and output files can be found in online documentation hosted at: https://github.com/usbr/et-demands. The monthly ET Demands .csv output field/column definitions are as follows:

Date – the date (start of month) in the format YYYY-MM

Year – model simulation year in format YYYY.

Month – model simulation numerical month value.

PMeto_mm – input grass reference evapotranspiration (ET) adjusted using OpenET bias correction surface values in units of mm/month.

ETact – ET_a estimates including stress adjustments in units of mm/month. ETact includes transpiration and evaporation from the soil surface from both precipitation and irrigation.

ETpot – crop specific potential ET in units of mm/month.

ETbas – basal evaporation component of ET in units of mm/month.

Kc – monthly average crop coefficient (unitless).

Kcb – monthly average basal crop coefficient (unitless).

PPT – total monthly precipitation in units of mm/month.

Irrigation – total monthly irrigation simulated by ET Demands in units of mm/month.

Runoff – total monthly runoff in units of mm/month.

DPerc – total monthly deep percolation from the root zone in units of mm/month.

P_rz – monthly total precipitation residing in the root zone available for either evaporation or transpiration in units of mm/month (see full description in Appendix 3).

P_eft – monthly total precipitation residing in the root zone available for transpiration only in units of mm/month (see full description in Appendix 3).

P_rz_fraction – fraction of monthly total P_rz to monthly total precipitation (unitless).

P_eft_fraction – fraction of monthly total P_eft to monthly total precipitation (unitless).

NIWR – monthly total net irrigation water requirement in units of mm/month.

Season – total number of active growing season days within simulation month.

Cutting – total number of cutting events during simulation month.